

CALIFORNIA INSTITUTE OF TECHNOLOGY

EARTHQUAKE ENGINEERING RESEARCH LABORATORY

**MODAL COUPLING AND EARTHQUAKE
RESPONSE OF TALL BUILDINGS**

BY
JOHN BRENT HOERNER

EERL 71-07

A REPORT ON RESEARCH CONDUCTED UNDER A
GRANT FROM THE NATIONAL SCIENCE FOUNDATION

PASADENA, CALIFORNIA

1971

MODAL COUPLING AND EARTHQUAKE RESPONSE
OF TALL BUILDINGS

Thesis by
John Brent Hoerner

In partial fulfillment of the requirements
for the Degree of
Doctor of Philosophy

California Institute of Technology
Pasadena, California
1971
(Submitted May 24, 1971)

ACKNOWLEDGMENTS

The author is pleased to thank Professor P.C. Jennings for his guidance and assistance in the preparation of this thesis. The cooperation of the San Diego Gas and Electric Company in making dynamic tests possible is appreciated.

The author is grateful to the California Institute of Technology and the National Science Foundation for financial assistance which made this thesis possible.

The author thanks Mrs. Karen Current for her patience and perseverance in typing this manuscript.

Special thanks are given to the author's wife, Margie, for her help and encouragement in the years of graduate study.

ABSTRACT

The major dynamic features of tall buildings are within the scope of a shear beam model. Herein the usual one-dimensional model is extended to three dimensions to include modes with translational and rotational components. The analysis is restricted to the continuous model with linear response.

A class of models for tall buildings is presented which possesses three sets of mutually orthogonal coupled modes. The amount of modal coupling is related to the eccentricities divided by the translational-torsional frequency differences. Strong modal coupling can occur if the eccentricities and frequency differences are small, as in a rectangular building with a smooth distribution of columns. A perturbation scheme is developed for buildings almost in this class. The perturbation method is applicable to buildings with nearly vertical mass and rigidity centers and with i^{th} modes of nearly the same shape.

Rotational components of earthquake response in buildings primarily results from modal coupling, and it is shown that modal coupling can increase response on the building's perimeter. Furthermore, rectangular buildings with modal coupling can show a beating-type frequency response, for which the more usual r.m.s. combination should be replaced by an absolute sum. These effects can significantly increase certain response parameters. The corners of a rectangular building can have a 95% increase in shear, as compared with 30% implied by a 5% eccentricity in the codes. Base shears and overturning moments can be increased by 40%.

TABLE OF CONTENTS

<u>Part</u>	<u>Title</u>	<u>Page</u>
I	INTRODUCTION	1
II	DYNAMIC MODELS OF TALL BUILDINGS	7
III	DYNAMIC PROPERTIES OF TALL BUILDINGS	35
IV	APPLICATION OF PERTURBATION THEORY	66
V	THE EFFECT OF EARTHQUAKES ON TALL BUILDINGS	96
VI	APPLICATION TO THE SAN DIEGO GAS AND ELECTRIC BUILDING	122
VII	SUMMARY AND CONCLUSIONS	141
	REFERENCES	145
	APPENDIX I	152
	APPENDIX II	154
	APPENDIX III	157

LIST OF FIGURES

<u>Figure</u>	<u>Title</u>	<u>Page</u>
1	MILLIKAN LIBRARY RESPONSE TO THE SAN FERNANDO EARTHQUAKE	9
2	FUNDAMENTAL MODES FOR SOME TALL BUILDINGS	10
3	SECOND MODES FOR SOME TALL BUILDINGS	11
4	THIRD MODES FOR SOME TALL BUILDINGS	12
5	n-STORY BUILDING MODEL	17
6	ONE-STORY BUILDING MODEL	19

<u>Figure</u>	<u>Title</u>	<u>Page</u>
7	FLOOR INTERACTION IN FINITE MODEL	21
8	CONTINUOUS MODEL	25
9	MOTION IN CONTINUOUS MODEL	27
10	BUILDINGS WITH COUPLING DUE TO ECCENTRICITY	48
11	BUILDINGS WITH COUPLING DUE TO FREQUENCY DIFFERENCES	53
12	T-BUILDING MODEL	60
13	MODES FOR T-BUILDING	61
14	MOHR'S CIRCLE	64
15	PERTURBATION MODEL	79
16	CHARACTERISTIC MOMENT ARMS FOR OVERTURNING	113
17	SAN DIEGO GAS AND ELECTRIC BUILDING	124
18	TYPICAL PLAN, 4th - 17th FLOORS, SAN DIEGO GAS AND ELECTRIC BUILDING	125
19	FUNDAMENTAL MODES AT THE 20th FLOOR	127
20	FIRST AND SECOND FUNDAMENTAL MODES	128
21	THIRD FUNDAMENTAL MODE	129
22	NORMALIZED FUNDAMENTAL MODES - 20th FLOOR	131
23	FUNDAMENTAL MODES FROM PERTURBATION THEORY	137
24	ESTIMATED EARTHQUAKE RESPONSES OF THE SAN DIEGO GAS AND ELECTRIC BUILDING	139

I. INTRODUCTION

The earthquake response of tall buildings has become of particular importance because the number of tall buildings in seismic regions of the western United States has increased rapidly in recent years. In Los Angeles, for example, where until recently all buildings were restricted by code⁽¹⁾ to thirteen stories with the exception of the twenty-seven story city hall, there are now several buildings of over thirty stories and buildings of over fifty stories are currently under construction. With the increase in the number of tall buildings which have certain common properties, such as a rectangular plan, a uniform cross-section and an open moment resisting frame, it appears that a general formulation which describes the earthquake response of many tall buildings can be attained. So motivated, the response of tall buildings in general is the subject of this thesis. For simplicity, attention is restricted to linear response.

The more important features of the dynamic response of many tall buildings, such as mode shapes and frequency spacings, can be represented with a planar shear beam model. For a structure with a nominally symmetric rectangular plan, this model is usually assumed to respond in a single translational plane or in rotation about the neutral axis. Such a model is basically one-dimensional and the mode shapes for such a model are said to be uncoupled. However, some tall

buildings with rectangular plans, such as the San Diego Gas and Electric Building, respond as a complete three-dimensional structure.⁽²⁾ Inspired by this type of response, attention herein is focused on a three-dimensional shear beam model for which strong modal coupling is a possibility. Another incentive for considering a three-dimensional model is that it can respond in rotation to excitation which is purely translational. Hence, the earthquake response may be significantly greater than would be expected from the more common one-dimensional model.

The possibility of modal coupling in a shear beam model, whether continuous or discrete, appears to have been first considered by R.S. Ayre^(3,4,5,6) who noted that mode shapes could be composed of both translational and rotational components if the centers of mass and rigidity are not coincident. Although strong modal coupling is likely with large eccentricities⁽⁷⁾, R. Shepherd and others^(8,9,10) observed that strong modal coupling can occur for small eccentricities if the corresponding natural frequencies are close together. Furthermore, it was noted that if the frequencies are close together, a beating-type phenomenon would be likely, and hence the traditional r.m.s. maxima applicable to well-separated frequencies should be replaced by an absolute sum.⁽⁸⁾ Other investigators have found coupled modes, either mathematically for specific models of building structures^(10,11,12,13,14) or from vibration tests of actual buildings.^(2,15)

The coupling of translational and rotational vibrations in modes is similar to other types of coupled vibration, for example,

the vibrations of buildings with light towers or setbacks, which have been discussed in the literature.^(9,10) A building with a small symmetrically placed appendage will have strongly coupled modes if the fixed base natural frequencies of the building and the appendage are close together;⁽¹⁶⁾ this result is fundamentally similar to translational-rotational coupling. Buildings with eccentric setbacks also exhibit coupled vibrational modes and have been investigated by G.V. Berg.⁽¹⁷⁾ Coupling between vertical motions and rotation about a horizontal axis as applied to one-story structures with asymmetric end walls; that is, coupling of motions in a vertical rather than horizontal plane, is considered by Loyar.⁽¹⁸⁾ Other instances of modal coupling, which is strong when the corresponding natural frequencies are close together, occur, for example, in machine structures.⁽¹⁹⁾

There are other effects related to torsional response of buildings which are not considered in this thesis, one of which is non-linear response of eccentric buildings.⁽²⁰⁾ It also may be possible for the earthquake itself to exhibit eccentric or torsional components arising from the spatial derivatives of the horizontal components of acceleration,⁽²¹⁾ but eccentricity is herein confined to the building itself.

Apparent modal coupling may result if resonance of a single mode is not attained during a building vibration test. This type of coupling, which seems in accord with the large shift in center of twist with slight changes in forcing frequency noted by Englekirk

and Matthiesen,⁽²²⁾ is a result of the response of two modes as discussed elsewhere,⁽²³⁾ and is not a property of modal coupling as defined in this thesis.

Since strong modal coupling and large torsional motions are possible in nominally symmetric buildings, it is of interest to compare the results of dynamic analyses with the design requirements of the building code. The current Uniform Building Code⁽²⁴⁾ recommends a static design for an accidental eccentricity of 5% of the maximum overall plan dimension. G.W. Housner and H. Outinen⁽²⁵⁾ found that traditional static methods of accounting for the effects of a real eccentricity on the earthquake response of buildings are not in accord with dynamic analysis. The inadequacy of this specification of building codes, especially when translational and torsional frequencies are close together, was observed also by Bustamante and Rosenbluth.^(26,27)

The purpose of this study is to estimate the effect of modal coupling on the earthquake response of tall buildings. Both discrete and continuous, three-dimensional shear beam models for tall buildings are developed in the second chapter. The manner in which the discrete model approaches the continuous model as the number of stories increases is examined, and, for simplicity, attention is henceforth restricted to the continuous model.

In the third chapter the dynamic properties for a particular class of models are displayed. This class, which is shown to be representative of many tall buildings, has a simple form of coupled

mode shapes. The three components, two translational and one rotational, of each of the mode shapes for a particular building are in one of three sets of constant ratios. A particularly simple subset of this class is one of uncoupled mode shapes with two sets in translation and one in rotation. It is noted that strong modal coupling in nominally symmetric structures occurs if and only if the translational and torsional frequencies are close together. As a result, it is observed that rectangular buildings with either central cores or peripheral shear walls as primary resistive elements tend to have relatively uncoupled modes, while a smooth even dispersion of columns can result in strong modal coupling in such buildings.

In Chapter Four perturbation theory is applied to the class of models developed in Chapter Three so that more tall buildings may be realistically included. It is found that, as long as the natural frequencies are not too close together, and the model is in a certain sense nearly in the class described by Chapter Three, the mode shapes and eigenvalues may be determined with good accuracy using this approach.

The earthquake response of buildings of this class is the subject of Chapter Five. In this chapter the responses due to strong modal coupling and uncoupled modes are compared. Relative displacements and absolute accelerations at the centroid and the perimeter of the building base shears and overturning moments are considered. It is noted that modal coupling can account for a 40% to 95% increase in response relative to that for uncoupled modes, depending upon

the response parameter chosen.

In Chapter Six an example of a building which possesses strong modal coupling, the San Diego Gas and Electric Building, is examined.⁽²⁾ The mode shapes and natural frequencies of this structure, determined from vibration tests, are compared with the theoretical results from Chapters Three and Four. Furthermore, the results of Chapter Five are applied to this example to determine the expected earthquake response, and to compare this with the response expected if the mode shapes are assumed to be uncoupled. From the results it is concluded that strong modal coupling can increase the earthquake response parameters much more than the 5% accidental eccentricity prescribed by the codes.⁽²⁴⁾

As a general conclusion it is recommended that tall buildings should either be designed for the increased response indicated by strong modal coupling, that is, more stringently than indicated by the codes, or they should be designed so that the modes are relatively uncoupled.

II. DYNAMIC MODELS OF TALL BUILDINGS

Introduction

To study the response of tall buildings to earthquakes or other dynamic loadings, it is necessary first to model the building so that the equations of motion may be formulated. A model should be chosen so that it displays only the more important dynamic properties of its prototype because a complete model, even if accurate, is usually too complex to be useful.

Because of the physical similarity of most tall buildings, it appears possible to describe the more important dynamic properties of a large number of such structures within the framework of a single model. Both ambient^(28,29,30,31,32) and forced^(2,15,33,34,35) vibration tests of tall buildings indicate that for sufficiently small amplitudes the response closely resembles that of a multi-degree of freedom linear oscillator and this is the type of model used in the thesis.

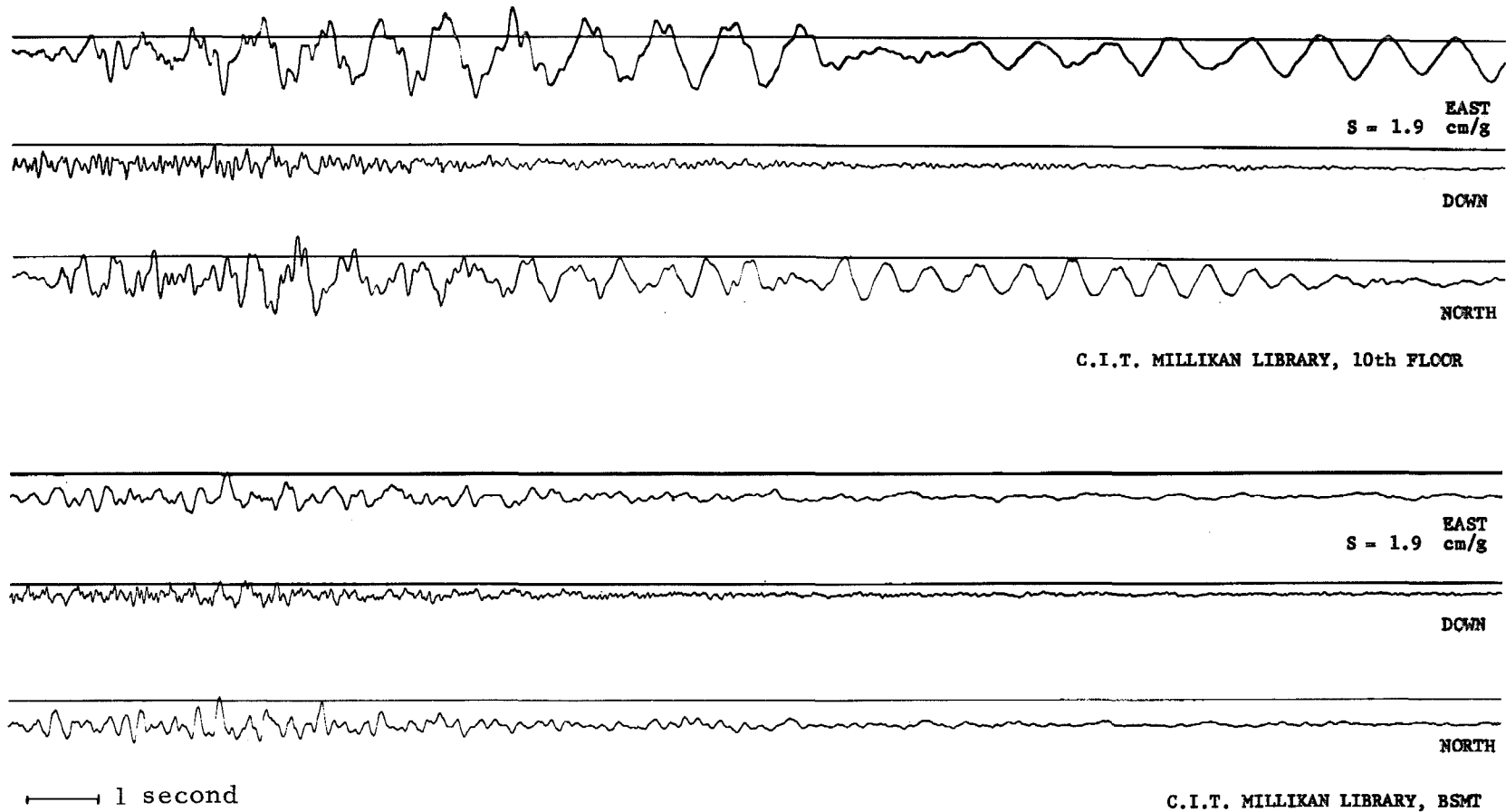
There are several dynamic features of building response which will be neglected, for example, vertical motions. This work is focused upon the interaction of horizontal motions, translational and rotational, in different directions, and therefore vertical motions are not of prime importance. It is possible, however, to include vertical motions by a natural extension of the dynamic models considered.

Non-linear response and hysteretic effects are also neglected for simplicity. Non-linear response, including yielding, certainly does

occur in strong earthquakes, but it is assumed that the earthquake responses of many structures, for which the Millikan Library response during the San Fernando earthquake of February 9, 1971 shown in figure 1 is typical, closely resemble that of a linear structure. This measurement and others suggest that many features of the response of structures to strong earthquakes are capable of description within the framework of linear analysis.

Because of the great convenience which results, columns and shear walls between adjacent floors are assumed to deform in horizontal shear only, with bending and axial extension or compression being neglected. Such an assumption implies that tall buildings should have dynamic properties, approximating those of a shear beam, for example, nearly sinusoidal fundamental mode shapes. Vibration tests indicate that the fundamental modes of tall buildings, as shown in figure 2, usually are close to straight lines, about halfway between the shape for a shear beam and that for bending beam, while the second and higher modes, as shown in figures 3 and 4, are close to the shape for a shear beam. A further indication that shear beam characteristics are predominant is the 1,3,5,7... spacing of natural frequency ratios; this frequency spacing differs greatly from that for a bending beam.

The floors of the buildings are assumed to be rigid in the analysis. This assumption is experimentally verified by demonstrating that at resonance certain straight lines on a floor remain straight or nearly so during a vibration test.^(33,34) Resonant frequencies of the floor can occur near the lower natural frequencies of some

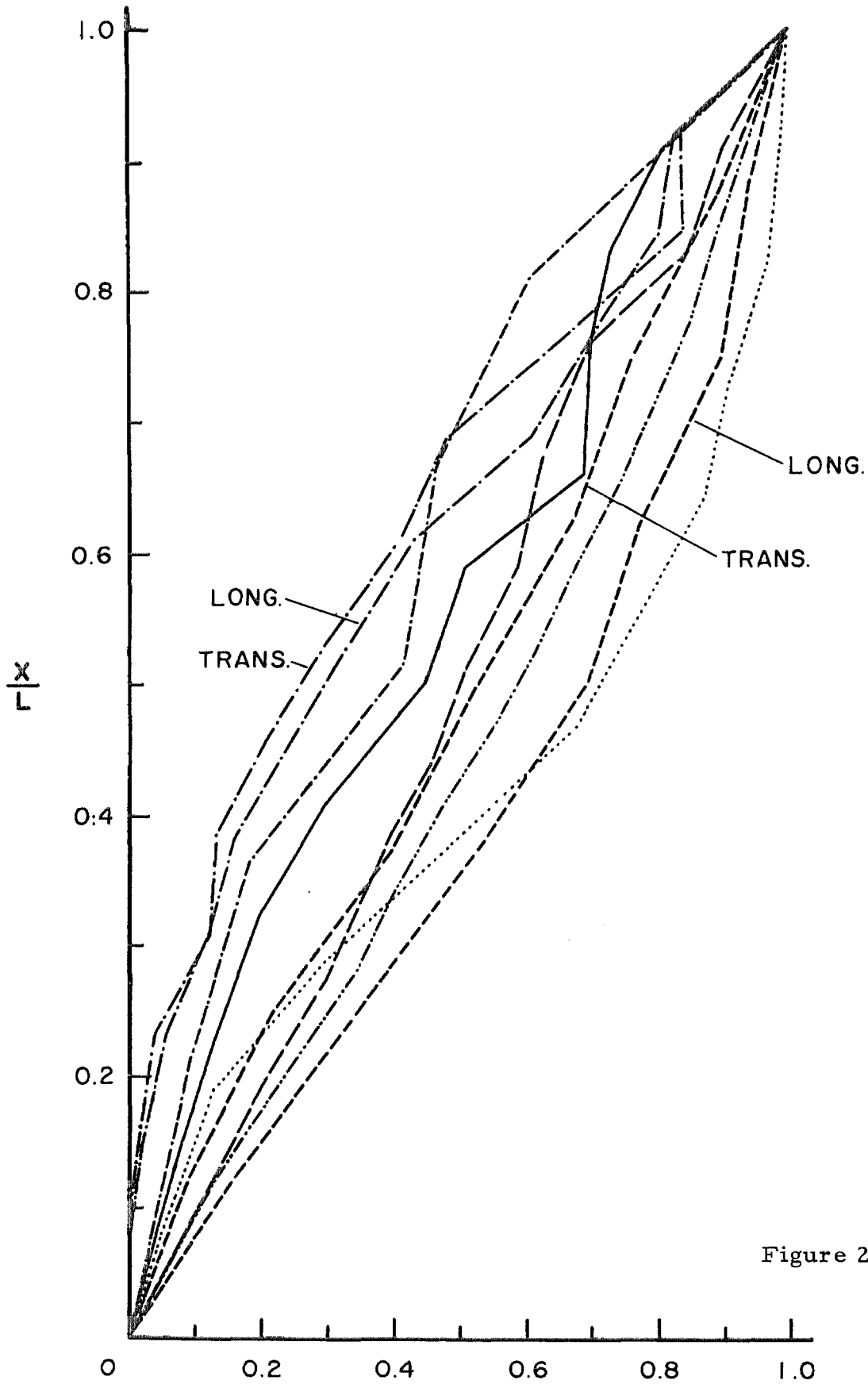


-6-

EARTHQUAKE OF 9 FEB 1971 0600PST

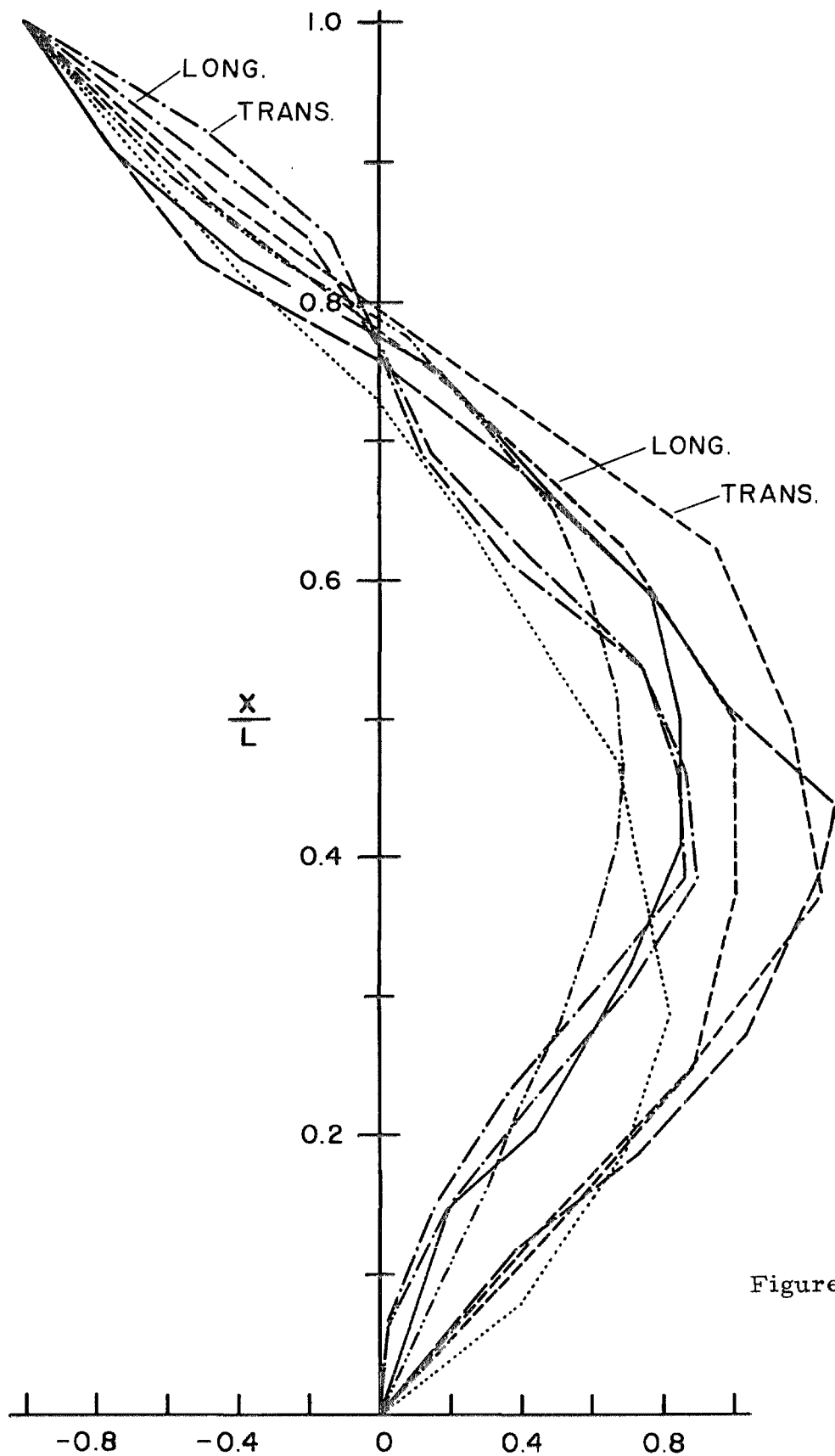
MILLIKAN LIBRARY RESPONSE TO THE SAN FERNANDO EARTHQUAKE

Figure 1



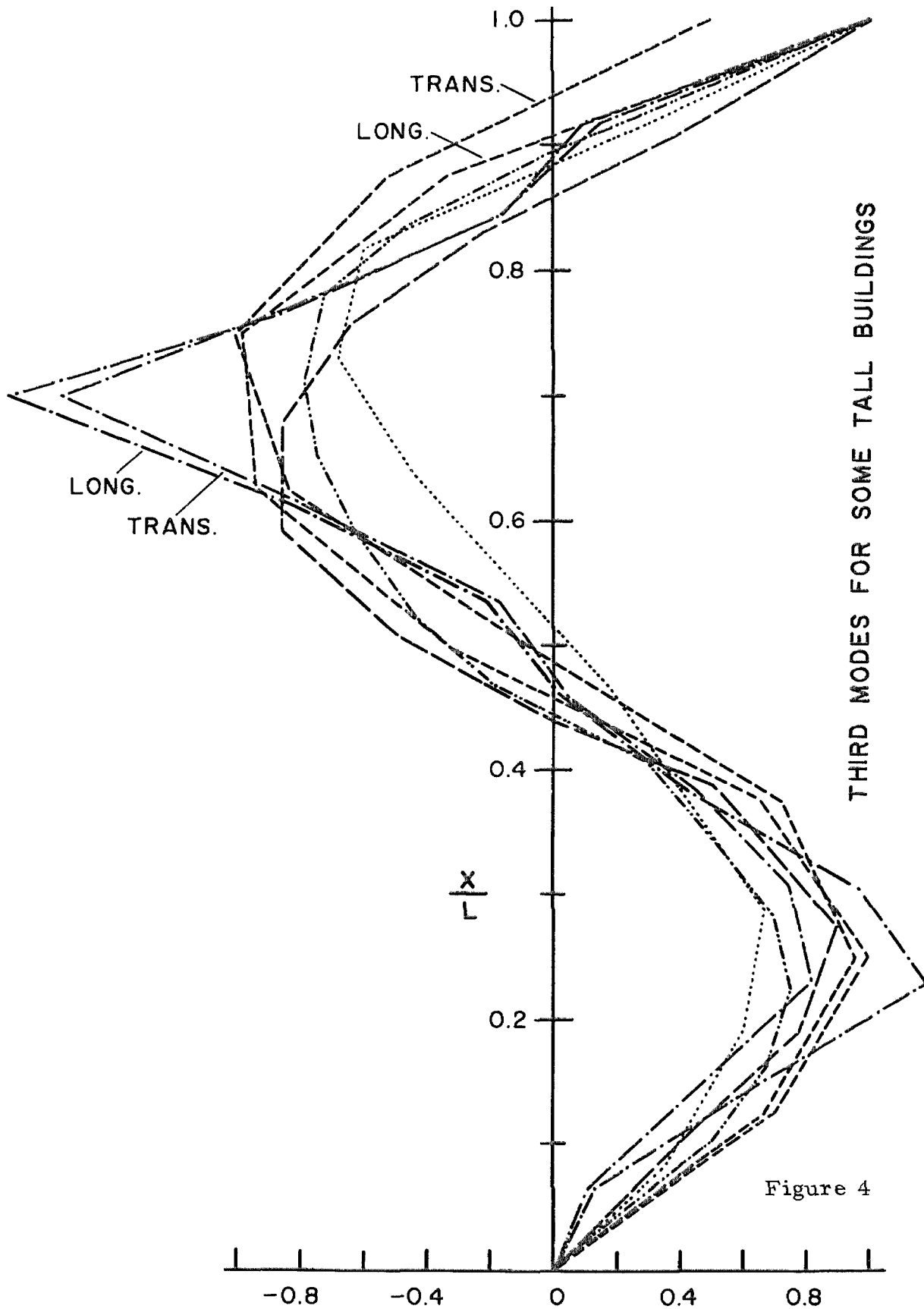
FUNDAMENTAL MODES FOR SOME TALL BUILDINGS

Figure 2



SECOND MODES FOR SOME TALL BUILDINGS

Figure 3



THIRD MODES FOR SOME TALL BUILDINGS

Figure 4

structures⁽³⁴⁾, but this effect is not thought to be of enough general importance to warrant inclusion in the analysis.

Finally, only buildings with perpendicular axes of stiffness are considered. Buildings which are rectilinear in form, as well as those which are circularly symmetric, for example, are included in this category.

The foregoing assumptions lead to a mathematical model which is a three dimensional generalization of the well-known shear beam. Both continuous and discrete forms of the model will be presented below, although for convenience most of the analysis will be done using the continuous version.

A list of symbols to be used is given below and they are defined again where they first appear in the text.

<u>Symbol</u>	<u>Explanation or definition</u>
$A(z)$	area at height z for continuous model
a, b	dimensions, overall dimensions of one-dimensional model are $2a$ by $2b$
$[C_{ij}]$	3×3 viscous damping matrix for finite model
$c_{xij}, c_{yij}, c_{\theta ij}$	dashpot constants in finite model
$F_x(z), F_y(z), F_\theta(z)$	shearing forces in continuous model
$G_{xz}(\hat{x}, \hat{y}, z), G_{yz}(\hat{x}, \hat{y}, z)$	moduli of rigidity in continuous model

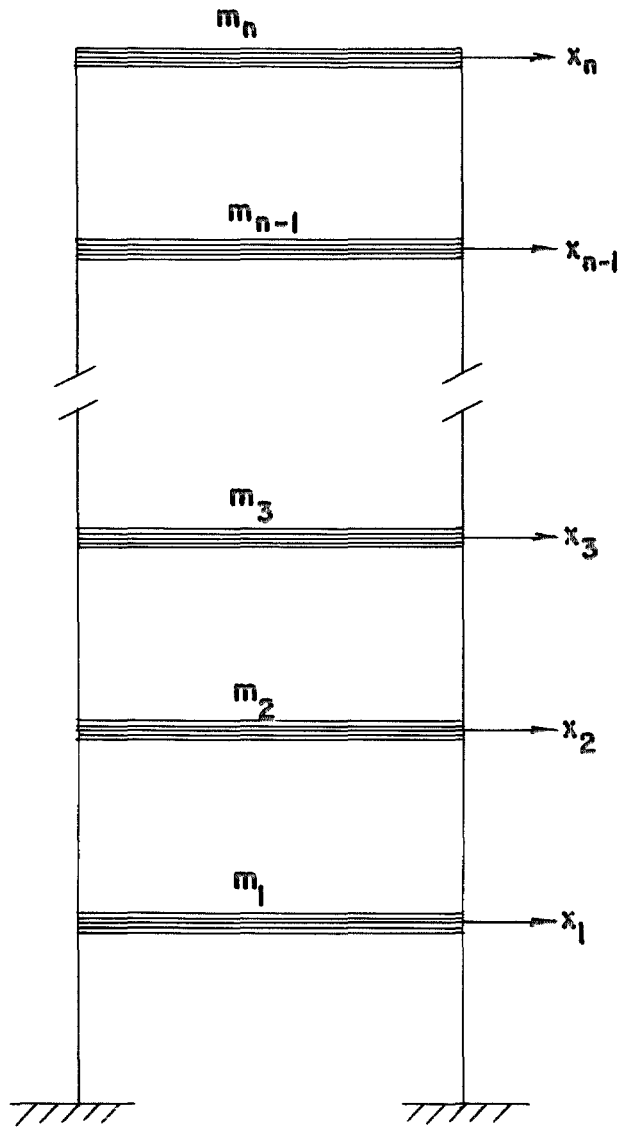
<u>Symbol</u>	<u>Explanation or definition</u>
h	interfloor distance or spacing
i, j	indices
$[K_{ij}]$	3 x 3 stiffness matrix for finite model
$[K(z)]$	3 x 3 stiffness matrix for continuous limit of finite model
$k_{x1}, k_{x2}, k_{x3}, k_{x4}, k_{y1}, k_{y2}, k_{y3}, k_{y4}$	column stiffnesses or spring constants in one-dimensional model
k_x, k_y, k_θ	spring constants in one-dimensional model
$k_{xij}, k_{yij}, k_{\theta ij}$	spring constants in finite model
ℓ	length or height of continuous model
$[M_i]$	3 x 3 mass matrix for finite model
$[M(z)]$	3 x 3 mass matrix for continuous limit of finite model
m_i	mass of i^{th} mass numbered from the base in finite model
$m(z)$	mass per unit length in continuous model
n	number of stories or levels
\bar{r}	polar radius of gyration of complete structure
r_i	radius of gyration of m_i about z axis in finite model

<u>Symbol</u>	<u>Explanation or definition</u>
$r(z)$	radius of gyration of $m(z)$ about z axis in continuous model
T	total kinetic energy of continuous model
t	time
u	relative displacement of a point in x direction in continuous model
V	total strain or potential energy of continuous model
v	relative displacement of a point in y direction in continuous model
\tilde{x}_i	3-vector of relative displacement for finite model
x, y	coordinate axes, relative displacements for one-dimensional model
\bar{x}, \bar{y}	locates center of rigidity for one-dimensional model
x_i, y_i	relative displacements for finite model
\bar{x}_i, \bar{y}_i	locates center of mass for finite model
$\bar{x}_{cij}, \bar{y}_{cij}$	locates center of viscous rigidity for finite model
$\bar{x}_{kij}, \bar{y}_{kij}$	locates center of rigidity for finite model
$x(z), y(z)$	relative displacements for continuous model

<u>Symbol</u>	<u>Explanation or definition</u>
\hat{x}, \hat{y}	coordinates of a point at height z in continuous model
$\bar{x}(z), \bar{y}(z)$	locates center of mass for continuous model
$\bar{x}_f(z), \bar{y}_f(z)$	locates center of rigidity for con- tinuous model
\ddot{z}	3-vector of earthquake acceleration
z	centroidal vertical axis
\ddot{z}_x, \ddot{z}_y	components of earthquake excitation
θ	relative rotation for one-dimensional model
θ_i	relative rotation for finite model
$\theta(z)$	relative rotation for continuous model
$\rho(\hat{x}, \hat{y}, z)$	density function for continuous model

The Finite Model

In tall buildings much of the mass is concentrated in the floor slabs, and therefore the model is taken to be a lumped parameter system with the masses at the floor levels, and with interfloor springs and dashpots. Thus the model of an n story building would have n mass elements as shown in figure 5. Because of the assumptions that only motions in the horizontal plane occur and that the floors are rigid, there are three degrees of freedom per floor, two translational and one rotational, and hence $3n$ degrees of freedom in the model of an n story building.



y and θ motions not shown for clarity

n-STORY BUILDING MODEL

Figure 5

Consider now for simplicity the model of a one-story building with four corner columns and no damping or excitation. The model, shown in figure 6, has asymmetric stiffness. The equations of motion may be written in the form

$$\begin{aligned}
 m\ddot{x} + (k_{x1}+k_{x2})(x-b\theta) + (k_{x3}+k_{x4})(x+b\theta) &= 0, \\
 m\bar{r}^2\ddot{\theta} + b[(k_{x3}+k_{x4})(x+b\theta) - (k_{x1}+k_{x2})(x-b\theta)] + a[(k_{y1}+k_{y4})(y+a\theta) \\
 - (k_{y2}+k_{y3})(y-a\theta)] &= 0 \quad \text{and} \\
 m\ddot{y} + (k_{y1}+k_{y4})(y+a\theta) + (k_{y2}+k_{y3})(y-a\theta) &= 0 \quad (2-1)
 \end{aligned}$$

where x and y are principle axes and \bar{r} is the polar radius of gyration. The center of rigidity is located at \bar{x} and \bar{y} in the x and y directions respectively as defined by the equations

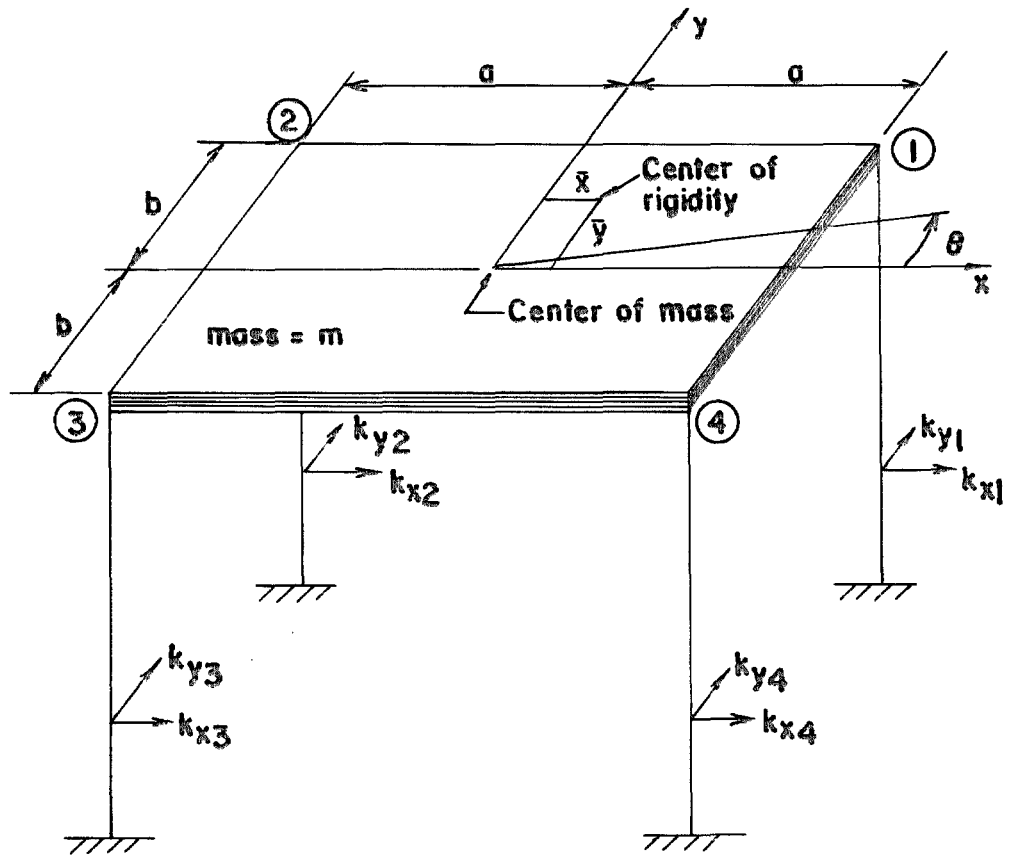
$$(k_{x1}+k_{x2})(b-\bar{y}) = (k_{x3}+k_{x4})(b+\bar{y}) \quad (2-2)$$

and

$$(k_{y1}+k_{y4})(a-\bar{x}) = (k_{y2}+k_{y3})(a+\bar{x}) \quad (2-3)$$

Substituting equations (2-2) and (2-3) into equation (2-1), it can be shown that

$$m \begin{Bmatrix} \ddot{x} \\ \bar{r}\ddot{\theta} \\ \ddot{y} \end{Bmatrix} + \begin{bmatrix} k_x & -\frac{\bar{y}}{\bar{r}}k_x & 0 \\ -\frac{\bar{y}}{\bar{r}}k_x & k_\theta & \frac{\bar{x}}{\bar{r}}k_y \\ 0 & \frac{\bar{x}}{\bar{r}}k_y & k_y \end{bmatrix} \begin{Bmatrix} x \\ \bar{r}\theta \\ y \end{Bmatrix} = \begin{Bmatrix} 0 \\ 0 \\ 0 \end{Bmatrix} \quad (2-4)$$



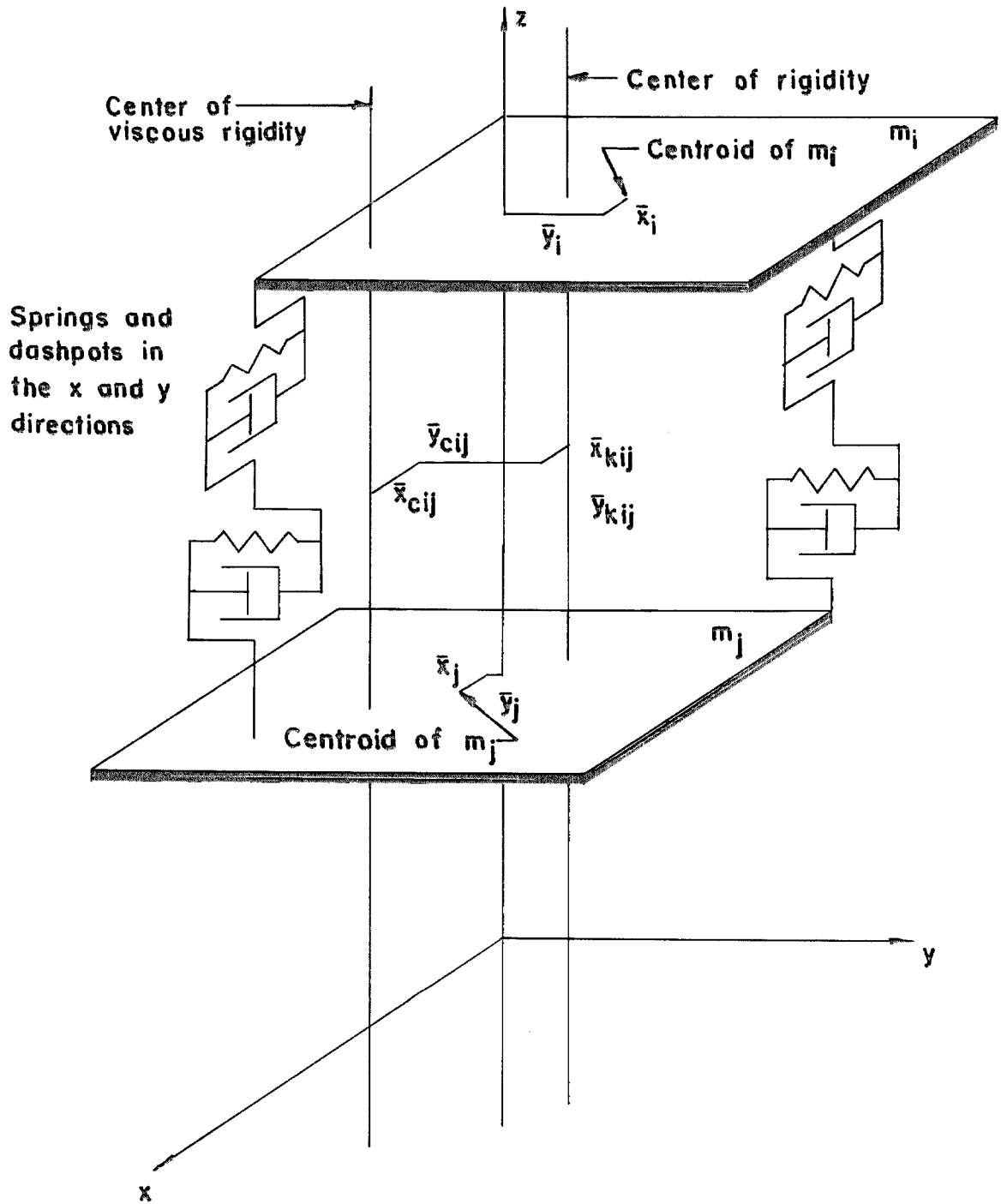
ONE - STORY BUILDING MODEL

Figure 6

where k_x , k_θ and k_y are the total stiffnesses in the x, θ and y directions respectively as defined by

$$\begin{aligned} k_x &= k_{x1} + k_{x2} + k_{x3} + k_{x4} , \\ k_\theta &= \frac{1}{\bar{r}^2} [b^2(k_{x1}+k_{x2}+k_{x3}+k_{x4}) + a^2(k_{y1}+k_{y2}+k_{y3}+k_{y4})] \\ k_y &= k_{y1} + k_{y2} + k_{y3} + k_{y4} . \end{aligned} \quad (2-5)$$

The foregoing model of a one-story building may be extended to the model of a multi-story building in which viscous damping and excitation is included. Consider, for example, the model of one particular floor of an n-story building and its spring and dashpot connection to other floors as shown in figure 7. Although the i^{th} and j^{th} floors may be arbitrarily selected, it is assumed that springs connect only adjacent floors. The vertical z axis locates the centroid of the complete structure and \bar{r} is defined as the radius of gyration of the structure about the z axis. The principle spring and dashpot orientations are x and y. Let \bar{x}_i and \bar{y}_i locate the centroid of the i^{th} floor numbered from the base and having mass m_i , and let r_i be the radius of gyration of m_i about the z axis. The dashpot and spring constants in the x,y and the rotation about the z axis directions are denoted by c_{xij} , c_{yij} , $c_{\theta ij}$, k_{xij} , k_{yij} and $k_{\theta ij}$ respectively. The center of rigidity is located by \bar{x}_{kij} and \bar{y}_{kij} relative to the z axis and \bar{x}_{cij} and \bar{y}_{cij} similarly locate the center of viscous rigidity. Earthquake excitation, assumed to have no rotational components, is described



FLOOR INTERACTION IN FINITE MODEL

Figure 7

by the accelerations $\ddot{z}_x(t)$ and $\ddot{z}_y(t)$ in the x and y directions, respectively. Treating the ground acceleration as an inertial force, let x_i and y_i be the relative displacements of a point fixed on the i^{th} floor and located on the z axis when the system is at rest, and let θ_i be the rotation of the i^{th} floor about the z axis with a rotation from plus x to plus y being positive. The equation of motion then is

$$\begin{bmatrix} [M_1] & 0 \\ & \ddots \\ 0 & [M_n] \end{bmatrix} \begin{Bmatrix} \ddot{x}_1 \\ \ddot{x}_2 \\ \vdots \\ \ddot{x}_n \end{Bmatrix} + \begin{bmatrix} \{ \sum_{j=1}^n [C_{1j}] \} & -[C_{12}] & \dots & -[C_{1n}] \\ & \vdots & & \vdots \\ & & -[C_{n-1,n}] & \\ -[C_{1n}] & \dots & -[C_{n-1,n}] & \{ \sum_{j=1}^n [C_{nj}] \} \end{bmatrix} \begin{Bmatrix} \dot{x}_1 \\ \dot{x}_2 \\ \vdots \\ \dot{x}_n \end{Bmatrix} \\
 + \begin{bmatrix} \{ [K_{01}] + [K_{12}] \} & -[K_{12}] & 0 \\ -[K_{12}] & \{ [K_{12}] + [K_{23}] \} & \\ & & \ddots \\ 0 & & -[K_{n-1,n}] & [K_{n-1,n}] \end{bmatrix} \begin{Bmatrix} \tilde{x}_1 \\ \tilde{x}_2 \\ \vdots \\ \tilde{x}_n \end{Bmatrix} = \begin{bmatrix} [M_1] & 0 \\ & \ddots \\ 0 & [M_n] \end{bmatrix} \begin{Bmatrix} \ddot{z} \\ \vdots \\ \ddot{z} \end{Bmatrix} \quad (2-6)$$

where $[M_i]$, $[C_{ij}]$ and $[K_{ij}]$ are 3 by 3 mass, viscous damping and stiffness matrices given by

$$[M_i] = m_i \begin{bmatrix} 1 & -\bar{y}_i/\bar{r} & 0 \\ -\bar{y}_i/\bar{r} & (r_i/\bar{r})^2 & \bar{x}_i/\bar{r} \\ 0 & \bar{x}_i/\bar{r} & 1 \end{bmatrix}, \quad (2-7)$$

$$[C_{ij}] = \begin{bmatrix} c_{xij} & -\frac{\bar{y}_{cij}}{\bar{r}} c_{xij} & 0 \\ -\frac{\bar{y}_{cij}}{\bar{r}} c_{xij} & c_{\theta ij} & \frac{\bar{x}_{cij}}{\bar{r}} c_{yij} \\ 0 & \frac{\bar{x}_{cij}}{\bar{r}} c_{yij} & c_{yij} \end{bmatrix}, \quad (2-8)$$

and

$$[K_{ij}] = \begin{bmatrix} k_{xij} & -\frac{\bar{y}_{kij}}{\bar{r}} k_{xij} & 0 \\ -\frac{\bar{y}_{kij}}{\bar{r}} k_{xij} & k_{\theta ij} & \frac{\bar{x}_{kij}}{\bar{r}} k_{yij} \\ 0 & \frac{\bar{x}_{kij}}{\bar{r}} k_{yij} & k_{yij} \end{bmatrix}, \quad (2-9)$$

and where the response vector \tilde{x}_i and the excitation vector \tilde{z} are given by

$$\tilde{x}_i = \begin{Bmatrix} x_i \\ \bar{r}\theta_i \\ y_i \end{Bmatrix} \quad (2-10)$$

and

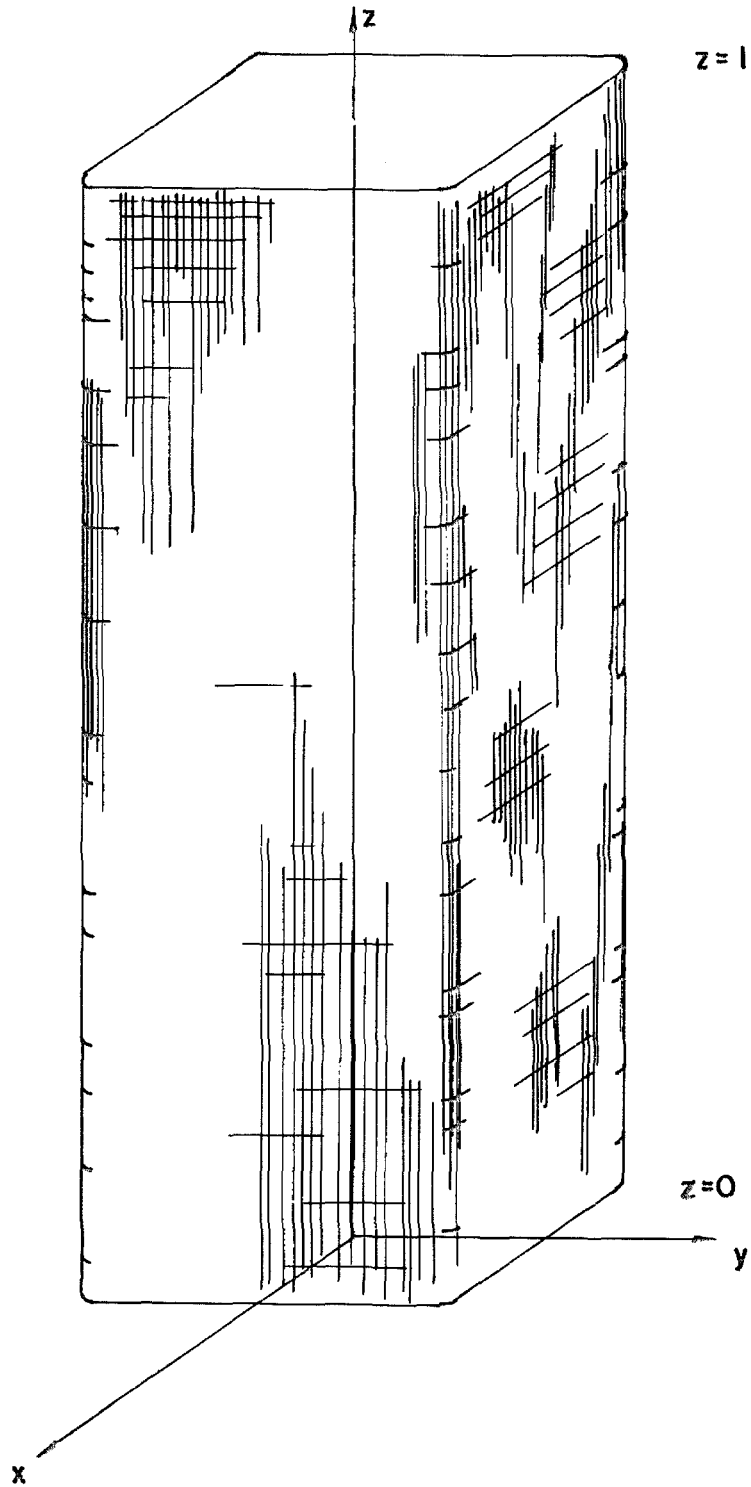
$$\ddot{z} = \begin{Bmatrix} \ddot{z}_x \\ 0 \\ \ddot{z}_y \end{Bmatrix} \quad (2-11)$$

The mass, viscous damping and stiffness matrices in equation (2-6) are symmetric. Furthermore, for all real building like structures the mass and stiffness matrices are positive definite and the viscous damping matrix is non-negative definite. The boundary conditions are obtained by noting that the relative displacements and rotation of the zeroth floor or the base are zero and that the relative displacements and rotation of an imaginary $(n+1)^{st}$ floor are the same as those for the n^{th} floor. Therefore, the boundary conditions are given by

$$\begin{aligned} \tilde{x}_0 &= \tilde{0} & \text{and} \\ \tilde{x}_{n+1} &= \tilde{x}_n \end{aligned} \quad (2-12)$$

Continuous Model

A common dynamic model whose planar vibrations have been studied extensively is the vertical shear beam shown in figure 8. The planar shear beam model, used to approximate the behavior of tall buildings, is herein extended to include x,y and θ motions simultaneously. The z axis is centroidal for this three-dimensional shear beam while the x and y axes are principle directions of stiffness. The moduli of elasticity in the x,y and z directions and the modulus of rigidity in the x-y planes are assumed to be infinite; thus the structure does



CONTINUOUS MODEL

Figure 8

not dilate or distort. The assumptions that there are no vertical motions and that the floors of a building are rigid are satisfied by these conditions. Lagrange's equations are used to derive the equations of motion in the undamped case.

Let $x(z)$ and $y(z)$ describe the motion of a fixed point on an x - y plane and lying on the z -axis when the structure, as shown in figure 9, is at rest. Define $\theta(z)$ as the rotation of the x - y plane about the z axis with a positive rotation being from plus x to plus y . Consider a particle at height z having the coordinates \hat{x} and \hat{y} in the x and y directions, respectively, when the structure is at rest. When the structure is excited the coordinates of the particle are given by $\hat{x} + u$ and $\hat{y} + v$ where u and v are functions of x, y and θ . For small values of θ , based upon the assumption that only small motions are encountered, the relative displacements u and v are approximated by

$$\begin{aligned} u &\approx x - \hat{y}\theta & \text{and} \\ v &\approx y + \hat{x}\theta \end{aligned} \quad (2-13)$$

The total kinetic energy, T , is given by

$$T = \int_0^{\ell} \iint_{A(z)} \frac{1}{2} \rho(\hat{x}, \hat{y}, z) [\dot{u}^2 + \dot{v}^2] d\hat{x}d\hat{y}dz \quad (2-14)$$

where $\rho(\hat{x}, \hat{y}, z)$ is the density function of the model and $A(z)$ is the cross-sectional area at height z . Define the mass per unit length, $m(z)$, by

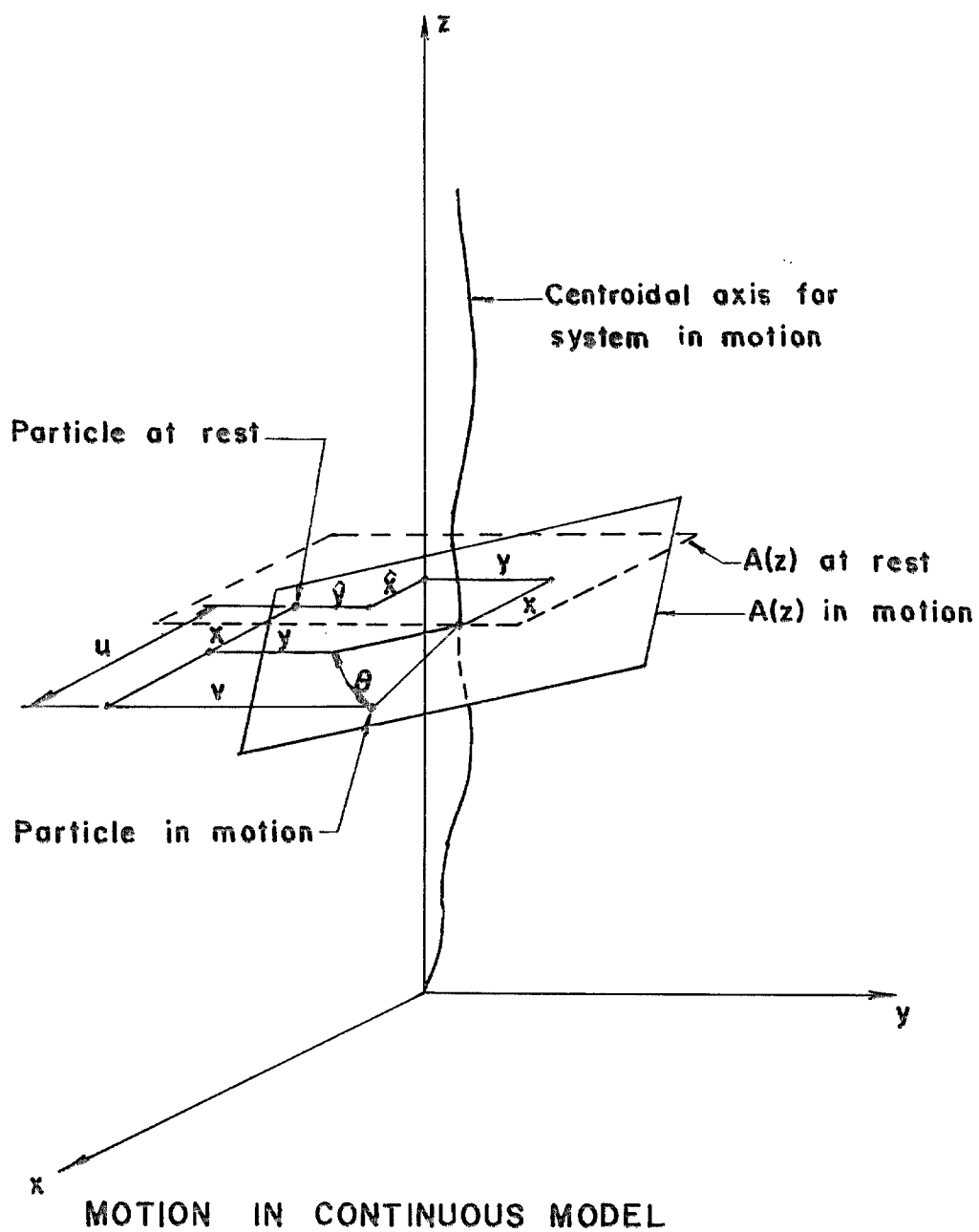


Figure 9

$$m(z) = \iint_{A(z)} \rho(\hat{x}, \hat{y}, z) d\hat{x}d\hat{y} \quad . \quad (2-15)$$

The center of mass of $m(z)$ is located at $\bar{x}(z)$ and $\bar{y}(z)$ in the x and y directions respectively as defined by

$$\bar{x}(z) = \frac{1}{m(z)} \iint_{A(z)} \hat{x}\rho(\hat{x}, \hat{y}, z) d\hat{x}d\hat{y} \quad \text{and} \quad (2-16)$$

$$\bar{y}(z) = \frac{1}{m(z)} \iint_{A(z)} \hat{y}\rho(\hat{x}, \hat{y}, z) d\hat{x}d\hat{y} \quad ; \quad (2-17)$$

while the radius of gyration, $r(z)$ of the mass $m(z)$ about the z axis, which does not, in general, coincide with the centroid of $m(z)$, is given by

$$r^2(z) = \frac{1}{m(z)} \iint_{A(z)} (\hat{x}^2 + \hat{y}^2)\rho(\hat{x}, \hat{y}, z) d\hat{x}d\hat{y} \quad . \quad (2-18)$$

Let \bar{r} be defined as the radius of gyration of the complete structure, about the z or centroidal axis, then

$$\bar{r}^2 = \frac{\int_0^{\ell} m(z) r^2(z) dz}{\int_0^{\ell} m(z) dz} \quad . \quad (2-19)$$

Equations (2-13) and (2-15) through (2-19) may be substituted into equation (2-14) to obtain

$$T = \frac{1}{2} \int_0^{\ell} m(z) \{ \dot{\bar{x}}^2(z) + \dot{\bar{y}}^2(z) - 2\dot{\bar{x}}(z) \frac{\bar{y}(z)}{\bar{r}} \bar{r}\dot{\theta}(z) + 2\dot{\bar{y}}(z) \frac{\bar{x}(z)}{\bar{r}} \bar{r}\dot{\theta}(z) + \left[\frac{r(z)}{\bar{r}} \right]^2 [\bar{r}\dot{\theta}(z)]^2 \} dz \quad . \quad (2-20)$$

Differentiating equation (2-20) with respect to the relative coordinate velocities at height z and then with respect to time gives

$$\begin{aligned} \frac{d}{dt} \frac{\partial T}{\partial \dot{\bar{x}}} \Big|_z &= m(z) dz \left\{ \ddot{x}(z) - \frac{\bar{y}(z)}{\bar{r}} \bar{r} \ddot{\theta}(z) \right\} \\ \frac{d}{dt} \frac{\partial T}{\partial \dot{\bar{r}\theta}} \Big|_z &= m(z) dz \left\{ -\frac{\bar{y}(z)}{\bar{r}} \ddot{x}(z) + \left[\frac{r(z)}{\bar{r}} \right]^2 \bar{r} \ddot{\theta}(z) + \frac{\bar{x}(z)}{\bar{r}} \ddot{y}(z) \right\} \\ \frac{d}{dt} \frac{\partial T}{\partial \dot{\bar{y}}} \Big|_z &= m(z) dz \left\{ \frac{\bar{x}(z)}{\bar{r}} \bar{r} \ddot{\theta}(z) + \ddot{y}(z) \right\} . \end{aligned} \quad (2-21)$$

Equation (2-21) has the required kinetic energy terms for Lagrange's equations.

The total strain energy, V , of the structure is given by

$$V = \int_0^l \iint_{A(z)} \frac{1}{2} \left\{ G_{xz}(\hat{x}, \hat{y}, z) \left[\frac{\partial u}{\partial z} \right]^2 + G_{yz}(\hat{x}, \hat{y}, z) \left[\frac{\partial v}{\partial z} \right]^2 \right\} d\hat{x} d\hat{y} dz \quad (2-22)$$

where $G_{xz}(\hat{x}, \hat{y}, z)$ and $G_{yz}(\hat{x}, \hat{y}, z)$ are the moduli of rigidity in the x - z and y - z planes respectively. The forces required to produce unit shearing displacements in the x and y directions are $F_x(z)$ and $F_y(z)$ respectively as defined by

$$F_x(z) = \iint_{A(z)} G_{xz}(\hat{x}, \hat{y}, z) d\hat{x} d\hat{y} \quad \text{and} \quad (2-23)$$

$$F_y(z) = \iint_{A(z)} G_{yz}(\hat{x}, \hat{y}, z) d\hat{x} d\hat{y} \quad . \quad (2-24)$$

The center of rigidity is located by $\bar{x}_f(z)$ and $\bar{y}_f(z)$ as defined by

$$\bar{x}_f(z) = \frac{1}{F_y(z)} \iint_{A(z)} \hat{x} G_{yz}(\hat{x}, \hat{y}, z) d\hat{x}d\hat{y} \quad \text{and} \quad (2-25)$$

$$\bar{y}_f(z) = \frac{1}{F_x(z)} \iint_{A(z)} \hat{y} G_{xz}(\hat{x}, \hat{y}, z) d\hat{x}d\hat{y} . \quad (2-26)$$

The torque about the z axis required to produce a rotation corresponding to a unit shearing displacement at a distance \bar{r} from the z axis is given by $\bar{r}F_\theta(z)$ where

$$\bar{r}F_\theta(z) = \frac{1}{\bar{r}} \iint_{A(z)} [\hat{x}^2 G_{yz}(\hat{x}, \hat{y}, z) + \hat{y}^2 G_{xz}(\hat{x}, \hat{y}, z)] d\hat{x}d\hat{y} . \quad (2-27)$$

From equations (2-13) and (2-23) through (2-27) it is readily seen that equation (2-22) may be cast in the form

$$V = \frac{1}{2} \int_0^l \left\{ F_x(z) x'^2 - \frac{2\bar{y}_f(z)}{\bar{r}} F_x(z) x' \bar{r}\theta' + F_\theta(z) (\bar{r}\theta')^2 + \frac{2\bar{x}_f(z)}{\bar{r}} F_y(z) y' \bar{r}\theta' + F_y(z) y'^2 \right\} dz . \quad (2-28)$$

The boundary conditions for this particular problem are

$$\begin{Bmatrix} x(0) \\ \bar{r}\theta(0) \\ y(0) \end{Bmatrix} = \begin{Bmatrix} 0 \\ 0 \\ 0 \end{Bmatrix} \quad \text{and} \quad (2-29)$$

$$\begin{Bmatrix} x'(l) \\ \bar{r}\theta'(l) \\ y'(l) \end{Bmatrix} = \begin{Bmatrix} 0 \\ 0 \\ 0 \end{Bmatrix} , \quad (2-30)$$

for the base can have no relative displacements or rotation, and the top of the structure, being a free end, must have vanishing first derivatives for the displacements and rotation. The variational equation for δV may be integrated by parts and, utilizing the boundary conditions, it follows that the required potential energy terms for Lagrange's equations are

$$\begin{aligned} \frac{\partial V}{\partial x} \Big|_z &= - \left\{ [F_x(z)x']' - \left[\frac{\bar{y}_f(z)}{\bar{r}} F_x(z)\bar{r}\theta' \right]' \right\} dz \quad , \\ \frac{\partial V}{\partial \bar{r}\theta} \Big|_z &= - \left\{ - \left[\frac{\bar{y}_f(z)}{\bar{r}} F_x(z)x' \right]' + [F_\theta(z)\bar{r}\theta']' + \left[\frac{\bar{x}_f(z)}{\bar{r}} F_y(z)y' \right]' \right\} dz \text{ and} \\ \frac{\partial V}{\partial y} \Big|_z &= - \left\{ \left[\frac{\bar{x}_f(z)}{\bar{r}} F_y(z)\bar{r}\theta' \right]' + [F_y(z)y']' \right\} dz \quad . \end{aligned} \quad (2-31)$$

The ground acceleration for an earthquake is again interpreted as an inertial force without rotational components. Therefore, applying Lagrange's equations with generalized forces, the undamped equations of motion are seen to be

$$\begin{aligned}
 & m(z) \begin{bmatrix} 1 & -\frac{\bar{y}(z)}{\bar{r}} & 0 \\ -\frac{\bar{y}(z)}{\bar{r}} & \left[\frac{\bar{r}(z)}{\bar{r}}\right]^2 & \frac{\bar{x}(z)}{\bar{r}} \\ 0 & \frac{\bar{x}(z)}{\bar{r}} & 1 \end{bmatrix} \begin{Bmatrix} \ddot{x}(z) \\ \bar{r}\ddot{\theta}(z) \\ \ddot{y}(z) \end{Bmatrix} \\
 & - \left\{ \begin{bmatrix} F_x(z) & -\frac{\bar{y}_f(z)}{\bar{r}}F_x(z) & 0 \\ -\frac{\bar{y}_f(z)}{\bar{r}}F_x(z) & F_\theta(z) & \frac{\bar{x}_f(z)}{\bar{r}}F_y(z) \\ 0 & \frac{\bar{x}_f(z)}{\bar{r}}F_y(z) & F_y(z) \end{bmatrix} \begin{Bmatrix} x'(z) \\ \bar{r}\theta'(z) \\ y'(z) \end{Bmatrix} \right\}' \\
 & = -m(z) \begin{bmatrix} 1 & -\frac{\bar{y}(z)}{\bar{r}} & 0 \\ -\frac{\bar{y}(z)}{\bar{r}} & \left[\frac{\bar{r}(z)}{\bar{r}}\right]^2 & \frac{\bar{x}(z)}{\bar{r}} \\ 0 & \frac{\bar{x}(z)}{\bar{r}} & 1 \end{bmatrix} \begin{Bmatrix} \ddot{z}_x(t) \\ 0 \\ \ddot{z}_y(t) \end{Bmatrix}. \tag{2-32}
 \end{aligned}$$

The Continuous Limit of the Finite Model

In much of the work which follows, the continuous equations of motion will be preferred over the more standard finite equations of motion because of their simplicity. It is desirable therefore to know how the finite equations approach the continuous equations as n increases or as the interfloor spacing decreases. In the undamped case, with springs between adjacent floors only, equation (2-6) may be

written in the form

$$[M_i] \ddot{\tilde{x}}_i - [K_{i-1,i}] \tilde{x}_{i-1} + [K_{i-1,i} + K_{i,i+1}] \tilde{x}_i - [K_{i,i+1}] \tilde{x}_{i+1} = -[M_i] \ddot{\tilde{z}}(t)$$

for $i = 1, 2, \dots, n$ (2-33)

subject to the boundary conditions given by equation (2-12). Let the i^{th} floor be at a height z above the base and let the interfloor spacing be a small distance h . Taylor series representations of $[M_i]$, \tilde{x}_{i-1} , \tilde{x}_i , \tilde{x}_{i+1} , $[K_{i-1,i}]$ and $[K_{i,i+1}]$ based upon the smallness of h relative to the appropriate derivatives are approximated by

$$[M_i] = [M(z)],$$

$$\tilde{x}_{i-1} = \tilde{x}(z-h) \approx \tilde{x}(z) - h\tilde{x}'(z) + \frac{h^2}{2} \tilde{x}''(z),$$

$$\tilde{x}_i = x(z), \tag{2-34}$$

$$\tilde{x}_{i+1} = \tilde{x}(z+h) \approx \tilde{x}(z) + h\tilde{x}'(z) + \frac{h^2}{2} \tilde{x}''(z),$$

$$[K_{i-1,i}] = [K(z - h/2)] \approx [K(z)] - \frac{h}{2}[K'(z)] + \frac{h^2}{8}[K''(z)] \text{ and}$$

$$[K_{i,i+1}] = [K(z + h/2)] \approx [K(z)] + \frac{h}{2}[K'(z)] + \frac{h^2}{8}[K''(z)].$$

Substitution of equation (2-34) into equation (2-33) results in a cancellation of zeroth and first order terms in h involving $[K(z)]$ and its derivatives. Thus keeping only the second order terms, equation (2-33) is approximated by

$$[M(z)] \ddot{\tilde{x}}(z) - h^2 \{ [K(z)] \tilde{x}'(z) \}' = -[M(z)] \ddot{\tilde{z}}(t). \tag{2-35}$$

Dividing equation (2-35) by h yields equation (2-32) for

$$\frac{1}{h}[M(z)] = m(z) \begin{bmatrix} 1 & -\frac{\bar{y}(z)}{\bar{r}} & 0 \\ -\frac{\bar{y}(z)}{\bar{r}} & \left[\frac{\bar{r}(z)}{\bar{r}}\right]^2 & \frac{\bar{x}(z)}{\bar{r}} \\ 0 & \frac{\bar{x}(z)}{\bar{r}} & 1 \end{bmatrix} \quad \text{and} \quad (2-36)$$

$$h[K(z)] = \begin{bmatrix} F_x(z) & -\frac{\bar{y}_f(z)}{\bar{r}}F_x(z) & 0 \\ -\frac{\bar{y}_f(z)}{\bar{r}}F_x(z) & F_\theta(z) & \frac{\bar{x}_f(z)}{\bar{r}}F_y(z) \\ 0 & \frac{\bar{x}_f(z)}{\bar{r}}F_y(z) & F_y(z) \end{bmatrix}. \quad (2-37)$$

The boundary conditions for the finite model, given by equation (2-12), are easily seen to be equivalent to the boundary conditions for the continuous model given by equations (2-29) and (2-30). It can be shown, using a more complete form of Taylor series, that the error introduced by using equation (2-35) as an approximation of equation (2-33) is of $O(h^4)$. Hence the equations of motion for the finite model may be approximated by the equations of motion for the continuous model as long as the building has a sufficient number of stories, and as long as the higher modes of the finite structure are not considered. Equation (2-35) is not valid if the higher order derivatives are too large, a condition which occurs in the finite model during vibration in the higher modes. This limitation is a consequence of the fact that the finite model has exactly $3n$ modes while the continuous model has an infinite number of modes.

III. DYNAMIC PROPERTIES OF TALL BUILDINGS

Introduction

The purpose of this chapter is to discuss the dynamic properties of the continuous model developed in chapter II with viscous damping included. Assuming classical normal modes exist, the free vibration response, as a function of height and time, can be uncoupled and subsequent attention is focused on the response as a function of height only, i.e., on the mode shapes. These mode shapes, in general, have three components of motion, two translational and one rotational. Although most attention in the literature has been focused on cases for which two of the components of motion in any particular mode shape vanish, herein the modes are not confined to one or two components of motion and are not restricted to specific examples. Instead a broad class of structural models is defined which includes many cases of practical interest and the dynamic properties of this class of structures are studied in detail.

A particularly interesting and mathematically simple case arises when the relative values of the three components of each mode shape are constant with height. As shown below there exists in this case a 3×3 , constant, orthogonal matrix of modal components with eigenvectors which specify the relative values of the three components of motion in three related mode shapes. As will be seen there are several types of buildings which lead to mode shapes of this type. For this general class of structures it is found explicitly how the

mode shapes are affected by the eccentricity of the center of rigidity relative to the center of mass, and by the closeness of the natural frequencies. It is shown that the presence of pure or nearly pure mode shapes (those for which one component of motion is dominant) requires not only small eccentricities, as might be expected, but also well separated natural frequencies. Finally, exact and approximate methods of determining the matrix of modal components are presented.

An explanation of the symbols used in this chapter is given below and they are defined again where they first appear in the text. Wherever possible the symbols of the previous chapter are used.

<u>Symbol</u>	<u>Explanation or definition</u>
A_i	a constant
a, b	constants defined by equation (3-33)
C_k	normalization constant
$\{\tilde{e}_k\}$	unit vector defined by equation (3-20)
$[F(z)]$	shearing force matrix
$[F_\lambda(z)]$	diagonal shearing force matrix similar to $[F(z)]$
$F_k(z)$	elements of $[F_\lambda(z)]$
F_m	one-third the trace of $[F_\lambda(z)]$
f	a particular damping function
G_k	a constant defined by equation (3-35)
i, j, k, s, p	indices

<u>Symbol</u>	<u>Explanation or definition</u>
[I]	identity matrix
p,q	difference between diagonals of [F (z)] and F_m
$\{\tilde{x}(z,t)\}$	response vector
$\{\ddot{z}(z,t)\}$	excitation vector
z_1, z_2	arbitrary values of z.
α, β	off-diagonal elements of $[F_\lambda(z)]$ as defined by equation (3-32)
$\eta(t)$	response as a function of time
$\bar{\theta}$	angle defined by equation (3-49)
$\rho_{ik}(z)$	scaler mode shape function defined by equation (3-19)
$[\phi(z)]$	orthogonal matrix which diagonalizes [F(z)]
$[\phi]$	constant $[\phi(z)]$, also matrix of modal components
$[\phi]_\Lambda$	approximate matrix of modal components defined by equation (3-47)
ϕ_k	k^{th} column of $[\phi]$
Ω	an angle defined by equation (3-34)
ω	frequency
ω_{ik}	natural frequency defined by equation (3-24)
$\{\psi(z)\}, \{\psi_{ik}(z)\}$	mode shapes

The Equation of Motion with Damping

Damping has heretofore been excluded from the continuous model for convenience in the application of Lagrange's equations. Viscous damping was included, however, in the finite model and the damping matrix utilized was somewhat general as neither relative nor absolute damping nor a combination of the two are able to account satisfactorily for the observed damping values in tall buildings. Damping values for the modes of buildings have been found to be nearly the same, independent of modal frequency. Most observed values are in the range of 2-5% of critical depending on the amplitude of response.^(2,33,34,36) Therefore a damping function is introduced into the equations of motion for the continuous model, such that classical normal modes with constant damping exist.

The floors of most tall buildings have the same geometry and their centroids lie on the same vertical line. Also the polar radii of gyration of the floor masses are equal. Adopting these conditions, the mass matrix for the continuous model reduces to a scalar multiple of the identity matrix. Introducing damping and this assumption into the equations of motion for the continuous model gives

$$\begin{aligned}
 & m(z) \begin{Bmatrix} \ddot{x} \\ \overline{r}\ddot{\theta} \\ \ddot{y} \end{Bmatrix} (z,t) + f \left(\begin{Bmatrix} \dot{x} \\ \overline{r}\dot{\theta} \\ \dot{y} \end{Bmatrix} (z,t) \right) \\
 & - \left\{ \begin{bmatrix} F_x(z) & -\frac{\overline{y}_f(z)}{\overline{r}}F_x(z) & 0 \\ -\frac{\overline{y}_f(z)}{\overline{r}}F_x(z) & F_\theta(z) & \frac{\overline{x}_f(z)}{\overline{r}}F_y(z) \\ 0 & \frac{\overline{x}_f(z)}{\overline{r}}F_y(z) & F_y(z) \end{bmatrix} \begin{Bmatrix} x' \\ \overline{r}\theta' \\ y' \end{Bmatrix} (z,t) \right\}' \\
 & = -m(z) \begin{Bmatrix} \ddot{z}_x \\ 0 \\ \ddot{z}_y \end{Bmatrix} (t) \tag{3-1}
 \end{aligned}$$

where f is a matrix function chosen to produce classical normal modes. This equation can be written in the more compact form

$$m(z)\{\ddot{\tilde{x}}(z,t)\} + f(\{\ddot{\tilde{x}}(z,t)\}) - \{[F(z)]\{\tilde{x}'(z,t)\}\}' = -m(z)\{\ddot{\tilde{z}}(t)\} \tag{3-2}$$

where the displacement vector, excitation vector and stiffness matrix are defined by

$$\{\tilde{x}(z,t)\} = \begin{Bmatrix} x \\ \overline{r}\theta \\ y \end{Bmatrix} (z,t) , \tag{3-3}$$

$$\{\ddot{\mathbf{z}}(t)\} = \begin{Bmatrix} \ddot{z}_x \\ 0 \\ \ddot{z}_y \end{Bmatrix} (t) \quad (3-4)$$

, and

$$[F(z)] = \begin{bmatrix} F_x(z) & -\frac{\bar{y}_f(z)}{r}F_x(z) & 0 \\ -\frac{\bar{y}_f(z)}{r}F_x(z) & F_\theta(z) & \frac{\bar{x}_f(z)}{r}F_y(z) \\ 0 & \frac{\bar{x}_f(z)}{r}F_y(z) & F_y(z) \end{bmatrix} \quad (3-5)$$

respectively.

Equation (3-1), or (3-2), is sufficiently general to describe the linear elastic response of many tall buildings to earthquakes, yet is restrictive enough to permit a useful discussion of its solutions. Throughout the remainder of this chapter, the solutions to this particular equation are examined, and the dynamic properties of the buildings it models are extracted.

Some Properties of the Mode Shapes

The modal solutions of equation (3-2), that is, the mode shapes, are unaltered by the excitation and the damping, hence both may be neglected in an examination of the mode shapes and their inter-relationships. Let $\{\tilde{\mathbf{x}}(z,t)\}$ be one of the modal solutions of the equation

$$m(z)\{\ddot{\tilde{\mathbf{x}}}(z,t)\} - \{[F(z)]\{\tilde{\mathbf{x}}'(z,t)\}\}' = \{\tilde{\mathbf{0}}\} \quad (3-6)$$

with the substitution

$$\{\tilde{x}(z,t)\} = \eta(t)\{\tilde{\psi}(z)\} . \quad (3-7)$$

Employment of the separation of variables technique results in the equations

$$\ddot{\eta}(t) + \omega^2\eta(t) = 0, \quad \text{and} \quad (3-8)$$

$$\{[F(z)]\{\tilde{\psi}'(z)\}\}' + m(z)\omega^2\{\tilde{\psi}(z)\} = \{\tilde{0}\} . \quad (3-9)$$

The boundary conditions for this problem are

$$\{\tilde{x}(0)\} = \{\tilde{x}'(\ell)\} = \{\tilde{0}\} . \quad (3-10)$$

Equation (3-8) implies that the time functions for free vibrations are sinusoidal as long as the frequencies ω are real, and equation (3-9) with (3-10) is a three-dimensional form of an ordinary self-adjoint, differential equation. Sturm-Liouville theory, as applied to one-dimensional, self-adjoint, ordinary differential equations subject to appropriate boundary conditions^(37,38) may also be applied to the three-dimensional equation in (3-9). Using a double subscript for reasons which will be clear later, let ω_{ik}^2 and ω_{js}^2 be two different eigenvalues of equation (3-9) with corresponding non-trivial mode shapes or eigenvectors $\{\tilde{\psi}_{ik}(z)\}$ and $\{\tilde{\psi}_{js}(z)\}$, then

$$\begin{aligned} \{[F(z)]\{\tilde{\psi}'_{ik}(z)\}\}' + m(z)\omega_{ik}^2\{\tilde{\psi}_{ik}(z)\} &= \{\tilde{0}\} \quad \text{and} \\ \{[F(z)]\{\tilde{\psi}'_{js}(z)\}\}' + m(z)\omega_{js}^2\{\tilde{\psi}_{js}(z)\} &= \{\tilde{0}\} . \end{aligned} \quad (3-11)$$

Subtract the transpose of $\{\tilde{\psi}_{ik}(z)\}$, $\{\tilde{\psi}_{ik}(z)\}^T$, times the second equation from $\{\tilde{\psi}_{js}(z)\}^T$ times the first equation and integrate by parts to obtain

$$\begin{aligned} & [\{\tilde{\psi}_{js}(z)\}^T [F(z)] \{\tilde{\psi}'_{ik}(z)\}]_0^\ell - \int_0^\ell \{\tilde{\psi}'_{js}(z)\}^T [F(z)] \{\tilde{\psi}'_{ik}(z)\} dz \\ & - [\{\tilde{\psi}_{ik}(z)\}^T [F(z)] \{\tilde{\psi}'_{js}(z)\}]_0^\ell + \int_0^\ell \{\tilde{\psi}'_{ik}(z)\}^T [F(z)] \{\tilde{\psi}'_{js}(z)\} dz \\ & + \omega_{ik}^2 \int_0^\ell m(z) \{\tilde{\psi}_{js}(z)\}^T \{\tilde{\psi}_{ik}(z)\} dz - \omega_{js}^2 \int_0^\ell m(z) \{\tilde{\psi}_{ik}(z)\}^T \{\tilde{\psi}_{js}(z)\} dz = 0 . \end{aligned} \quad (3-12)$$

Because of the fact that $[F(z)]$ is symmetric, it follows that

$$\begin{aligned} \{\tilde{\psi}'_{js}(z)\}^T [F(z)] \{\tilde{\psi}'_{ik}(z)\} &= \{\{\tilde{\psi}'_{js}(z)\}^T [F(z)] \{\tilde{\psi}'_{ik}(z)\}\}^T \\ &= \{\tilde{\psi}'_{ik}(z)\}^T [F(z)] \{\tilde{\psi}'_{js}(z)\} \end{aligned} \quad (3-13)$$

as well as

$$\{\tilde{\psi}_{js}(z)\}^T \{\tilde{\psi}_{ik}(z)\} = \{\{\tilde{\psi}_{js}(z)\}^T \{\tilde{\psi}_{ik}(z)\}\}^T = \{\tilde{\psi}_{ik}(z)\}^T \{\tilde{\psi}_{js}(z)\}. \quad (3-14)$$

Equations (3-13) and (3-14) may be substituted into equation (3-12), and since $\{\tilde{\psi}_{ik}(z)\}$ and $\{\tilde{\psi}_{js}(z)\}$ or their first derivatives vanish at both ends, it may be concluded that

$$(\omega_{ik}^2 - \omega_{js}^2) \int_0^\ell m(z) \{\tilde{\psi}_{js}(z)\}^T \{\tilde{\psi}_{ik}(z)\} dz = 0 . \quad (3-15)$$

Since it has been postulated that ω_{ik}^2 and ω_{js}^2 are different,

it follows that

$$\int_0^{\ell} m(z) \{\tilde{\psi}_{js}(z)\}^T \{\tilde{\psi}_{ik}(z)\} dz = 0 . \quad (3-16)$$

Therefore, the mode shapes corresponding to different eigenvalues are orthogonal with respect to the weighting function $m(z)$.

Analogously, the first equation in (3-11) may be multiplied by $\{\tilde{\psi}_{ik}(z)\}^T$ and integrated by parts to obtain

$$\omega_{ik}^2 = \frac{\int_0^{\ell} \{\tilde{\psi}'_{ik}(z)\}^T [F(z)] \{\tilde{\psi}'_{ik}(z)\} dz}{\int_0^{\ell} m(z) \{\tilde{\psi}_{ik}(z)\}^T \{\tilde{\psi}_{ik}(z)\} dz} . \quad (3-17)$$

Since the matrix $[F(z)]$ is positive definite, $m(z)$ is positive and the mode shapes are non-trivial, both the numerator and the denominator of the right hand side of equation (3-17) and hence the eigenvalues ω_{ik}^2 are positive. This means, of course, that all frequencies are real and positive.

The Matrix of Mode Shapes

The stiffness matrix is symmetric and positive definite, and hence there exists an orthogonal matrix $[\phi(z)]$ and a positive definite diagonal matrix $[F_{\lambda}(z)]$ such that

$$[F(z)] = [\phi(z)] [F_{\lambda}(z)] [\phi(z)]^T . \quad (3-18)$$

An interesting and useful subcase results when $[\phi(z)]$ is given by a constant $[\phi]$. In this case only, (Appendix I), $[\phi]$ is

also a matrix of modal components, and the mode shapes may be expressed in the form

$$\{\tilde{\psi}_{ik}(z)\} = \rho_{ik}(z)[\phi]\{\tilde{e}_k\} = \rho_{ik}(z)\phi_k \quad \text{for } k = 1,2,3 \quad (3-19)$$

where

$$\{\tilde{e}_1\} = \begin{Bmatrix} 1 \\ 0 \\ 0 \end{Bmatrix} ; \quad \{\tilde{e}_2\} = \begin{Bmatrix} 0 \\ 1 \\ 0 \end{Bmatrix} ; \quad \{\tilde{e}_3\} = \begin{Bmatrix} 0 \\ 0 \\ 1 \end{Bmatrix} \quad (3-20)$$

and ϕ_k is the k^{th} column of $[\phi]$. It is here that the usefulness of double subscript on $\{\tilde{\psi}(z)\}$ and ω is realized.

With $[\phi]$ constant the modal components, the relative values of $x(z)$, $\bar{r}\theta(z)$ and $y(z)$ for all z in a particular mode, are given by the components of the column vectors of $[\phi]$. Thus as i varies, there are three types of modes corresponding to the three values of k . The modal components of each type are orthogonal to the modal components of the other two types, and hence an orthogonality condition on mode shapes of different types evaluated at arbitrary levels exists.

$$\{\tilde{\psi}_{jp}(z_1)\}^T \{\tilde{\psi}_{ik}(z_2)\} = 0 \quad \text{if } k \neq p \text{ for all } i,j \text{ and } 0 \leq z_1, z_2 \leq \ell . \quad (3-21)$$

However, from (3-19) mode shapes of the same type differ only by a scalar function of z as the equation

$$\rho_{ik}(z)\{\tilde{\psi}_{jk}(z)\} = \rho_{jk}(z)\{\tilde{\psi}_{ik}(z)\} \quad (3-22)$$

holds. In this case the product, $\{\tilde{\psi}_{jk}(z)\}^T \{\tilde{\psi}_{ik}(z)\}$, as defined by

equation (3-19), may be multiplied by $m(z)$ and integrated to obtain the one-dimensional orthogonality condition

$$\int_0^{\ell} m(z) \rho_{jk}(z) \rho_{ik}(z) dz = 0 \quad \text{for } i \neq j \quad . \quad (3-23)$$

Thus different mode shapes of the same type are orthogonal only in an integral sense, while mode shapes of different types are everywhere orthogonal. This is more easily seen if $[\phi]$ equals $[I]$. Then the three classes of modes are purely x , purely y and purely rotational and the orthogonality between classes is obvious.

Assuming there exists a constant orthogonal matrix of modal components, $[\phi]$, satisfying (3-18) equation (3-9) may be reduced to three one-dimensional self-adjoint equations.

$$\{F_k(z) \rho_{ik}'(z)\}' + m(z) \omega_{ik}^2 \rho_{ik}(z) = 0 \quad \text{for } k = 1, 2, 3 \quad (3-24)$$

and

$$[F_{\lambda}(z)] = \begin{bmatrix} F_1(z) & 0 & 0 \\ 0 & F_2(z) & 0 \\ 0 & 0 & F_3(z) \end{bmatrix} . \quad (3-25)$$

The boundary conditions for (3-24) follow from equation (3-10) and are

$$\rho_{ik}(0) = \rho_{ik}'(\ell) = 0 \quad \text{for } k = 1, 2, 3 . \quad (3-26)$$

Equation (3-24) with boundary conditions may reduce to a zeroeth order Bessel's equation or to a second order linear differential equation in

certain cases. (39) Some of the more important results from Sturm Liouville theory applicable to equation (3-24) are reviewed here. (37)

The Rayleigh quotient, as defined by equation (3-17), is replaced by the more elementary equation

$$\omega_{ik}^2 = \frac{\int_0^{\ell} F_k(z) [\rho'_{ik}(z)]^2 dz}{\int_0^{\ell} m(z) \rho_{ik}^2(z) dz} \quad (3-27)$$

As a convenience, the eigenvalues may be ordered so that

$$\omega_{1k}^2 < \omega_{2k}^2 < \omega_{3k}^2 < \dots \quad \text{for } k = 1, 2, 3 \quad (3-28)$$

A further consequence of the constancy of $[\phi]$, from Sturm-Liouville theory, is that each of the three k^{th} mode shapes, $\{\tilde{\psi}_{ik}(z)\}$, vanish at exactly i points on the closed interval $[0, \ell]$. (37) This fact makes identification of the i^{th} mode shape an easy matter. Thus, the second index, k , in $\{\tilde{\psi}_{ik}(z)\}$ places the mode shape into one of three mutually orthogonal classes, and the first index, i , numbers the modes in any one class in order of increasing natural frequency or increasing number of zero crossings.

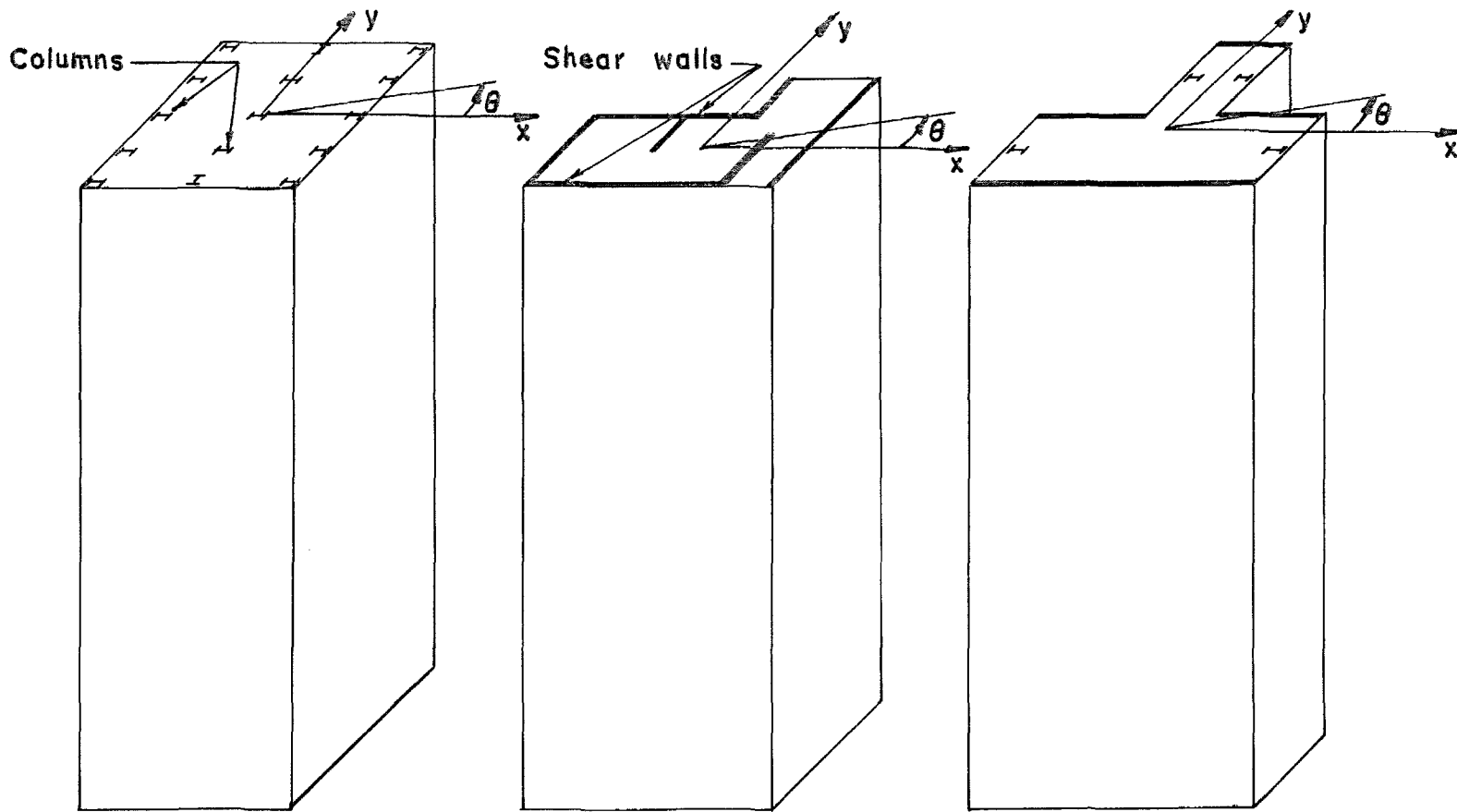
The convenience of having a constant $[\phi]$ matrix which diagonalizes $[F(z)]$ lies, in part, in the fact that it is also a matrix of modal components, as given by equation (3-19). Not only does a constant $[\phi]$ reduce the three-dimensional coupled problem to three uncoupled one-dimensional problems of a well known type, (37) but also the modal solutions are relatively easy to envision and describe.

Therefore, special attention is given to this circumstance throughout the remainder of this chapter. Of particular interest is the applicability to real buildings.

Building Types for Which $[\phi]$ is Constant

There are two primary conditions sufficient for $[\phi]$ to be a constant. One, $[\phi]$ equal $[I]$, the identity matrix, occurs if the centers of rigidity lie directly on the vertical axis of mass centers. This condition, for which $\bar{x}_f(z)$ and $\bar{y}_f(z)$ both vanish, is particularly applicable to structures which have perfect, two-fold mass, column and shear wall symmetry in plan. Rectangular buildings, as shown in figure (10-a) are a common and important example. There are no restrictions on the relative stiffness values in the x, y and rotational directions in this case as the two-fold symmetry is sufficient to guarantee that $[\phi]$ is constant. For this type of building the mode shapes are pure in the sense that any mode shape has exactly one of $x(z)$, $\bar{r}\theta(z)$ or $y(z)$ motions, provided that no two natural frequencies are identical. (The situations which arise when there are identical natural frequencies will be discussed in the next section.)

The second condition occurs if 1) the centers of rigidity lie along a vertical line so that the eccentricity is constant with height; and if 2) the relative values of $F_x(z)$, $F_\theta(z)$ and $F_y(z)$ are invariant with height. Buildings which have a constant but arbitrary geometry at each level and which have columns and shear walls tapered in such a way that the stiffness ratios in the x, y and rotational directions are constant with height satisfy this condition. Buildings



(a)
pure $x, \bar{\theta}$ and y modes

(b)
 $x, \bar{\theta}$ and y motions
in each mode shape

(c)
pure y mode shape with
 x and $\bar{\theta}$ coupled

BUILDINGS WITH COUPLING DUE TO ECCENTRICITY

Figure 10

with shear walls as primary resistive elements normally maintain the same stiffness ratios between floors and hence they fit into this second category rather well. Figure (10-b) exemplifies a building of this type for which the mode shapes are completely coupled; that is, each mode shape has each of the three principle motions, $x(z)$, $\bar{r}\theta(z)$ and $y(z)$ represented. Similarly, framed buildings with columns at the same points at every level would normally maintain about the same stiffness ratios over the height of the structure.

There are also two intermediate conditions of interest for constancy of $[\phi]$, one being the case for which $\bar{y}_f(z)$ vanishes and the ratio of $F_\theta(z)$ to $F_y(z)$ is a constant, and the similar case for which $\bar{x}_f(z)$ vanishes and the ratio of $F_\theta(z)$ to $F_x(z)$ is a constant. Either of these equivalent conditions stipulates that the vertical center of rigidity lies on one of the principle axes and that the translational stiffness in the direction of the other principle axis maintains a constant ratio with the torsional stiffness. This condition can apply to buildings with one-fold plan symmetry, such as the T-shaped structure shown in figure (10-c) or to U-shaped buildings which have shear walls aligned perpendicular to the axis of symmetry. In this case one set of mode shapes is purely translational with motion in the same direction as the axis of symmetry while the other two sets of mode shapes involve a mixture of both translational (in the other direction) and rotational motions. There are other conditions for which $[\phi]$ is constant but they have varying eccentricities and stiffness ratios and as such do not appear

to be useful from the standpoint of the dynamics of buildings.

(Appendix II)

It is considered that a large fraction of tall buildings are such that their dynamic properties can be modeled satisfactorily within the framework indicated by $[\phi] = \text{constant}$. The perturbation analysis developed in the next chapter may be applied to buildings which nearly satisfy one of the conditions for $[\phi]$ to be constant.

The Effect of Close Frequencies Upon $[\phi]$

Assuming that $[\phi]$ is constant, it is already known that $[\phi]$ is the identity matrix $[I]$ when $\bar{x}_f(z)$ and $\bar{y}_f(z)$ both vanish and none of the diagonal terms, $F_x(z)$, $F_\theta(z)$ or $F_y(z)$, are equal. The conditions of $\bar{x}_f(z)$ and $\bar{y}_f(z)$ both vanishing is equivalent to having the vertical lines of centroids and centers of rigidity coincident, as in the case for a rectangular building with two-fold plan symmetry. Furthermore, when $[\phi]$ is the identity matrix, the mode shapes are purely x , purely y or purely rotational, a situation which because of its simplicity has been discussed at length in the literature.

If $\bar{x}_f(z)$ and $\bar{y}_f(z)$ vanish and the diagonal terms $F_x(z)$ and $F_\theta(z)$ and $F_y(z)$ are all equal, the matrix $[\phi]$ can be any orthogonal matrix, for the matrix $[F(z)]$ is then a scalar multiple of $[I]$. In this case the mode shapes are arbitrary combinations of $x(z)$, $\bar{r}\theta(z)$ and $y(z)$ subject to the orthogonality condition. Furthermore, since the diagonals of $[F(z)]$ are identical in this case, so also are the diagonals of $[F_\lambda(z)]$, and hence it follows from equation (3-24)

that the natural frequencies ω_{i1} , ω_{i2} and ω_{i3} are all equal. If only two of the diagonal terms are identical, the matrix $[\phi]$ has two columns which are orthogonal but otherwise arbitrary, the third column must be the same as the corresponding column of the identity matrix. One class of mode shapes in this case has only one component of $x(z)$, $\bar{r}\theta(z)$ or $y(z)$ motion, that component corresponding to the diagonal which is distinct. The other mode shapes are arbitrary, orthogonal combinations of the other two components of $x(z)$, $\bar{r}\theta(z)$ and $y(z)$, and have equal i^{th} frequencies.

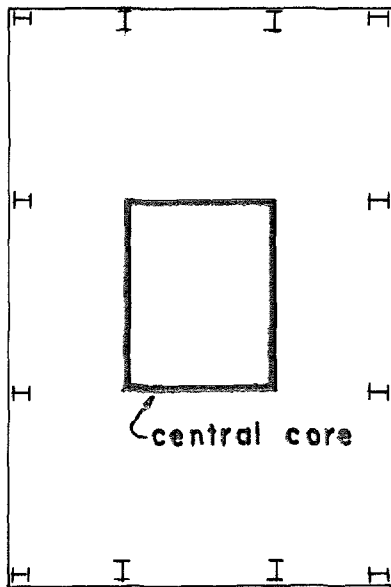
The foregoing discussion suggests that if the eccentricities $\bar{x}_f(z)$ and $\bar{y}_f(z)$ are sufficiently close to zero, then the matrix $[\phi]$ is close to the identity matrix unless two or all of the diagonal elements of $[F(z)]$ are nearly equal. Furthermore, the diagonal elements of $[F(z)]$ are closely approximated by the corresponding elements in $[F_\lambda(z)]$ when the eccentricities are small and as such, equation (3-24) suggests that if two diagonals of $[F(z)]$ are nearly equal, the corresponding i^{th} frequencies are nearly the same. These suggestions, which are established in the following text, are of particular importance for earthquake response because torsional response to the purely translational excitation can only be manifested through the matrix $[\phi]$. The torsional response can give rise to relatively large motions and shears on the perimeter of a structure.

One of the properties of $[F(z)]$ is that the off-diagonal terms, $\bar{x}_f(z)$ are $\bar{y}_f(z)$ only couple translational and torsional motions directly. Translational coupling of $x(z)$ and $y(z)$ motions

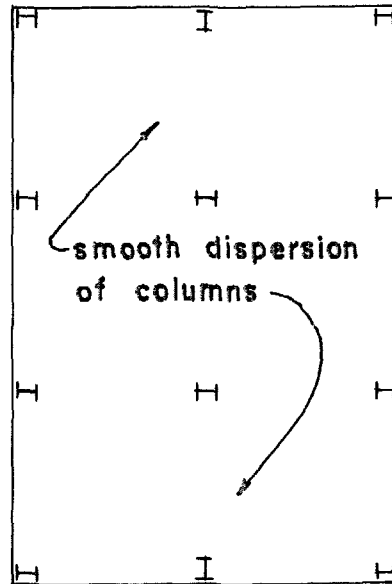
can only occur indirectly, that is, by way of torsion. Therefore the closeness of $F_x(z)$ to $F_y(z)$, $F_1(z)$ to $F_3(z)$ or ω_{i1} to ω_{i3} should not be as influential as the closeness of corresponding translational and rotational parameters.

Buildings with a central core, a smooth dispersion of columns or peripheral shear walls as shown in plan in figure 11 tend to have, respectively, low, nearly equal or high torsional frequencies relative to the corresponding translational frequencies. As such it can be inferred that rectangular buildings with small eccentricities and central cores or peripheral shear walls have $[\phi]$ matrices, if constant, nearly equal to $[I]$, i.e., nearly uncoupled modes, while rectangular buildings with a smooth even dispersion of columns over the floor can have $[\phi]$ quite far from $[I]$, that is, strongly coupled modes. For example, a rectangular building with an even dispersion of columns could have significant torsional response to translational excitation, as in an earthquake, while a rectangular building with a central core or peripheral shear walls would not respond as much in rotation.

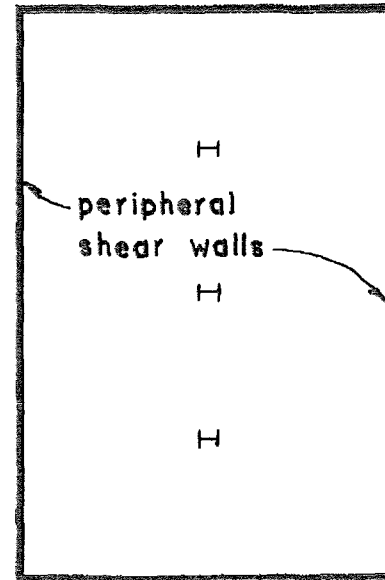
The same inferences do not hold regarding the closeness of frequencies for buildings which do not have small eccentricities, such as L-shaped buildings. In this last case, for example, $[\phi]$ may be quite far from $[I]$ while the corresponding natural frequencies are well-separated.



Torsional frequencies smaller than corresponding translational frequencies, $[\Phi]$ near $[I]$.



Torsional frequencies nearly equal corresponding translational frequencies, $[\Phi]$ may not be near $[I]$.



Torsional frequencies larger than corresponding translational frequencies, $[\Phi]$ near $[I]$.

BUILDINGS WITH COUPLING DUE TO FREQUENCY DIFFERENCES

Figure 11

Determination of $[\phi]$

Assuming conditions sufficient for the matrix $[\phi]$ to be constant, $[\phi]$ may be evaluated at any height z . Therefore, evaluating $[F(z)]$ and $[F_\lambda(z)]$ at the same value of z it follows from equation (3-18) that

$$\begin{bmatrix} F_x - F_k & -\frac{\bar{y}_f}{\bar{r}} F_x & 0 \\ -\frac{\bar{y}_f}{\bar{r}} F_x & F_\theta - F_k & \frac{\bar{x}_f}{\bar{r}} F_y \\ 0 & \frac{\bar{x}_f}{\bar{r}} F_y & F_y - F_k \end{bmatrix} \begin{Bmatrix} \phi_{1k} \\ \phi_{2k} \\ \phi_{3k} \end{Bmatrix} = \begin{Bmatrix} 0 \\ 0 \\ 0 \end{Bmatrix} \text{ for } k = 1, 2, 3 \quad (3-29)$$

where the z dependence has been dropped. The average value of the diagonal elements of $[F]$ is defined by F_m where

$$F_m = \frac{1}{3}(F_x + F_\theta + F_y) \quad (3-30)$$

The differences between the translational stiffness and the average translational-torsional stiffness are given by p and q .

$$\begin{aligned} p &= F_x - F_m & \text{and} \\ q &= F_y - F_m \end{aligned} \quad (3-31)$$

By introducing α and β , the off-diagonal elements of $[F]$ are simplified by the relations

$$\alpha = -\frac{\bar{y}_f}{\bar{r}} F_x \quad \text{and} \quad (3-32)$$

$$\beta = \frac{\bar{x}_f}{\bar{r}} F_y$$

where it is assumed that neither α nor β vanish. The case in which either α or β vanish is discussed later in this section, and if both α and β vanish, $[\phi]$, is equal to $[I]$ with F_1 , F_2 and F_3 equal to F_x , F_θ and F_y , respectively. For convenience the eccentricities divided by the radius of gyration \bar{r} , that is, \bar{y}_f/\bar{r} and \bar{x}_f/\bar{r} are henceforth referred to as eccentricity ratios.

Two new parameters, a and b , are introduced and defined by the equations

$$a = p^2 + pq + q^2 + \alpha^2 + \beta^2 \quad \text{and} \quad (3-33)$$

$$b = pq(p + q) + \alpha^2 q + \beta^2 p \quad .$$

Equations (3-30) through (3-33) are definitions introduced for algebraic convenience in solving the eigenvalue and eigenvector problem given by equation (3-29). Using these definitions, a solution for Ω in the equation

$$\cos \Omega = \frac{-b}{\sqrt{\left(\frac{a}{3}\right)^3}} \quad (3-34)$$

first must be found. If G_k is defined by the equation

$$G_k = 2\sqrt{\frac{a}{3}} \cos\left(\frac{\Omega + 2\pi k}{3}\right) \quad \text{for } k = 1, 2, 3 \quad (3-35)$$

it can be shown that,

$$F_k = F_m + G_k \quad \text{for } k = 1,2,3 \quad (3-36)$$

and that the eigenvectors of $[\phi]$, the ratios of modal components, are given by

$$\begin{Bmatrix} \phi_{1k} \\ \phi_{2k} \\ \phi_{3k} \end{Bmatrix} = C_k \begin{Bmatrix} \alpha(G_k - q) \\ (G_k - p)(G_k - q) \\ \beta(G_k - p) \end{Bmatrix} \quad \text{for } k = 1,2,3 \quad (3-37)$$

where C_k is a scalar which normalizes the eigenvector. In some cases the vectors of $[\phi]$ may be permuted so that the resultant $[\phi]$ matrix is near $[I]$.

In the special case for which the eccentricity ratios, as functions of z , $\bar{x}_f(z)/\bar{r}$ and $\bar{y}_f(z)/\bar{r}$, are constants both $[F(z)]$ and $[F_\lambda(z)]$ are scalar multiples of constant matrices. (Appendix III). If this is the case it follows from equation (3-24) that

$$\left(\frac{\omega_{ik}}{\omega_{is}} \right)^2 = \frac{F_k}{F_s} \quad \text{for } k,s = 1,2,3. \quad (3-39)$$

Assuming that F_k and $[\phi]$ have been determined, the solutions of equation (3-24) for the three values of k give the corresponding natural frequencies and components of the mode shapes which combine to give the total modes as specified by the appropriate vector of $[\phi]$.

Though complete, the above determination of $[\phi]$ does not clarify the relationship between $[\phi]$ and the eccentricities or the difference between natural frequencies.

However, if the condition

$$\text{Minimum } ([F_x - F_\theta]^2, [F_x - F_y]^2, [F_\theta - F_y]^2) \gg \alpha^2 + \beta^2 \quad (3-40)$$

is satisfied, the F_k 's and the matrix $[\phi]$ may be approximated by greatly simplified expressions. This assumption implies that the minimum fractional difference between the diagonals of $[F]$ is somewhat greater than the maximum eccentricity ratio, a case for which one would expect $[\phi]$ to be near $[I]$. In this case, the F_k 's are given approximately by

$$F_1 \approx F_x + \frac{\alpha^2}{F_x - F_\theta} \quad , \quad (3-41)$$

$$F_2 \approx F_\theta + \frac{\alpha^2}{F_\theta - F_x} + \frac{\beta^2}{F_\theta - F_y} \quad \text{and} \quad (3-42)$$

$$F_3 \approx F_y + \frac{\beta^2}{F_y - F_\theta} \quad . \quad (3-43)$$

If the eccentricity ratios are constant, equation (3-39) holds and

$$\omega_{i1}^2 \approx A_i \left(F_x + \frac{\alpha^2}{F_x - F_\theta} \right) \quad (3-44)$$

$$\omega_{i2}^2 \approx A_i \left(F_\theta + \frac{\alpha^2}{F_\theta - F_x} + \frac{\beta^2}{F_\theta - F_y} \right) \quad \text{and} \quad (3-45)$$

$$\omega_{i3}^2 \approx A_i \left(F_y + \frac{\beta^2}{F_y - F_\theta} \right) \quad (3-46)$$

where A_i is a constant. Therefore, the fractional differences between natural frequencies are large in comparison to the eccentricity ratios.

In the simplified case the orthogonal matrix $[\phi]$ is approximated by $[\phi]_A$ where

$$[\phi]_A = \begin{bmatrix} 1 & \frac{\alpha}{F_\theta - F_x} & \frac{\alpha\beta}{(F_y - F_x)(F_y - F_\theta) + \beta^2} \\ \frac{\alpha}{F_x - F_\theta} & 1 & \frac{\beta}{F_y - F_\theta} \\ \frac{\alpha\beta}{(F_x - F_\theta)(F_x - F_y) + \alpha^2} & \frac{\beta}{F_\theta - F_y} & 1 \end{bmatrix} \quad (3-47)$$

From equation (3-47) it is seen that when the eccentricity ratios are small relative to the fractional difference between rigidities or natural frequencies, the orthogonal matrix $[\phi]$ is close to the identity matrix, and furthermore the off-diagonal terms which specify the modal coupling are proportional to the eccentricity ratios and inversely proportional to the fractional differences in stiffness. Because of equations (3-44) through (3-46) this implies that a sufficient condition for $[\phi]$ to be near $[I]$, i.e. for the mode shapes to be nearly uncoupled is that the eccentricities be small with respect to the difference in corresponding natural frequencies. Realistic building properties for any orthogonal $[\phi]$ are, however, possible.

The determination of $[\phi]$ when either α or β , but not both, vanish is now considered, and since the two cases are equivalent, only that for which β equals zero is examined. An example of a building of this type is one which is symmetric about the y axis such as the T-shaped building shown in figure 12. In this case equation (3-29) becomes

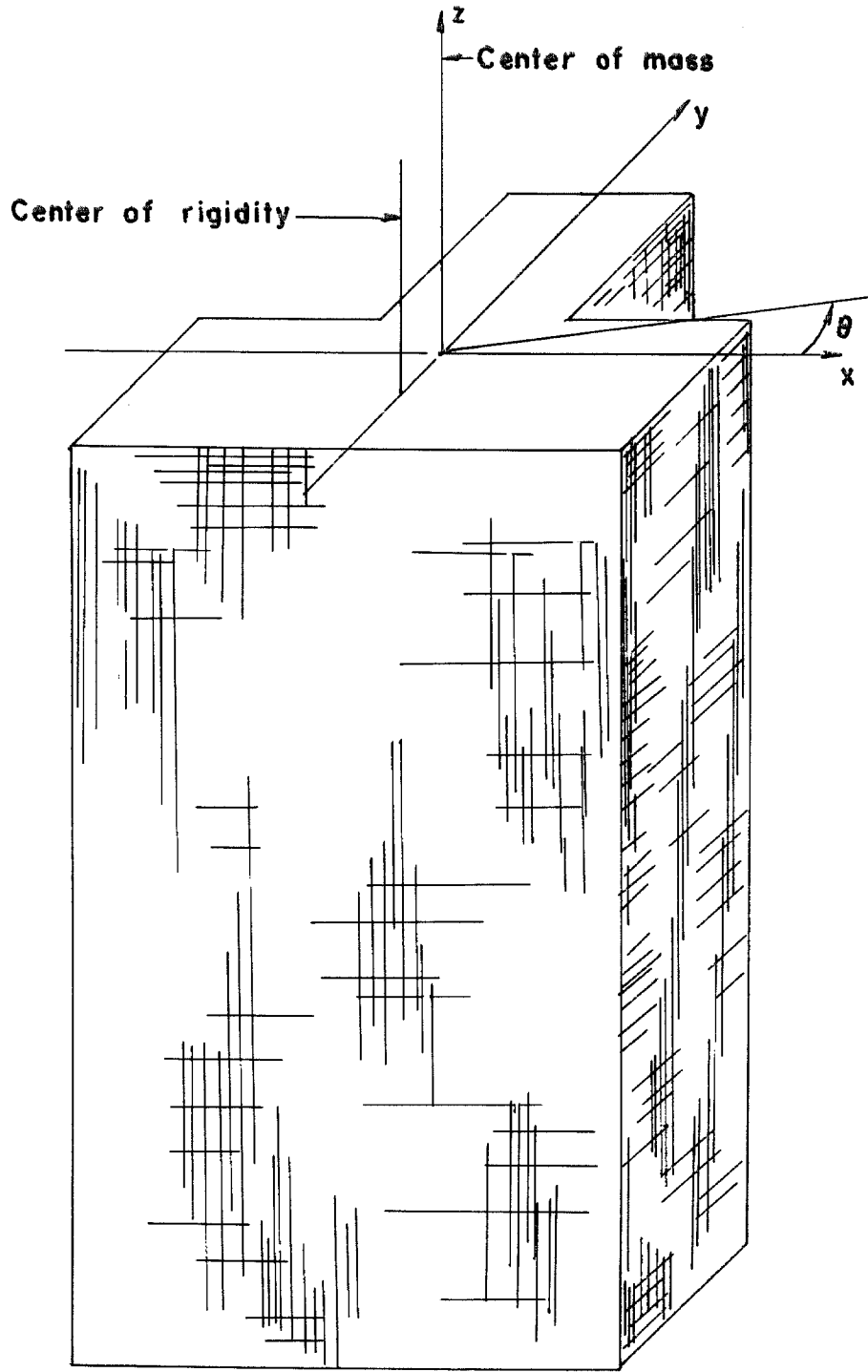
$$\begin{bmatrix} F_x - F_k & -\frac{\bar{y}_f}{\bar{r}} F_x & 0 \\ -\frac{\bar{y}_f}{\bar{r}} F_x & F_\theta - F_k & 0 \\ 0 & 0 & F_y - F_k \end{bmatrix} \begin{Bmatrix} \phi_{1k} \\ \phi_{2k} \\ \phi_{3k} \end{Bmatrix} = \begin{Bmatrix} 0 \\ 0 \\ 0 \end{Bmatrix} \text{ for } k = 1, 2, 3$$

(3-48)

for which it is seen that in any mode shape there is either $y(z)$ motion or a combination of $x(z)$ and $\bar{r}\theta(z)$ motion. Hence by orthogonality $[\phi]$ must have the form

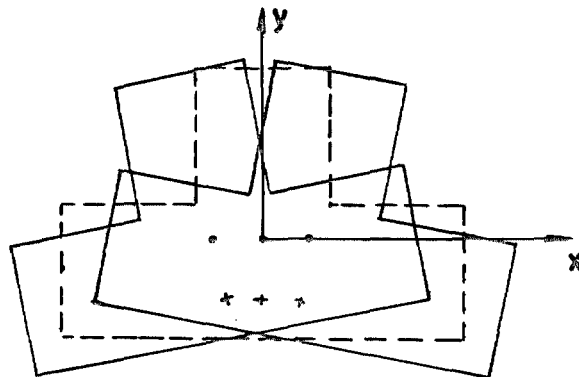
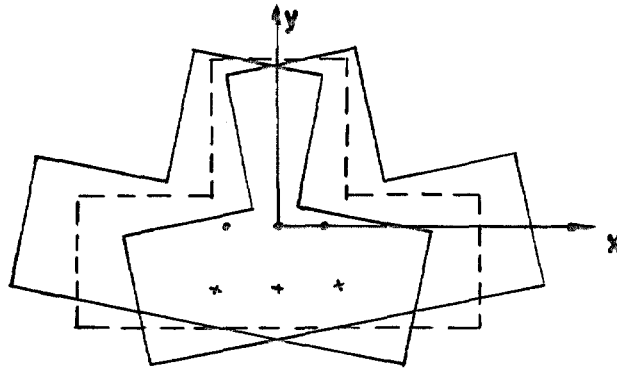
$$[\phi] = \begin{bmatrix} \cos\bar{\theta} & -\sin\bar{\theta} & 0 \\ \sin\bar{\theta} & \cos\bar{\theta} & 0 \\ 0 & 0 & 1 \end{bmatrix} \quad (3-49)$$

which is a function of a single variable, the angle $\bar{\theta}$. A $[\phi]$ of this type is illustrated in figure 13 which shows the three possible modal ratios for a T-shaped building. During vibration in each mode shape the building plan proceeds from one solid outline to the other passing



T-BUILDING MODEL

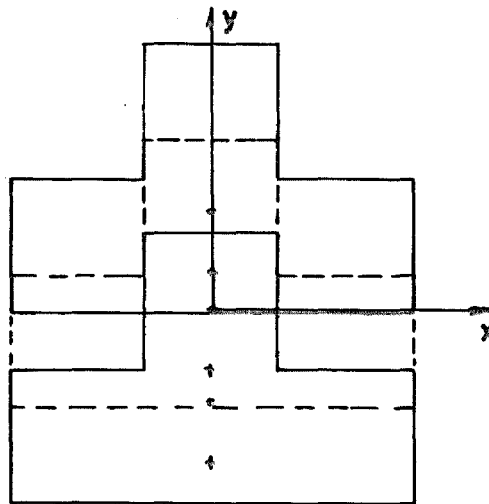
Figure 12



Two modes exhibit an orthogonal combination of $x(z)$ and $T\theta(z)$ motions

LEGEND

- Center of mass
- + Center of rigidity



One mode exhibits only $y(z)$ motion

MODES FOR T-BUILDING

Figure 13

through the neutral dashed outline.

Because of the fact that the first two columns of $[\phi]$ may be interchanged or multiplied by minus one, it is always possible to let the angle $\bar{\theta}$ be less than or equal to $\pi/4$ in absolute value. Substituting this representation of $[\phi]$ into equation (3-18) implies that

$$[F] = \begin{bmatrix} \frac{F_1+F_2}{2} + \frac{F_1-F_2}{2} \cos 2\bar{\theta} & \frac{F_1-F_2}{2} \sin 2\bar{\theta} & 0 \\ \frac{F_1-F_2}{2} \sin 2\bar{\theta} & \frac{F_1+F_2}{2} - \frac{F_1-F_2}{2} \cos 2\bar{\theta} & 0 \\ 0 & 0 & F_3 \end{bmatrix}, \quad (3-50)$$

and by comparing equations (3-48) and (3-50) it follows that

$$F_1 = \frac{1}{2}(F_x + F_\theta) + \frac{1}{2}(F_x - F_\theta) \sqrt{1 + \left(\frac{2 \frac{\bar{y}_f}{\bar{r}} F_x}{F_x - F_\theta} \right)^2}, \quad (3-51)$$

$$F_2 = \frac{1}{2}(F_x + F_\theta) - \frac{1}{2}(F_x - F_\theta) \sqrt{1 + \left(\frac{2 \frac{\bar{y}_f}{\bar{r}} F_x}{F_x - F_\theta} \right)^2}, \quad (3-52)$$

$$F_3 = F_y \quad \text{and} \quad (3-53)$$

$$\tan 2\bar{\theta} = \frac{-2 \frac{\bar{y}_f}{\bar{r}} F_x}{(F_x - F_\theta)}. \quad (3-54)$$

Assuming a constant eccentricity ratio, equation (3-39) holds and hence

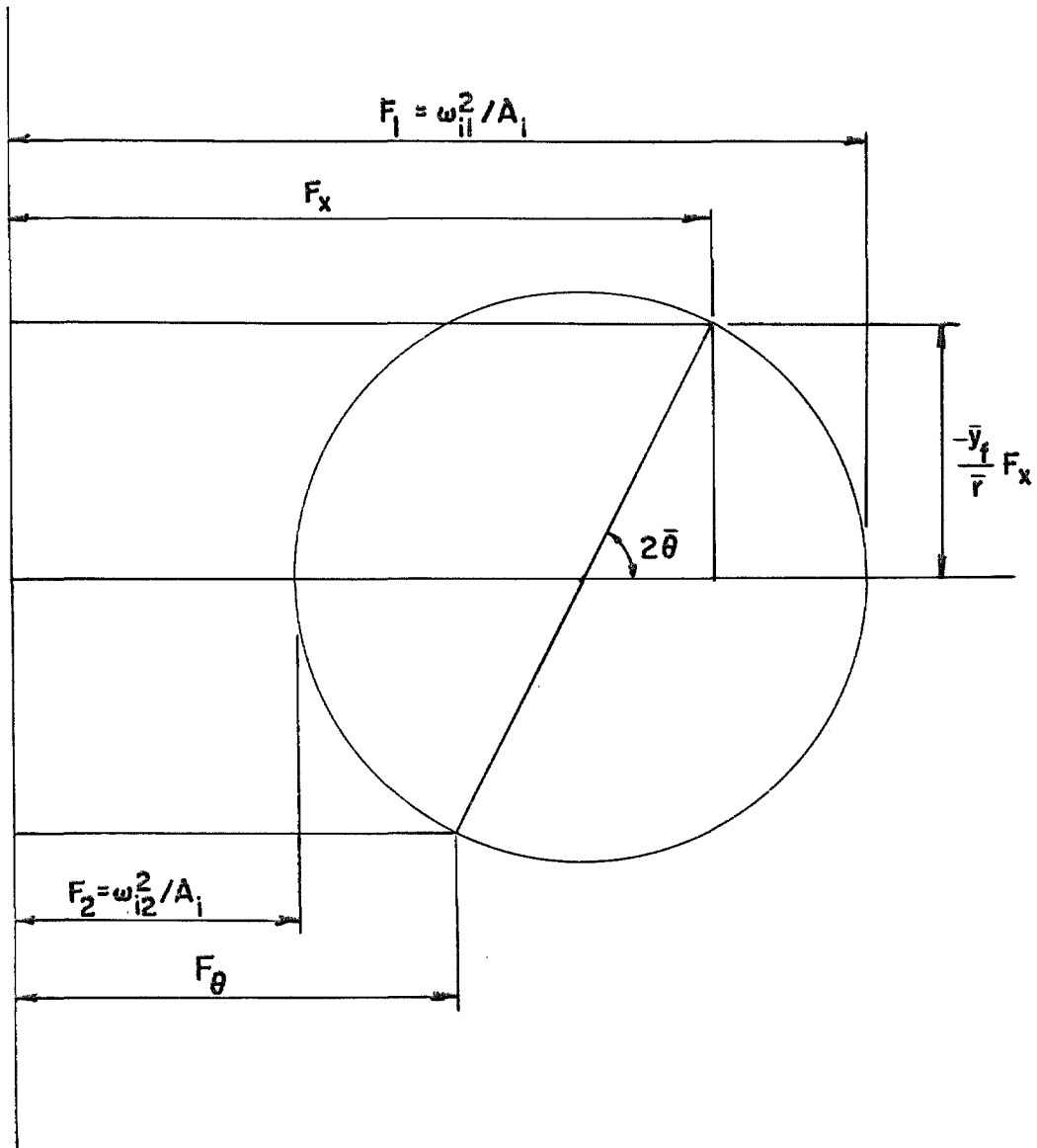
$$\omega_{i1}^2 = A_i F_1^2, \quad \omega_{i2}^2 = A_i F_2^2 \quad \text{and} \quad \omega_{i3}^2 = A_i F_3^2. \quad (3-55)$$

A comparison of equation (3-50) with the definition of [F] implies that a Mohr's circle plot of the elements of [F] as shown in figure 14 is applicable. In this particular figure F_x is assumed to be greater than F_θ and hence F_1 is greater than F_x and F_2 is less than F_θ .

From figure 14 and the above equations it can be seen that $[\phi]$ is near [I] if and only if the eccentricity ratio is small relative to the fractional frequency difference. The sufficiency, but not the necessity, of this condition for $[\phi]$ to be near [I] has already been established in the case for which neither α nor β vanish.

Summary

In this chapter it is seen that there exists a constant matrix of modal components, $[\phi]$, for tall buildings with certain typical properties. If $[\phi]$ is constant, the mode shapes have the same properties, such as general shape and number of zero crossings, as uncoupled modes with the exception that the vectors of $[\phi]$ denote the three orthogonal directions of the mode shapes in $(x, \bar{r}\theta, y)$ space. Sufficient building properties for $[\phi] = \text{constant}$ are non-eccentric symmetry or constant eccentricity and stiffness ratios. If the translational and torsional stiffnesses are well separated and the eccentricities are small, as for a rectangular building with either a central core or peripheral shear walls, $[\phi]$ is near [I] and there is little modal coupling. However, if these stiffnesses



MOHR'S CIRCLE

Figure 14

are nearly equal, as would be likely for a smooth dispersion of many columns across the floor area, strong modal coupling can be expected.

Methods of determining $[\phi]$ from the pertinent building properties, i.e. stiffness and eccentricity, are presented. After $[\phi]$ is found the mode shape factors and eigenvalues may be determined from three differential equations, just as when the modes are uncoupled. With the shape factors $\rho_{ik}(z)$ and the ratios of the modal components, ϕ_k , the eigenvectors, $\{\tilde{\psi}_{ik}(z)\}$, can be assembled to form, with the associated eigenvalues ω_{ik} , the mode shapes and natural frequencies of the structure.

One important practical result of the analysis is that nominally symmetric buildings can have significant modal coupling, for such structures the ratio of eccentricities to the difference in corresponding translational and rotational stiffnesses or frequencies is a measure of the extent of modal coupling; thus a small eccentricity combined with a small frequency difference can produce strong modal coupling.

IV. APPLICATION OF PERTURBATION THEORY

Introduction

In Chapter III the exact form of modal interaction for a class of models for tall buildings was presented, a class characterized by the existence of a constant orthogonal matrix of modal components, $[\phi]$, for each structure. It was also noted what properties of tall buildings are sufficient to make the buildings members of this class. Since the properties of many tall buildings tend to be similar to the properties for this class, it is logical to extend the analysis to include structures approximately describable by a constant $[\phi]$. In this chapter the building properties, equations of motion and solutions are studied by a perturbation analysis of the constant $[\phi]$ case.⁽⁴⁰⁾ Damping and excitation are neglected for simplicity as only the mode shapes and natural frequencies are of interest.

An explanation of the symbols used in this chapter is given below and they are defined again where they first appear in the text. Wherever possible the symbols of previous chapters are used.

<u>Symbol</u>	<u>Explanation or definition</u>
$F_{jk}(z)$	elements of $[\phi]^T [F(z)] [\phi]$ as defined by equation (4-4)
M	mass of the structure
$[R(z)]$	dimensionless mass matrix defined by equation (4-2)

<u>Symbol</u>	<u>Explanation or definition</u>
$R_{jk}(z)$	elements of $[\phi]^T[R(z)][\phi]$ as defined by equation (4-5)
$\{\tilde{u}_{ik}(z)\}$	mode shape correction vector
$u_{ikj}(z)$	elements of $\{\tilde{u}_{ik}(z)\}$
α_{iksj}	constants defined by equation (4-13)
δ_{is}	kroncker delta
λ_{ik}	natural frequency or eigenvalue correction term
μ	a positive dimensionless constant
$\rho_i(z)$	i^{th} mode shape function when each of the three $\rho_{ik}(z)$'s are equal
$[\phi]_P$	matrix of modal components determined from perturbation theory
$[\phi]_{AN}$	$[\phi]_A$ with normalized vectors
ω_{aik}	natural frequency defined by equation (4-11)

Mode Shape to First Order

By extending the results of Chapter III to include a mass distribution which varies with z , it is seen that the mode shapes and natural frequencies are given by solutions of the equation

$$\{[F(z)]\{\tilde{\psi}'_{ik}(z)\}\}' + m(z) \omega_{ik}^2 [R(z)]\{\tilde{\psi}_{ik}(z)\} = \{\tilde{0}\} \quad (4-1)$$

for $k = 1, 2, 3$ and $i = 1, 2, \dots$

which reduces to equation (3-11) if $[R(z)]$ is equal to the identity matrix. The matrix $[R(z)]$ is a dimensionless mass matrix defined by

$$[R(z)] = \begin{bmatrix} 1 & -\frac{\bar{y}(z)}{\bar{r}} & 0 \\ -\frac{\bar{y}(z)}{\bar{r}} & \left[\frac{\bar{r}(z)}{\bar{r}}\right]^2 & \frac{\bar{x}(z)}{\bar{r}} \\ 0 & \frac{\bar{x}(z)}{\bar{r}} & 1 \end{bmatrix} \quad (4-2)$$

while $[F(z)]$ is given by equation (3-5). The boundary conditions again are

$$\{\tilde{\psi}_{ik}(0)\} = \{\tilde{\psi}_{ik}'(\ell)\} = \{0\} \quad (4-3)$$

Equation (3-18) defines an orthogonal matrix as a function of z which diagonalizes the stiffness matrix and that orthogonal matrix, if constant, is seen also to be a matrix of modal components with the mode shapes expressed by equation (3-19). If $[R(z)]$ is not equal to $[I]$ but the matrices $[\phi]^T[F(z)][\phi]$ and $[\phi]^T[R(z)][\phi]$ are both diagonal with $[\phi]$ constant, then equation (3-19) is still valid.

If no constant orthogonal matrix $[\phi]$ exists which diagonalizes both $[F(z)]$ and $[R(z)]$ then there is no constant matrix of modal components. However, for a number of tall buildings it is thought that a constant orthogonal matrix $[\phi]$ does exist which nearly diagonalizes $[F(z)]$ and $[R(z)]$; in other words the off-diagonal elements of $[\phi]^T[F(z)][\phi]$ and $[\phi]^T[R(z)][\phi]$ are small relative to the diagonal

elements. In addition to nearly symmetric rectangular buildings for which small eccentricities imply that $[\phi]$ may be chosen equal to $[I]$, this representation may be applied to buildings of uniform but irregular cross-section for which the eccentricities, though large, are nearly constant. By defining $[\phi]$ in this manner, it is convenient to express the nearly diagonal, symmetric matrices in the forms

$$[\phi]^T [F(z)] [\phi] = \begin{bmatrix} F_{11}(z) & F_{12}(z) & F_{13}(z) \\ F_{21}(z) & F_{22}(z) & F_{23}(z) \\ F_{31}(z) & F_{32}(z) & F_{33}(z) \end{bmatrix} \quad \text{and} \quad (4-4)$$

$$[\phi]^T [R(z)] [\phi] = \begin{bmatrix} R_{11}(z) & R_{12}(z) & R_{13}(z) \\ R_{21}(z) & R_{22}(z) & R_{23}(z) \\ R_{31}(z) & R_{32}(z) & R_{33}(z) \end{bmatrix} . \quad (4-5)$$

From equations (3-5) and (4-2) it is clear that $F_{13}(z)$, $F_{31}(z)$, $R_{13}(z)$ and $R_{31}(z)$ are identically equal to zero if the application suggests that the perturbation should be about $[\phi] = [I]$.

For the analysis the mode shapes and eigenvalues may be cast in the forms

$$\{\tilde{\psi}_{ik}(z)\} = \rho_{ik}(z) [\phi] \{\tilde{e}_k\} + [\phi] \{\tilde{u}_{ik}(z)\} = \rho_{ik}(z) \phi_k + [\phi] \{\tilde{u}_{ik}(z)\} \quad (4-6)$$

and

$$\omega_{ik}^2 = \omega_{aik}^2 + \lambda_{ik} \quad \text{for } k = 1, 2, 3 \quad (4-7)$$

where $\rho_{ik}(z)\phi_k$ and ω_{aik}^2 are, respectively, the mode shapes and eigenvalues which would exist if $[\phi]^T[F(z)][\phi]$ and $[\phi]^T[R(z)][\phi]$ are both diagonal, and where $\{\tilde{u}_{ik}(z)\}$ and λ_{ik} are small corrections to the mode shapes and eigenvalues.

Substitute equations (4-4) through (4-7) into equation (4-1), premultiply by $[\phi]^T$, subtract the zeroth order equation

$$\left\{ \begin{bmatrix} F_{11}(z) & 0 & 0 \\ 0 & F_{22}(z) & 0 \\ 0 & 0 & F_{33}(z) \end{bmatrix} \rho'_{ik}(z) \{\tilde{e}_k\} \right\} + m(z)\omega_{aik}^2 \begin{bmatrix} R_{11}(z) & 0 & 0 \\ 0 & R_{22}(z) & 0 \\ 0 & 0 & R_{33}(z) \end{bmatrix} \rho_{ik}(z) \{\tilde{e}_k\} = \begin{Bmatrix} 0 \\ 0 \\ 0 \end{Bmatrix} \quad (4-8)$$

and neglect the higher order correction terms. The first order equation which results is

$$\begin{aligned}
 & \left\{ \begin{bmatrix} F_{11}(z) & 0 & 0 \\ & F_{22}(z) & 0 \\ 0 & 0 & F_{33}(z) \end{bmatrix} \begin{Bmatrix} u'_{ik1}(z) \\ u'_{ik2}(z) \\ u'_{ik3}(z) \end{Bmatrix} \right\}' \\
 & + \left\{ \begin{bmatrix} 0 & F_{12}(z) & F_{13}(z) \\ F_{21}(z) & 0 & F_{23}(z) \\ F_{31}(z) & F_{32}(z) & 0 \end{bmatrix} \rho'_{ik}(z) \{\tilde{e}_k\} \right\}' \\
 & + m(z) \omega_{aik}^2 \begin{bmatrix} R_{11}(z) & 0 & 0 \\ 0 & R_{22}(z) & 0 \\ 0 & & R_{33}(z) \end{bmatrix} \begin{Bmatrix} u_{ik1}(z) \\ u_{ik2}(z) \\ u_{ik3}(z) \end{Bmatrix} \\
 & + m(z) \omega_{aik}^2 \begin{bmatrix} 0 & R_{12}(z) & R_{13}(z) \\ R_{21}(z) & 0 & R_{23}(z) \\ R_{31}(z) & R_{32}(z) & 0 \end{bmatrix} \rho_{ik}(z) \{\tilde{e}_k\} \\
 & + m(z) \lambda_{ik} \begin{bmatrix} R_{11}(z) & 0 & 0 \\ 0 & R_{22}(z) & 0 \\ 0 & 0 & R_{33}(z) \end{bmatrix} \rho_{ik}(z) \{\tilde{e}_k\} = \begin{Bmatrix} 0 \\ 0 \\ 0 \end{Bmatrix} \quad (4-9)
 \end{aligned}$$

for $k = 1, 2, 3$

where

$$\{\tilde{u}_{ik}(z)\} = \begin{Bmatrix} u_{ik1}(z) \\ u_{ik2}(z) \\ u_{ik3}(z) \end{Bmatrix} \quad (4-10)$$

Application of Sturm Liouville Theory

The zeroeth order equation of the preceding section, equation (4-8), which would be exact in the unperturbed case, may be written as

$$[F_{kk}(z)\rho'_{ik}(z)]' + m(z)\omega_{aik}^2 R_{kk}(z)\rho_{ik}(z) = 0 \quad \text{for } k = 1,2,3, \quad (4-11)$$

a one-dimensional differential equation in self-adjoint form. From Sturm Liouville theory⁽³⁷⁾ it is possible to show that the functions $\rho_{ik}(z)$ for each of the three values of k form a complete set of eigenfunctions which satisfy the weighted orthogonality condition

$$\int_0^{\ell} m(z)R_{kk}(z)\rho_{ik}(z)\rho_{sk}(z)dz = \delta_{is} \int_0^{\ell} m(z)R_{kk}(z)\rho_{ik}^2(z)dz = \delta_{is} \mu M^2 \quad (4-12)$$

where δ_{is} is the Kronecker delta, M is the total mass of the structure and μ is a positive dimensionless constant. Therefore, the correction terms, $u_{ikj}(z)$, may be expanded in a generalized Fourier series of the form

$$u_{ikj}(z) = \sum_{s=1}^{\infty} \alpha_{iks} \rho_{sj}(z) \quad \text{for } k,j = 1,2,3 \quad (4-13)$$

If $[\phi]$ is equal to $[I]$, the k , or j , direction corresponds to the x , $\bar{r}\theta$ or y direction as the index takes the values 1,2, or 3, respectively; while in general the k direction corresponds to the direction of the k^{th} vector of $[\phi]$. Hence $u_{ikj}(z)$ may be interpreted as the first order correction term from the j^{th} direction to be applied to the i^{th} mode in the k^{th} direction, and α_{iks_j} may be thought of as specifying the first order contribution of the s^{th} mode in the j^{th} direction to the i^{th} mode in the k^{th} direction.

Now the k^{th} row of equation (4-9), the first order equation, has no contribution from off-diagonal matrix terms and is given by

$$[F_{kk}(z)u'_{ikk}(z)]' + m(z)\omega_{aik}^2 R_{kk}(z)u_{ikk}(z) + m(z)\lambda_{ik} R_{kk}(z)\rho_{ik}(z) = 0$$

$$\text{for } k = 1,2,3. \quad (4-14)$$

Substitute equation (4-13) into equation (4-14) and then add and subtract the term $m(z)R_{kk}(z) \sum_{s=1}^{\infty} \omega_{ask}^2 \alpha_{iksk} \rho_{sk}(z)$ to obtain the equation

$$\sum_{s=1}^{\infty} \alpha_{iksk} \{ [F_{kk}(z)\rho'_{sk}(z)]' + m(z)\omega_{ask}^2 R_{kk}(z)\rho_{sk}(z) \}$$

$$+ m(z)R_{kk}(z) \sum_{s=1}^{\infty} (\omega_{aik}^2 - \omega_{ask}^2) \alpha_{iksj} \rho_{sk}(z)$$

$$+ m(z)\lambda_{ik} R_{kk}(z) \rho_{ik}(z) = 0 \quad \text{for } k = 1,2,3. \quad (4-15)$$

The first summation term in this equation is a sum of vanishing differential equations of the form given by equation (4-11). Hence the equation

$$m(z)R_{kk}(z) \sum_{s=1}^{\infty} (\omega_{aik}^2 - \omega_{ask}^2) \alpha_{iksk} \rho_{sk}(z) + m(z) \lambda_{ik} R_{kk}(z) \rho_{ik}(z) = 0$$

for $k = 1, 2, 3$ (4-16)

may be multiplied by $\rho_{pk}(z)$ and integrated to give

$$[(\omega_{aik}^2 - \omega_{apk}^2) \alpha_{ikpk} + \lambda_{ik} \delta_{ip}] \mu M^2 = 0 \quad \text{for } k = 1, 2, 3 \quad (4-17)$$

where the orthogonality condition, equation (4-12) has been used.

Since μM^2 is positive, its coefficient must be equal to zero. If i and p are different, the Kronecker delta vanishes while ω_{aik} and ω_{apk} are distinct, thus it follows that

$$\alpha_{ikpk} = 0 \quad \text{for } i \neq p \quad \text{and } k = 1, 2, 3. \quad (4-18)$$

Furthermore, if p equals i , the coefficient of the integral reduces to λ_{ik} , and hence the first order correction to the natural frequencies vanishes, that is

$$\lambda_{ik} = 0 \quad \text{for } k = 1, 2, 3. \quad (4-19)$$

From equations (4-6), (4-13) and (4-18) it can be shown that

$$\{\tilde{\psi}_{i1}(z)\} = [\phi] \begin{Bmatrix} (1+\alpha_{i1i1})\rho_{i1}(z) \\ u_{i12}(z) \\ u_{i13}(z) \end{Bmatrix}, \quad \{\tilde{\psi}_{i2}(z)\} = [\phi] \begin{Bmatrix} u_{i21}(z) \\ (1+\alpha_{i2i2})\rho_{i2}(z) \\ u_{i23} \end{Bmatrix}$$

$$\text{and } \{\tilde{\psi}_{i3}(z)\} = [\phi] \begin{Bmatrix} u_{i31}(z) \\ u_{i32}(z) \\ (1+\alpha_{i3i3})\rho_{i3}(z) \end{Bmatrix}. \quad (4-20)$$

Equation (4-20) states that the first order correction to the mode shape in the direction of the principle component of the mode shape is only a scalar multiple of the principle component. Therefore, since only the relative values of the modal components to first order are of interest, this scalar multiple may be taken equal to zero.

Hence, in combination with equation (4-18) it follows that

$$\alpha_{ikpk} = 0 \quad \text{for } k = 1,2,3 \quad (4-21)$$

holds for all i and p. The desired relation

$$u_{ikk}(z) = 0 \quad \text{for } k = 1,2,3 \quad (4-22)$$

follows directly from equation (4-21). These relations insure the convenient simplification that the first order correction to a mode shape has no component in the direction of the principle component of that mode shape.

Using these results, in particular equation (4-19), the j^{th} row of equation (4-9) for j not equal to k may be written in the form

$$\begin{aligned}
 & [F_{jj}(z)u'_{ikj}(z)] + [F_{jk}(z)\rho'_{ik}(z)] + m(z)\omega_{aik}^2 [R_{jj}(z)u'_{ikj}(z) + R_{jk}(z)\rho'_{ik}(z)] \\
 & = 0 \quad \text{for } k = 1, 2, 3 \text{ and } k \neq j. \quad (4-23)
 \end{aligned}$$

Substitute equation (4-13) into this equation and add and subtract the term $m(z)R_{jj}(z)\sum_{s=1}^{\infty}\omega_{asj}^2\alpha_{iks_j}\rho_{sj}(z)$ to obtain

$$\begin{aligned}
 & \sum_{s=1}^{\infty}\alpha_{iks_j}\{[F_{jj}(z)\rho'_{sj}(z)] + m(z)\omega_{asj}^2 R_{jj}(z)\rho_{sj}(z) + [F_{jk}(z)\rho'_{ik}(z)] \\
 & + m(z)\omega_{aik}^2 R_{jk}(z)\rho_{ik}(z) + m(z)R_{jj}(z)\sum_{s=1}^{\infty}(\omega_{aik}^2 - \omega_{asj}^2)\alpha_{iks_j}\rho_{sj}(z)\} = 0
 \end{aligned}$$

$$\text{for } k, j = 1, 2, 3 \text{ and } k \neq j \quad (4-24)$$

From equation (4-11) it is easily seen that the first summation term vanishes and hence the resulting equation

$$\begin{aligned}
 & [F_{jk}(z)\rho'_{ik}(z)] + m(z)\omega_{aik}^2 R_{jk}(z)\rho_{ik}(z) \\
 & + m(z)R_{jj}(z)\sum_{s=1}^{\infty}(\omega_{aik}^2 - \omega_{asj}^2)\alpha_{iks_j}\rho_{sj}(z) = 0
 \end{aligned}$$

$$\text{for } k, j = 1, 2, 3 \text{ and } k \neq j \quad (4-25)$$

may be multiplied by $\rho_{pj}(z)$ and integrated, using the orthogonality condition, to obtain

$$\int_0^{\ell} [F_{jk}(z)\rho'_{ik}(z)] \rho'_{pj}(z) dz + \omega_{aik}^2 \int_0^{\ell} m(z)R_{jk}(z)\rho_{ik}(z)\rho_{pj}(z) dz$$

$$+ \alpha_{ikpj} (\omega_{aik}^2 - \omega_{apj}^2) \mu M \bar{r}^2 = 0 \quad (4-26)$$

for $k, j = 1, 2, 3$ and $k \neq j$.

The first integral may be integrated by parts to give

$$\int_0^{\ell} F_{jk}(z)\rho'_{ik}(z)\rho'_{pj}(z) dz - \omega_{aik}^2 \int_0^{\ell} m(z)R_{jk}(z)\rho_{ik}(z)\rho_{pj}(z) dz$$

$$= \alpha_{ikpj} (\omega_{aik}^2 - \omega_{apj}^2) \mu M \bar{r}^2 \quad (4-27)$$

for $k, j = 1, 2, 3$ and $k \neq j$

where the boundary conditions, $\rho_{ik}(0)$ and $\rho'_{ik}(\ell)$ equal zero, have been used.

If the matrix $[\phi]$ is chosen equal to the identity matrix, as would be the case for a nearly symmetric rectangular building, $F_{13}(z)$, $F_{31}(z)$, $R_{13}(z)$ and $R_{31}(z)$ are all identically equal to zero and hence the left hand side of equation (4-27) vanishes when j and k are equal to 1 and 3 in either order. Therefore the right hand side of equation (4-27) also vanishes, and it follows that

$$\alpha_{ikpj} (\omega_{aik}^2 - \omega_{apj}^2) = 0 \quad \text{if } [\phi] = [I] \text{ and } k, j = 1, 3 \text{ or } 3, 1.$$

(4-28)

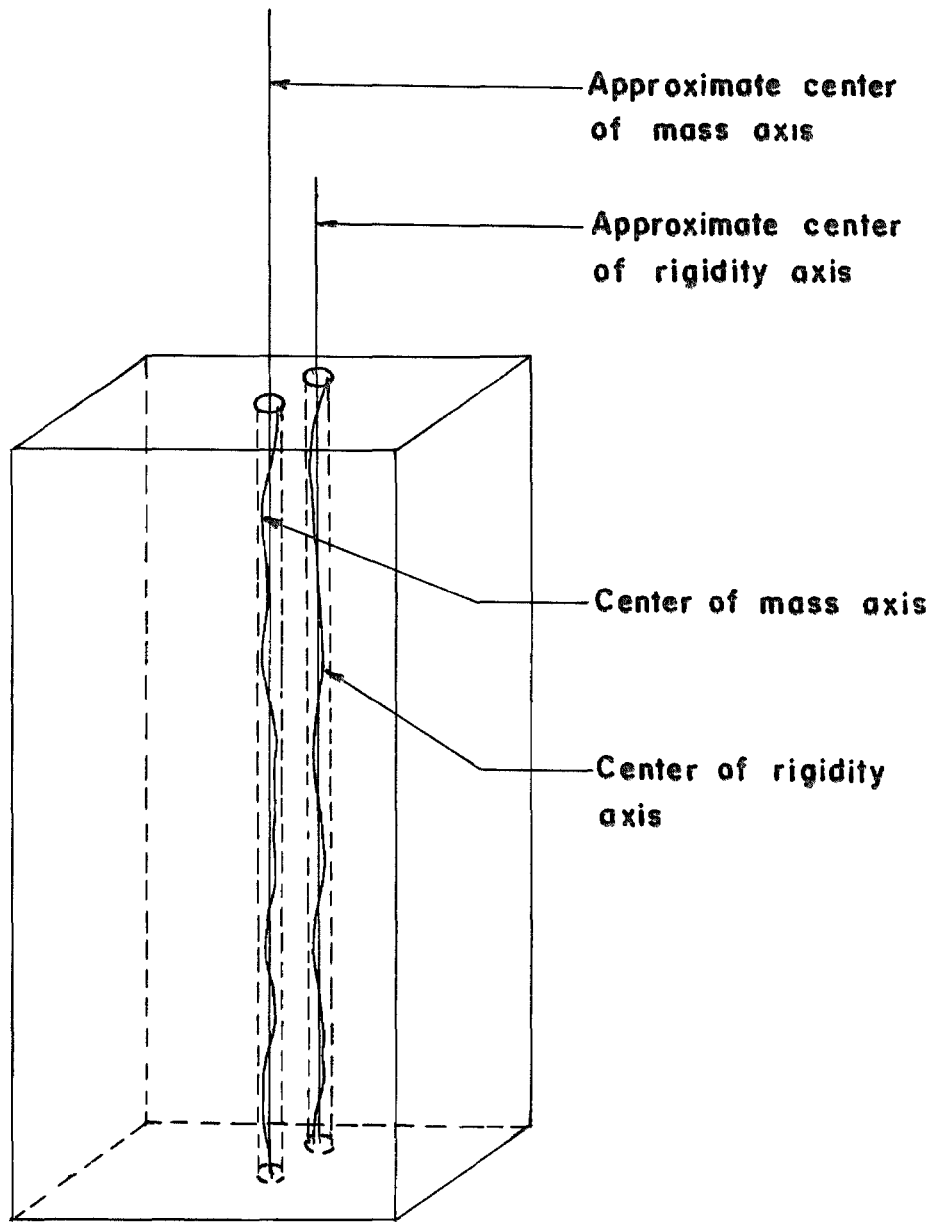
In the case, for which $[\phi]$ equals $[I]$, the principle components of the mode shapes are purely x,y or rotational and the k and j values of 1 and 3 correspond to the translational directions. Therefore if the principle components of the mode shapes are purely x,y or rotational, the first order contribution in one translational direction to a mode shape whose principle component is in the other translational direction is zero unless a certain pair of natural frequencies are equal; that is, the equation

$$u_{ikj}(z) = 0 \quad \text{if } [\phi] = [I] \text{ and } k,j = 1,3 \text{ or } 3,1 \quad (4-29)$$

holds, unless ω_{aik} is equal to ω_{apj} for some value of p. If there does exist a p such that ω_{aik} and ω_{apj} are equal, then the corresponding value of α_{ikpj} is not restricted by equation (4-28). This removal of the restriction for ω_{aik} equal to ω_{apj} indicates that higher order terms should not be neglected in the formulation of an equation like (4-9) when the difference between ω_{aik} and ω_{apj} for some p is small. Consequently, a more thorough examination of the particular aspect of the problem is included later in this chapter.

Approximation to the First Order Corrections

At this point it is profitable to make a few reasonable assumptions regarding the properties of the structure and its mode shapes so that certain useful results may be obtained. First assume that the mass is nearly of uniform distribution with height; that is, assume that each floor of the building was virtually the same shape and mass distribution in plan and as shown in figure 15 that



PERTURBATION MODEL

Figure 15

the centroids are almost vertically aligned. This means that the matrix $[R(z)]$ as defined in equation (4-2) is nearly equal to the identity matrix and furthermore that $[\phi]^T[R(z)][\phi]$ as expressed in equation (4-5) is to first order equal to $[I]$. The second assumption is that the three zeroth order components of the i^{th} mode shapes in the three k^{th} directions, $\rho_{ik}(z)$, are to first order equal to a general i^{th} mode shape $\rho_i(z)$. This assumption does not violate the orthogonality condition, equation (4-12), for $R_{kk}(z)$ to first order equals unity, and it is in reasonable concurrence with experimentally⁽²⁾ or theoretically⁽¹³⁾ determined mode shapes. The mode shapes for several tall buildings are shown in figures 2,3, and 4.⁽⁴¹⁾ If these two assumptions are satisfied, then from equation (4-11) it follows that

$$\frac{F_{kk}(z)}{F_{jj}(z)} \approx \frac{\omega_{aik}^2}{\omega_{aij}^2} \quad \text{for all } i; \quad (4-30)$$

in other words, the diagonal elements of $[\phi]^T[F(z)][\phi]$ are almost in a particular constant ratio. A third and final assumption is that each of the off-diagonal elements divided by any one of the diagonal elements of $[\phi]^T[F(z)][\phi]$ is nearly constant. This assumption implies, as illustrated in figure 15, that the eccentricity ratios $\bar{x}_f(z)/\bar{r}$ and $\bar{y}_f(z)/\bar{r}$ are nearly constant. If all three of these assumptions are satisfied exactly, then $[\phi(z)]$, as defined in equation (3-18), is indeed constant, and the perturbation approach is not necessary. However, the concern here is with approximate, first order results,

not exact solutions.

Based upon these assumptions, $F_{jk}(z)/F_{kk}(z)$ is assigned a constant value, and hence equation (4-27) may be written in the form

$$\frac{F_{jk}}{\sqrt{F_{kk}F_{jj}}} \int_0^{\ell} \sqrt{F_{jj}F_{kk}} \rho'_i(z) \rho'_p(z) dz = \alpha_{ikpj} (\omega_{aik}^2 - \omega_{apj}^2) \mu M \bar{F}^2. \quad (4-31)$$

It follows from Sturm-Liouville theory⁽³⁷⁾, equation (4-30) and the orthogonality condition, equation (4-12), that

$$\int_0^{\ell} \sqrt{F_{jj}(z)F_{kk}(z)} \rho'_i(z) \rho'_p(z) dz = \delta_{ip} \omega_{aik} \omega_{aij} \mu M \bar{F}^2 \quad (4-32)$$

and hence

$$\alpha_{ikij} = \frac{F_{jk}}{\sqrt{F_{jj}F_{kk}}} \frac{\omega_{aik} \omega_{aij}}{(\omega_{aik}^2 - \omega_{aij}^2)}, \quad \text{and} \quad (4-33)$$

$$\alpha_{ikpj} = 0 \quad \text{if } i \neq p. \quad (4-34)$$

Furthermore $[F(z)]$ and therefore $[\phi]^T [F(z)] [\phi]$ are symmetric; thus $F_{jk}(z)$ and $F_{kj}(z)$ are equal, and from equation (4-33) it follows that

$$\alpha_{ikij} = -\alpha_{ijik}. \quad (4-35)$$

Since the perturbation procedure is based upon small correction terms, the absolute value of the expression for α_{ikij} in equation (4-33)

must be small relative to unity if equation (4-33) is to be valid.

If the estimated matrix of modal components, $[\phi]$, and $[I]$ are equal, as in the rectangular building case, a slightly different approach is preferred. Then $F_{13}(z)$ and $F_{31}(z)$ vanish and the non-zero, off-diagonal elements of the symmetric matrix, $[\phi]^T[F(z)][\phi]$, which in this case equals $[F(z)]$, may be denoted by F_{2k} for k equal to 1 or 3. In this case it follows from equations (4-30) and (4-33) that

$$\alpha_{iki2} = -\alpha_{i2ik} = \frac{F_{2k}}{F_{kk}} \frac{\omega_{aik}^2}{\omega_{aik}^2 - \omega_{ai2}^2} \quad \text{for } k = 1 \text{ or } 3, \quad (4-36)$$

and

$$\alpha_{ilp3} = \alpha_{p3il} = 0 \quad \text{for all } i \text{ and } p. \quad (4-37)$$

Using equation (3-5), which defines both $[F(z)]$ and $[\phi]^T[F(z)][\phi]$, it follows that equation (4-36) may be written in the forms

$$\alpha_{i2i1} = -\alpha_{i1i2} = \frac{\bar{y}_f}{\bar{r}} \frac{\omega_{ai1}^2}{\omega_{ai1}^2 - \omega_{ai2}^2}, \quad \text{and} \quad (4-38)$$

$$\alpha_{i3i2} = -\alpha_{i2i3} = \frac{\bar{x}_f}{\bar{r}} \frac{\omega_{ai3}^2}{\omega_{ai3}^2 - \omega_{ai2}^2} \quad (4-39)$$

where the eccentricity ratios are presumed constant or nearly so.

Second Order Translational Interaction and Frequency Shifts

It has been shown that if the off-diagonal elements of $[F(z)]$ are relatively small, then the approximate matrix of modal components,

$[\phi]$, may be chosen equal to $[I]$. Furthermore, if $[\phi]$ equals $[I]$, then the first order interaction between the translational modes vanishes unless certain natural frequencies are equal. A discontinuity in the first order solution occurs if a pair of translational frequencies in the two directions approach equality, and this suggests that second and higher order effects should be considered. Without yet presuming that $[\phi]$ equals $[I]$, utilize the three assumptions presented in the foregoing section, substitute equations (4-4) through (4-7) into equation (4-1) and premultiply by $[\phi]^T$ to obtain

$$\begin{aligned} & \left\{ \begin{bmatrix} F_{11}(z) & F_{12}(z) & F_{13}(z) \\ F_{21}(z) & F_{22}(z) & F_{23}(z) \\ F_{31}(z) & F_{32}(z) & F_{33}(z) \end{bmatrix} \left\{ \rho_i(z) \{ \tilde{e}_k \} + \begin{bmatrix} u_{ik1}(z) \\ u_{ik2}(z) \\ u_{ik3}(z) \end{bmatrix} \right\} \right\} \\ & + m(z) (\omega_{aik}^2 + \lambda_{ik}) \left\{ \rho_i(z) \{ \tilde{e}_k \} + \begin{bmatrix} u_{ik1}(z) \\ u_{ik2}(z) \\ u_{ik3}(z) \end{bmatrix} \right\} = \begin{bmatrix} 0 \\ 0 \\ 0 \end{bmatrix} \quad (4-40) \end{aligned}$$

Equation (4-40) is complete in that it contains terms of all orders, while equations (4-8) and (4-9) contain only zeroth and first order terms, respectively.

Now, if j and k are chosen equal to 1 and 3 in either order and the condition that $[\phi]$ equals $[I]$ is used so that $F_{13}(z)$ and $F_{31}(z)$ vanish, the j^{th} row of equation (4-40) becomes

$$[F_{jj}(z)u'_{ikj}(z)]' + [F_{j2}(z)u'_{ik2}(z)]' + m(z)(\omega_{aik} + \lambda_{ik})u_{ikj}(z) = 0$$

$$\text{for } k, j = 1, 3 \text{ or } 3, 1 . \quad (4-41)$$

Assume that ω_{ai1} and ω_{ap3} are well separated for unequal i and p , then from equation (4-28), equation (4-34) is valid as a discontinuity is not approached. Therefore, the second and higher order interaction between translational modes results only from the terms α_{ili3} and α_{i3il} . It follows from equations (4-13) and (4-34) for any k and j equal to 1, 2, or 3 independently that

$$u_{ikj}(z) = \alpha_{ikij} \rho_i(z) \quad (4-42)$$

where the assumption that the three i^{th} mode shapes are to first order equal is used. This equation with k equal to 1 or 3 and j equal to 2 is substituted into the preceding equation and the term $\alpha_{ikij} m(z) \omega_{aij}^2 \rho_i(z)$ is added and subtracted to obtain

$$\begin{aligned} & \alpha_{ikij} \{ [F_{jj}(z)\rho'_i(z)]' + m(z)\omega_{aij}^2 \rho_i(z) \} + \alpha_{iki2} [F_{j2}(z)\rho'_i(z)]' \\ & + \alpha_{ikij} m(z) (\omega_{aik}^2 + \lambda_{ik} - \omega_{aij}^2) \rho_i(z) = 0 \quad \text{for } k, j = 1, 3 \text{ or } 3, 1. \end{aligned} \quad (4-43)$$

Since $\rho_{ik}(z)$ equals $\rho_i(z)$, the first term vanishes and the remaining equation is multiplied by $\rho_i(z)$ and integrated. Thus α_{ikij} is given by

$$\alpha_{ikij} = \frac{\alpha_{iki2} \int_0^{\ell} F_{j2} [\rho_i'(z)]^2 dz}{\mu M \bar{r}^2 (\omega_{aik}^2 + \lambda_{ik} - \omega_{aij}^2)} \quad \text{for } k,j = 1,3 \text{ or } 3,1 . \quad (4-44)$$

Using the equation

$$\int_0^{\ell} F_{j2}(z) [\rho_i'(z)]^2 dz = \frac{F_{j2}}{F_{jj}} \int_0^{\ell} F_{jj}(z) [\rho_i'(z)]^2 dz = \frac{F_{j2}}{F_{jj}} \omega_{aij}^2 \mu M \bar{r}^2 \quad (4-45)$$

and equation (4-36), equation (4-44) becomes

$$\alpha_{ikij} = \frac{F_{2k}}{F_{kk}} \frac{F_{j2}}{F_{jj}} \frac{\omega_{aik}^2 \omega_{aij}^2}{(\omega_{aik}^2 - \omega_{ai2}^2)(\omega_{aik}^2 + \lambda_{ik} - \omega_{aij}^2)} \quad \text{for } k,j = 1,3 \text{ or } 3,1 . \quad (4-46)$$

Furthermore, since $[\phi]$ equals $[I]$ in this case, equation (4-46) can be expressed as

$$\alpha_{ikij} = - \frac{\bar{x}_f \bar{y}_f}{\bar{r}^2} \frac{\omega_{ai1}^2 \omega_{ai3}^2}{(\omega_{aik}^2 - \omega_{ai2}^2)(\omega_{aik}^2 + \lambda_{ik} - \omega_{aij}^2)} \quad \text{for } k,j = 1,3 \text{ or } 3,1 . \quad (4-47)$$

where, in light of the assumptions used in this and the preceding section, it is necessary that the eccentricity ratios be nearly constant.

It has been shown that the first order expression for λ_{ik} is zero; however, as can be seen from equation (4-47), λ_{ik} must be known more accurately for the determination of α_{ikij} if ω_{aik} and ω_{aij}

are close together. The k^{th} row of equation (4-40), which does not presume that $[\phi]$ is the identity matrix, may be written in the form

$$[F_{kk}(z)\rho_i'(z)]' + \sum_{j=1}^3 [F_{kj}(z)u_{ikj}'(z)]' + m(z)(\omega_{aik} + \lambda_{ik}) [\rho_i(z) + u_{ikk}(z)] = 0. \quad (4-48)$$

Substitute equations (4-11) with $\rho_{ik}(z)$ equal to $\rho_i(z)$, (4-22) and (4-42) into equation (4-48) and neglect the third and higher order terms. The resulting equation is

$$\sum_{\substack{j=1 \\ j \neq k}}^3 \alpha_{ikij} [F_{kj}(z)\rho_i'(z)]' + \lambda_{ik} m(z)\rho_i(z) = 0. \quad (4-49)$$

Multiply this equation by $\rho_i(z)$, integrate by parts, and use orthogonality and boundary conditions to obtain the equation

$$\sum_{\substack{j=1 \\ j \neq k}}^3 \alpha_{ikij} \int_0^{\ell} F_{kj}(z) [\rho_i'(z)]^2 dz = \lambda_{ik} \mu M \bar{r}^2. \quad (4-50)$$

If $[\phi]$ and $[I]$ are unequal, it is useful to substitute the equation

$$\int_0^{\ell} F_{kj}(z) [\rho_i'(z)]^2 dz = \frac{F_{kj}}{\sqrt{F_{kk} F_{jj}}} \omega_{aik} \omega_{aij} \mu M \bar{r}^2 \quad (4-51)$$

which holds for any k and j independently equal to 1,2 or 3 and equation (4-33) into equation (4-50) to obtain

$$\lambda_{ik} = \sum_{\substack{j=1 \\ j \neq k}}^3 \frac{F_{kj}^2}{F_{kk}F_{jj}} \frac{\omega_{aik}^2 \omega_{aij}^2}{\omega_{aik}^2 - \omega_{aij}^2} . \quad (4-52)$$

However, if $[\phi]$ equals $[I]$, then $F_{13}(z)$ and $F_{31}(z)$ vanish in equation (4-50) and equations (4-36) and (4-45) are substituted into equation (4-50). The resulting equations for λ_{i1} , λ_{i2} and λ_{i3} are

$$\lambda_{i1} = \left(\frac{F_{12}}{F_{11}} \right)^2 \frac{\omega_{ai1}^4}{\omega_{ai1}^2 - \omega_{ai2}^2} , \quad \lambda_{i3} = \left(\frac{F_{32}}{F_{33}} \right)^2 \frac{\omega_{ai3}^4}{\omega_{ai3}^2 - \omega_{ai2}^2}$$

and $\lambda_{i2} = -(\lambda_{i1} + \lambda_{i3})$. (4-53)

Using equation (3-5) one may then write

$$\lambda_{i1} = \left(\frac{\bar{y}_f}{\bar{r}} \right)^2 \frac{\omega_{ai1}^4}{\omega_{ai1}^2 - \omega_{ai2}^2}$$

$$\lambda_{i2} = \left(\frac{\bar{y}_f}{\bar{r}} \right)^2 \frac{\omega_{ai1}^4}{\omega_{ai2}^2 - \omega_{ai1}^2} + \left(\frac{\bar{x}_f}{\bar{r}} \right)^2 \frac{\omega_{ai3}^4}{\omega_{ai2}^2 - \omega_{ai3}^2} \quad \text{and}$$

$$\lambda_{i3} = \left(\frac{\bar{x}_f}{\bar{r}} \right)^2 \frac{\omega_{ai3}^4}{\omega_{ai3}^2 - \omega_{ai2}^2} . \quad (4-54)$$

Equation (4-54), for which the natural frequency corrections are determined to second order, may be substituted into equation (4-47)

to obtain

$$\alpha_{i1i3} = -\frac{\bar{x}_f \bar{y}_f}{\bar{r}^2} \frac{\omega_{ai1}^2 \omega_{ai3}^2}{(\omega_{ai1}^2 - \omega_{ai3}^2)(\omega_{ai1}^2 - \omega_{ai2}^2) + \left(\frac{\bar{y}_f}{\bar{r}}\right)^2 \omega_{ai1}^4} \quad \text{and}$$

$$\alpha_{i3i1} = -\frac{\bar{x}_f \bar{y}_f}{\bar{r}^2} \frac{\omega_{ai1}^2 \omega_{ai3}^2}{(\omega_{ai3}^2 - \omega_{ai1}^2)(\omega_{ai3}^2 - \omega_{ai2}^2) + \left(\frac{\bar{x}_f}{\bar{r}}\right)^2 \omega_{ai3}^4} .$$

(4-55)

The Natural Frequencies and Matrix of Modal Components

Since the three i^{th} mode shapes, $\rho_{ik}(z)$, have been taken equal to a general i^{th} mode shape, $\rho_i(z)$, the mode shape equation, equation (4-6), in conjunction with equation (4-42), may be written as

$$\{\tilde{\psi}_{ik}(z)\} = \rho_{ik}(z) [\phi] \left\{ \begin{matrix} \{\tilde{e}_k\} + \begin{matrix} \alpha_{iki1} \\ \alpha_{iki2} \\ \alpha_{iki3} \end{matrix} \end{matrix} \right\} \quad (4-56)$$

where α_{ikik} is zero. Therefore, the matrix of modal components which results from perturbation theory is denoted by $[\phi]_p$ where

$$[\phi]_p = [\phi] \begin{bmatrix} 1 & \alpha_{i2i1} & \alpha_{i3i1} \\ \alpha_{i1i2} & 1 & \alpha_{i3i2} \\ \alpha_{i1i3} & \alpha_{i2i3} & 1 \end{bmatrix} \quad \text{for } i = 1, 2, 3 \dots \quad (4-57)$$

In this equation the α_{ikij} terms to first order are determined from equation (4-33) if $[\phi]$ is unequal to $[I]$. The natural frequency correction terms are of second order, and if $[\phi]$ and $[I]$ are unequal, they are given by equation (4-52) which may be substituted into equation (4-7) to determine the natural frequencies.

Now if $[\phi]$ is chosen equal to $[I]$ equation (4-57) becomes simply

$$[\phi]_p = \begin{bmatrix} 1 & \alpha_{i2i1} & \alpha_{i3i1} \\ \alpha_{i1i2} & 1 & \alpha_{i3i2} \\ \alpha_{i1i3} & \alpha_{i2i3} & 1 \end{bmatrix} \quad \text{for } i = 1, 2, 3 \dots \quad (4-58)$$

The terms α_{ikij} for which one of k or j is equal to 2 are of first order but α_{i1i3} and α_{i3i1} are second order terms in this case. To determine $[\phi]_p$, substitute the appropriate equations, equations (4-38), (4-39) and (4-55) into equation (4-58) to obtain

$$[\phi]_P = \begin{bmatrix} 1 & \frac{-\bar{y}_f}{\bar{r}} \frac{\omega_{ai1}^2}{(\omega_{ai2}^2 - \omega_{ai1}^2)} & \frac{-\bar{x}_f \bar{y}_f}{\bar{r}^2} \frac{\omega_{ai1}^2 \omega_{ai3}^2}{(\omega_{ai3}^2 - \omega_{ai1}^2)(\omega_{ai3}^2 - \omega_{ai2}^2) + \left(\frac{\bar{x}_f}{\bar{r}}\right)^2 \omega_{ai3}^4} \\ \frac{-\bar{y}_f}{\bar{r}} \frac{\omega_{ai1}^2}{(\omega_{ai1}^2 - \omega_{ai2}^2)} & 1 & \frac{\bar{x}_f}{\bar{r}} \frac{\omega_{ai3}^2}{(\omega_{ai3}^2 - \omega_{ai2}^2)} \\ \frac{-\bar{x}_f \bar{y}_f}{\bar{r}^2} \frac{\omega_{ai1}^2 \omega_{ai3}^2}{(\omega_{ai1}^2 - \omega_{ai3}^2)(\omega_{ai1}^2 - \omega_{ai2}^2) + \left(\frac{\bar{y}_f}{\bar{r}}\right)^2 \omega_{ai1}^4} & \frac{\bar{x}_f}{\bar{r}} \frac{\omega_{ai3}^2}{(\omega_{ai2}^2 - \omega_{ai3}^2)} & 1 \end{bmatrix}$$

The natural frequencies, to second order, are determined from equations (4-7) and (4-54).

$$\begin{aligned} \omega_{i1}^2 &= \omega_{ai1}^2 + \left(\frac{\bar{y}_f}{\bar{r}}\right)^2 \frac{\omega_{ai1}^4}{(\omega_{ai1}^2 - \omega_{ai2}^2)} \quad , \\ \omega_{i2}^2 &= \omega_{ai2}^2 + \left(\frac{\bar{y}_f}{\bar{r}}\right)^2 \frac{\omega_{ai1}^4}{(\omega_{ai2}^2 - \omega_{ai1}^2)} + \left(\frac{\bar{x}_f}{\bar{r}}\right)^2 \frac{\omega_{ai3}^4}{(\omega_{ai2}^2 - \omega_{ai3}^2)} \quad \text{and} \\ \omega_{i3}^2 &= \omega_{ai3}^2 + \left(\frac{\bar{x}_f}{\bar{r}}\right)^2 \frac{\omega_{ai3}^4}{(\omega_{ai3}^2 - \omega_{ai2}^2)} \quad . \end{aligned} \quad (4-60)$$

If the perturbation procedure as presented herein is to be valid, it is necessary for the first and second order correction terms, as determined in the above equations, to be small.

It is of interest to compare equations (4-59) and (4-60) with the results obtained in Chapter III for the case when the off-diagonal elements are small. Assuming that equation (3-40) holds, and that $[\phi]$ as defined in Chapter III is constant, the natural frequencies and the matrix of modal components are determined approximately in equations (3-44) through (3-47). If the eccentricity ratios, α and β , as defined by equation (3-32), vanish, then a comparison with equation (4-7) implies that ω_{ik}^2 should be replaced by ω_{aik}^2 . Therefore, from equations (3-44) through (3-46) it follows that

$$\omega_{ai1}^2 = A_i F_x^2 \quad , \quad \omega_{ai2}^2 = A_i F_\theta^2 \quad \text{and} \quad \omega_{ai3}^2 = A_i F_y^2 \quad \text{for } i = 1, 2, 3 \dots \quad (4-61)$$

Substituting equations (3-32) and this equation into equations (3-44) through (3-46) gives a set of equations identical to equation (4-60),

and the same substitutions applied to the matrix of modal components implies that equations (3-47) and (4-59) are identical. That is, the natural frequencies and the matrix of modal components, as determined approximately in Chapter III in the case for which $[\phi]$ is close to $[1]$ and constant, are the same as those determined from the perturbation procedure if the matrix of modal components is close to $[I]$ and approximately constant. This type of comparison is not made if the matrix of modal components is not close to $[I]$.

In this chapter the constant matrix $[\phi]_p$ is determined as representative of the nearly constant ratios of modal components. Therefore, the terms α_{ikij} appearing in equation (4-57) are independent of i , as is implied by the form of α_{ikij} and equation (4-61). However if equation (4-61) holds only in an approximate sense, the small frequency differences and hence the α_{ikij} may be strongly influenced by the choice of i . Therefore, the matrix $[\phi]_p$ may depend on i in applications and a weighted average of $[\phi]_p$'s for the various modes might be considered.

A Comparative Example

As an example consider a building for which, in the appropriate units, F_x , F_θ and F_y are given by 10, 15 and 11 respectively and the eccentricity ratios, \bar{y}_f/\bar{r} and \bar{x}_f/\bar{r} are given by 1/5 and 1/11 respectively. Then it can be shown that the eigenvalues F_1 , F_2 and F_3 , or the natural frequencies in the appropriate units, and the matrix of modal components $[\phi]$ are given exactly by

$$F_1 = \omega_{i1}^2 = 9.232, \quad F_2 = \omega_{i2}^2 = 15.884 \quad \text{and} \quad F_3 = \omega_{i3}^2 = 10.884 \quad (4-62)$$

and

$$[\phi] = \begin{bmatrix} 0.916 & -0.316 & 0.246 \\ 0.352 & 0.931 & -0.112 \\ -0.199 & 0.191 & 0.941 \end{bmatrix} . \quad (4-63)$$

Using the approximation technique developed in Chapter III or the perturbation analysis in which case $[\phi]$ is assumed to be $[I]$ it is found that the eigenvalues or natural frequencies are calculated to be

$$\begin{aligned} F_1 &= \omega_{i1}^2 = 9.20 , \\ F_2 &= \omega_{i2}^2 = 16.05 , \quad \text{and} \\ F_3 &= \omega_{i3}^2 = 10.75 , \end{aligned} \quad (4-64)$$

while the matrix of modal components determined from either equation (3-47) or (4-59) is found, after normalization of the vectors, to be

$$[\phi]_{AN} = \begin{bmatrix} 0.911 & -0.362 & 0.545 \\ 0.373 & 0.905 & -0.204 \\ -0.202 & 0.226 & 0.816 \end{bmatrix} . \quad (4-65)$$

It is of particular interest to note that the approximate and exact solutions are close enough for most applications, even though equation (3-40) is not satisfied. If equation (3-40) is satisfied, even better agreement between the approximate and exact solutions is attained. For example, assume that the eccentricity ratios for this

example are reduced by a factor of 10; that is, \bar{y}_f/\bar{r} and \bar{x}_f/\bar{r} are given by 1/50 and 1/110 respectively. Then equation (3-40) is satisfied and the exact solutions are given by

$$\begin{aligned} F_1 &= \omega_{i1}^2 = 9.9918 \quad , \\ F_2 &= \omega_{i2}^2 = 15.0106 \quad , \\ F_3 &= \omega_{i3}^2 = 10.9977 \quad \text{and} \end{aligned} \tag{4-66}$$

$$[\phi] = \begin{bmatrix} 0.999 & -0.040 & 0.005 \\ 0.041 & 0.999 & -0.023 \\ -0.004 & 0.025 & 0.999 \end{bmatrix} . \tag{4-67}$$

while the approximate eigenvalues or natural frequencies and normalized matrix of modal components as determined from either Chapter III or the perturbation procedure are found to be

$$\begin{aligned} F_1 &= \omega_{i1}^2 = 9.9920 \quad , \\ F_2 &= \omega_{i2}^2 = 15.0105 \quad , \\ F_3 &= \omega_{i3}^2 = 10.9975 \quad \text{and} \end{aligned} \tag{4-68}$$

$$[\phi]_{AN} = \begin{bmatrix} 0.999 & -0.040 & 0.005 \\ 0.040 & 0.999 & -0.025 \\ -0.004 & 0.025 & 0.999 \end{bmatrix} . \tag{4-69}$$

Although the results for both the approximate, based on constant $[\phi]$, and the perturbation techniques are the same, the

perturbation technique applies to a larger class of problems. The approximate technique developed in Chapter III applies only when there exists a constant matrix of modal components which is close to [I]. The perturbation analysis is applicable to any matrix of modal components which is almost constant. Thus in the first example above, the perturbation analysis would apply if the restraints on the eccentricity ratios were relaxed so that \bar{y}_f/\bar{r} and \bar{x}_f/\bar{r} for example varied from 0.18 to 0.22 and from 0.07 to 0.11 respectively. This of course would invalidate the approximation scheme of Chapter III for $[\phi]$ would not be constant.

V. THE EFFECT OF EARTHQUAKES ON TALL BUILDINGS

Introduction

From Chapter III it is seen that the models for building structures can possess mode shapes with a realistic mixture of translational and rotational components, and can therefore provide a means to study the effect of modal coupling in the earthquake response of buildings. The effect of modal coupling, and the resulting torsional vibrations, on the response is of practical interest, since buildings are designed primarily on the basis of purely translational response with the dynamic effects of modal coupling approximated by a small (5%) eccentricity in the applied static forces specified by the codes.⁽²⁴⁾

In this chapter the responses of tall buildings to earthquake ground motions for both arbitrarily complex mode shapes and pure mode shapes are computed and compared for a building uniform with height. This simplified model is used so that analytical results may be obtained from which trends in the response, particularly the effects of modal coupling, may be seen.⁽⁴¹⁾ It is found that some variables of the response may be significantly larger, by as much as 1.40 to 1.95, than would be expected if uncoupled modes existed. The results indicate that the dynamic effects of accidental eccentricities and the resulting modal coupling may be of major importance, even in buildings that are nominally symmetric.

The symbols used in this chapter are defined below, and wherever possible the symbols of the previous chapters are used.

<u>Symbol</u>	<u>Explanation or definition</u>
A	area of building in plan
g	acceleration of gravity
M_x, M_y	total overturning moments in the x and y directions respectively
M_{xi}, M_{yi}	overturning moments due to the i^{th} modes in the x and y directions respectively.
M_{xu}, M_{yu}	M_x and M_y if $[\phi]$ equals [I]
M_{xiu}, M_{yiu}	M_{xi} and M_{yi} if $[\phi]$ equals [I]
M_{Rx}, M_{Ry}	moments of resistance in the x and y directions respectively
S_v	constant or average velocity spectrum value
S_{vik}	velocity spectrum value at the i^{th} mode in the k^{th} direction
T_{ik}	fundamental period in the k^{th} direction
u	a subscript used to indicate uncoupled modes
V	total base shear in any direction
V_u	V if $[\phi]$ equals [I]
V_x, V_y	total base shears in the x and y directions, respectively
V_{xi}, V_{yi}	base shears due to the i^{th} modes in the x and y directions, respectively

<u>Symbol</u>	<u>Explanation or definition</u>
V_{xu}, V_{yu}	V_x and V_y if $[\phi]$ equals [I]
V_{xiu}, V_{yiu}	V_{xi} and V_{yi} if $[\phi]$ equals [I]
v	base shearing stress at a specific point in a particular direction
v_u	v if $[\phi]$ equals [I]
W_o	average weight of one floor
w_x, w_y	moment arms, one-half the overall plan dimen- sions in the x and y directions respective- ly for a rectangular building
$\{\tilde{x}(z,t)\}_{ik}$	response due to the i^{th} mode in the k^{th} direction
$\{\tilde{x}(z,t)\}_i$	response due to the i^{th} modes
$x_i(z,t), y_i(z,t)$	translational components of $\{x(z,t)\}_i$
x_u, y_u	translational displacements x and y if $[\phi]$ equals [I]
x_s, y_s	coordinates of a point in plan
$\ddot{z}(t)$	ground acceleration in a particular direction
β_k, β_o	constants
ξ	displacement of a specific point in any particular direction
ζ	constant fraction of critical damping
$\theta_i(z,t)$	rotational component of $\{\tilde{x}(z,t)\}_i$
θ_u	rotation θ if $[\phi]$ equals [I]
σ_x, σ_y	root mean square values of components of ground motion

Response to Ground Acceleration

Equation (3-2) is the equation of motion for the continuous model with damping and earthquake excitation. Assuming that the damping is classical, the response can be expressed as a sum of normal modes,

$$\{\tilde{x}(z,t)\} = \sum_{i=1}^{\infty} \sum_{k=1}^3 \eta_{ik}(t) \{\tilde{\psi}_{ik}(z)\} \quad , \quad (5-1)$$

where $\{\tilde{\psi}_{ik}(z)\}$ are the mode shapes as prescribed in Chapter III. It is again assumed that there exists a constant orthogonal matrix $[\phi]$ which diagonalizes $[F(z)]$, and which thereby specifies the amount of coupling between the translational and rotational components of the mode shapes. Equation (5-1) may be substituted into equation (3-2) to obtain

$$\begin{aligned} & \sum_{i=1}^{\infty} \sum_{k=1}^3 m(z) \ddot{\eta}_{ik}(t) \{\tilde{\psi}_{ik}(z)\} + f \left(\sum_{i=1}^{\infty} \sum_{k=1}^3 \dot{\eta}_{ik}(t) \{\tilde{\psi}_{ik}(z)\} \right) \\ & - \sum_{i=1}^{\infty} \sum_{k=1}^3 \eta_{ik}(t) \{[F(z)]\{\tilde{\psi}'_{ik}(z)\}\}' = -m(z)\{\ddot{z}(t)\} \quad . \quad (5-2) \end{aligned}$$

The mode shapes $\{\tilde{\psi}_{ik}(z)\}$ are prescribed by the self-adjoint form, equation (3-11), and it follows that the term $\{[F(z)]\{\tilde{\psi}'_{ik}(z)\}\}'$ may be eliminated from this equation and equation (5-2) giving

$$\sum_{i=1}^{\infty} \sum_{k=1}^3 m(z) [\ddot{\eta}_{ik}(t) + 2\zeta_{ik}\omega_{ik}\dot{\eta}_{ik}(t) + \omega_{ik}^2\eta_{ik}(t)] \{\tilde{\psi}_{ik}(z)\} \\ = -m(z)\{\ddot{\tilde{z}}(t)\} \quad (5-3)$$

where the classical damping assumption, is used with ζ_{ik} being the fraction of critical damping in the appropriate mode.

It has been assumed that there exists a constant orthogonal matrix of modal components $[\phi]$, and hence $\{\tilde{\psi}_{ik}(z)\}$ is given by equation (3-19). Substituting this equation into equation (5-3) and premultiplying both sides of the equation by $[\phi]^T$ gives the equation

$$\sum_{i=1}^{\infty} \sum_{k=1}^3 m(z) [\ddot{\eta}_{ik}(t) + 2\omega_{ik}\zeta_{ik}\dot{\eta}_{ik}(t) + \omega_{ik}^2\eta_{ik}(t)] \rho_{ik}(z) \{\tilde{e}_k\} \\ = -m(z)[\phi]^T\{\ddot{\tilde{z}}(t)\} \quad (5-4)$$

which can readily be uncoupled so that the matrix equation becomes three scalar equations given by

$$\sum_{i=1}^{\infty} m(z) [\ddot{\eta}_{ik}(t) + 2\omega_{ik}\zeta_{ik}\dot{\eta}_{ik}(t) + \omega_{ik}^2\eta_{ik}(t)] \rho_{ik}(z) \\ = -m(z) [\phi_{1k}\ddot{z}_x(z) + \phi_{3k}z_y(t)] \quad \text{for } k = 1, 2, 3. \quad (5-5)$$

Uncoupling, in this convenient way is a consequence of the existence of a constant orthogonal matrix of modal components. Equation (5-5) may now be multiplied by $\rho_{pk}(z)$ and integrated using the orthogonality condition to obtain

$$\ddot{\eta}_{pk}(t) + 2\omega_{pk}\zeta_{pk}\dot{\eta}_{pk}(t) + \omega_{pk}^2\eta_{pk}(t) = \frac{\int_0^{\ell} m(z)\rho_{pk}(z)dz}{\int_0^{\ell} m(z)\rho_{pk}^2(z)dz} [\phi_{1k}\ddot{z}_x(t) + \phi_{3k}\ddot{z}_y(t)]$$

for $k = 1, 2, 3$ $p = 1, 2, \dots$ (5-6)

Equation (5-6) can be solved for each mode of each type using Duhamel's integral. For the system initially at rest

$$\eta_{pk}(t) = \frac{-1}{\omega_{pk}\sqrt{1-\zeta_{pk}^2}} \frac{\int_0^{\ell} m(z)\rho_{pk}(z)dz}{\int_0^{\ell} m(z)\rho_{pk}^2(z)dz} \int_0^t [\phi_{1k}\ddot{z}_x(\tau) + \phi_{3k}\ddot{z}_y(\tau)] e^{-\zeta_{pk}\omega_{pk}(t-\tau)} \sin[\omega_{pk}\sqrt{1-\zeta_{pk}^2}(t-\tau)] d\tau$$

(5-7)

It is seen that, in general, each mode of the structure is excited by both components of the ground motion. By substituting equation (5-7) into equation (5-1) and using equation (3-19), the earthquake response for the continuous system, as a function of height and time, may be written.

$$\{\tilde{x}(z,t)\} = \sum_{i=1}^{\infty} \sum_{k=1}^3 \frac{-\rho_{ik}(z)[\phi]\{\tilde{e}_k\}}{\omega_{ik}\sqrt{1-\zeta_{ik}^2}} \frac{\int_0^{\ell} m(\bar{z})\rho_{ik}(\bar{z})d\bar{z}}{\int_0^{\ell} m(\bar{z})\rho_{ik}^2(\bar{z})d\bar{z}} \int_0^t [\phi_{1k}\ddot{z}_x(\tau) + \phi_{3k}\ddot{z}_y(\tau)] e^{-\zeta_{ik}\omega_{ik}(t-\tau)} \sin[\omega_{ik}\sqrt{1-\zeta_{ik}^2}(t-\tau)] d\tau$$

(5-8)

Simplification of the Ground Acceleration

It is customary to consider the velocity spectrum, spectrum intensity and root mean square of the ground acceleration as measures of the strength of earthquake acceleration. Assuming that the velocity spectrum is nearly constant, the root mean square of the ground acceleration, the spectrum intensity and the velocity spectrum are in relative agreement, especially if a small amount of damping is included.⁽⁴²⁾ With this in mind, a conservative estimate or a bound for the root mean square of the ground motion

given by $\left\{ \frac{1}{T} \int_0^T [\phi_{1k} \ddot{z}_x(\tau) + \phi_{3k} \ddot{z}_y(\tau)]^2 d\tau \right\}^{\frac{1}{2}}$ is sought. Letting $z(t)$

be the larger of $\ddot{z}_x(t)$ and $\ddot{z}_y(t)$ in the r.m.s. sense, the r.m.s. of the ground motion term in (5-8) is conservatively estimated by

$\left\{ \frac{1}{T} [\phi_{1k}^2 + \phi_{3k}^2] \int_0^T \ddot{z}^2(\tau) d\tau \right\}^{\frac{1}{2}}$. Although the r.m.s. values of two perpendicular directions of ground acceleration are not equal in general,⁽⁴²⁾ as can be seen in Table I, they are nearly equal and hence replacement of $\ddot{z}_x(t)$ and $\ddot{z}_y(t)$ by the larger of the two, $\ddot{z}(t)$ is considered satisfactory in view of the purposes of this chapter.

Therefore the ground acceleration term in equation (5-8), $[\phi_{1k} \ddot{z}_x(t) + \phi_{3k} \ddot{z}_y(t)]$, is replaced by $\sqrt{\phi_{1k}^2 + \phi_{3k}^2} \ddot{z}(t)$, or more simply by $\sqrt{1 - \phi_{2k}^2} \ddot{z}(t)$ since the vectors of $[\phi]$ are normalized to unit length.

TABLE I. ⁺ RELATIVE STRONG-MOTION EARTHQUAKE r.m.s. VALUES

Location and Date	Strong-Motion Duration (seconds)	Component	Acceleration r.m.s. ft./sec ²	Acceleration r.m.s. ratios (Maximum over Minimum)
El Centro, Calif. 18 May, 1940	25	x = N.S. y = E.W.	$\sigma_x = 2.20$ $\sigma_y = 1.82$	$\sigma_x/\sigma_y = 1.21$
El Centro, Calif. 30 Dec. 1934	17	x = N.S. y = E.W.	$\sigma_x = 1.43$ $\sigma_y = 1.27$	$\sigma_x/\sigma_y = 1.13$
Olympia, Wash. 13 April 1949	21	x = S80°W y = S10°E	$\sigma_x = 1.95$ $\sigma_y = 1.57$	$\sigma_x/\sigma_y = 1.24$
Taft, Calif. 21 July, 1952	14	x = S69°E y = N21°E	$\sigma_x = 1.45$ $\sigma_y = 1.42$	$\sigma_x/\sigma_y = 1.02$

⁺Housner and Jennings, 1964. (42)

Modal Response of a Uniform Structure

In order that simple results suitable for understanding trends can be found, $[F(z)]$ and $m(z)$ are assumed constant. In this case the model is uniform with height, and the mode shapes are, as indicated by equation (3-24), sinusoidal. Each mode shape has, however, translational and rotational components in general. The boundary conditions imply that the mode shape factors satisfy the equation

$$\rho_{ik}(z) = \sin \frac{(2i-1)\pi z}{2\ell} \quad (5-9)$$

The natural frequencies satisfy equations (3-24) and (3-26), hence

$$\omega_{ik} = (2i-1)\omega_{1k} = \frac{2\pi(2i-1)}{T_{1k}} = \frac{2\pi(2i-1)}{\beta_k n} \quad (5-10)$$

where T_{1k} ($k=1,2,3$) are the fundamental periods and are taken as a constant β_k times the number of stories or levels in the building. β_k is equal to about 1/10 of a second for steel frame structures and about 1/15 of a second for concrete shear wall buildings. As a further simplification guided by experimental results^(2,32,36) the dampings in all the modes is taken to be a constant ζ . Incorporating these assumptions into equation (5-9) with p replaced by i , and including the simplified estimate of the ground motion, it can be shown that

$$\eta_{ik}(t) = \frac{-2\beta_k n \sqrt{1-\zeta^2}}{\pi^2 (2i-1)^2 \sqrt{1-\zeta^2}} \int_0^t \ddot{z}(\tau) e^{\frac{-2\pi(2i-1)\zeta(t-\tau)}{\beta_k n}} \sin\left[\frac{2\pi(2i-1)}{\beta_k n} \sqrt{1-\zeta^2} (t-\tau)\right] d\tau. \quad (5-11)$$

In terms of the velocity spectrum value^(43,44) appropriate for each mode, the maximum value of $\eta_{ik}(t)$ and its derivatives are found to be

$$\begin{aligned} \eta_{ik} \Big|_{\max} &= \frac{2\beta_k n}{\pi^2 (2i-1)^2} \sqrt{1-\phi_{2k}^2} S_{vik} ; \dot{\eta}_{ik} \Big|_{\max} \\ &= \frac{4}{\pi(2i-1)} \sqrt{1-\phi_{2k}^2} S_{vik} ; \ddot{\eta}_{ik} + \frac{4\sqrt{1-\phi_{2k}^2}}{\pi(2i-1)} \ddot{z} \Big|_{\max} = \frac{8}{\beta_k n} \sqrt{1-\phi_{2k}^2} S_{vik} . \end{aligned} \quad (5-12)$$

It is of interest to combine the response in the different modes to determine the relative displacements, relative velocities and absolute accelerations of the structure. From equations (3-7), (3-19) and (5-9) the response due to the i^{th} mode in the k^{th} direction may be written in the form

$$\{\tilde{x}(z,t)\}_{ik} = \eta_{ik}(t) \{\tilde{\psi}_{ik}(z)\} = \eta_{ik}(t) \rho_{ik}(z) \phi_k = \eta_{ik}(t) \phi_k \sin \left[\frac{(2i-1)\pi z}{2\ell} \right] . \quad (5-13)$$

By defining $\{\tilde{x}(z,t)\}_i$ to be the summed response of the three i^{th} modes with components $x_i(z,t)$, $\bar{r}\theta_i(z,t)$ and $y_i(z,t)$, it follows that

$$\{\tilde{x}(z,t)\}_i = \sum_{k=1}^3 \eta_{ik}(t) \phi_k \sin \left[\frac{(2i-1)\pi z}{2\ell} \right] \quad (5-14)$$

from which it follows that

$$\begin{Bmatrix} x_i \\ \bar{F}\theta_i \\ y_i \end{Bmatrix} (z,t) = \begin{bmatrix} \phi_{11} & \phi_{12} & \phi_{13} \\ \phi_{21} & \phi_{22} & \phi_{23} \\ \phi_{31} & \phi_{32} & \phi_{33} \end{bmatrix} \begin{Bmatrix} \eta_{i1} \\ \eta_{i2} \\ \eta_{i3} \end{Bmatrix} (t) \sin \frac{(2i-1)\pi z}{2\ell} .$$

(5-15)

Estimates of $x_i|_{\max}$, etc., are desired so that shears, over-turning moments and other parameters of engineering interest may be calculated. Therefore, it is desirable to find a suitable scheme for combining the components $\eta_{i1}|_{\max}$, $\eta_{i2}|_{\max}$ and $\eta_{i3}|_{\max}$ or their derivatives in the three principle directions. R.m.s. combinations are good estimators of the maxima when the frequencies are well-separated, but even then they are not necessarily conservative. The familiar absolute sum combinations are upper bounds to the response but tend to be inaccurate estimates. As a further complication, when one of the components dominates the others, the difference between r.m.s. and absolute sum combinations is small, but when the components are of the same order, the absolute sum is significantly larger than the r.m.s. value. (45)

The cases of particular interest are those for which modal coupling is significant ($[\phi]$ not near $[I]$), and hence those for which the absolute sum and r.m.s. combinations are significantly different. From discussions in Chapter III it is seen that for many applications at least two of the i^{th} mode natural frequencies will be close together if $[\phi]$ is not near $[I]$ and the eccentricities are small. If the natural frequencies are close together, a beating-type

phenomena takes place during earthquake response and an absolute sum combination of the two modes would be fairly realistic. The beating may take place between all three of the i^{th} natural frequencies, but this seems rather unlikely. Beating between two frequencies is more likely and hence a r.m.s. combination of the absolute sum of the two largest components with the third component seems to be a realistic estimate of the maximum in this case.

It can also be shown that the ratio of the suggested combination to the usual r.m.s. combination of the three modes is at most $\sqrt{2}$. If beating between all three frequencies were to occur, an absolute sum of all three components would be indicated and in comparison with a r.m.s. combination the $\sqrt{2}$ factor would be replaced by $\sqrt{3}$.

Unfortunately, the desired r.m.s. combination of the absolute sum of the two largest components with the third component is difficult to calculate in general whereas a simple r.m.s. combination without absolute sums is easily calculated. Therefore, the usual r.m.s. of the maximized components is found and then multiplied by the scale factor $\sqrt{2}$ in order to achieve a better estimate of the maximum principle motions. This estimate is an upper bound to the desired root mean square combination of the absolute sum of the two largest components with the third component, and it is a useful estimate in the interesting case for which modal coupling is strong.

In the case for which the modes are uncoupled ($[\phi]$ equals $[I]$), the absolute sum and root mean square combinations for

$\{\tilde{x}(z,t)\}_i$ are identical and hence no scale factor should be applied to a r.m.s. combination. These two cases, one for strongly coupled modes and for which $\sqrt{2}$ times the r.m.s. of the maximized components is used, and the other for which the modes are uncoupled, and the scale factor of $\sqrt{2}$ is dropped are examined and compared. To help in the comparative study of the effect of modal coupling, the subscript u will be applied exclusively to all values for which $[\phi]$ equals [1].

Taking β_o and S_v to be average values of the nearly equal β_k 's and S_{vik} 's respectively, one may estimate using equations (5-12) and (5-15) that for strongly coupled modes

$$\begin{bmatrix}
 x_i |_{\max} & \dot{x}_i |_{\max} & \ddot{x}_i + \frac{4\ddot{z}_x \sin\left[\frac{(2i-1)\pi z}{2\ell}\right]}{\pi(2i-1)} \Big|_{\max} \\
 \bar{r}\theta_i |_{\max} & \dot{\bar{r}}\theta_i |_{\max} & \ddot{\bar{r}}\theta_i |_{\max} \\
 y_i |_{\max} & \dot{y}_i |_{\max} & \ddot{y}_i + \frac{4\ddot{z}_y \sin\left[\frac{(2i-1)\pi z}{2\ell}\right]}{\pi(2i-1)} \Big|_{\max}
 \end{bmatrix} = \sqrt{2} S_v \sin\left[\frac{(2i-1)\pi z}{2\ell}\right]$$

$$\begin{bmatrix}
 \sqrt{\phi_{11}^2(1-\phi_{21}^2)+\phi_{12}^2(1-\phi_{22}^2)+\phi_{13}^2(1-\phi_{23}^2)} & 0 & 0 \\
 0 & \sqrt{\phi_{21}^2(1-\phi_{11}^2)+\phi_{22}^2(1-\phi_{12}^2)+\phi_{23}^2(1-\phi_{13}^2)} & 0 \\
 0 & 0 & \sqrt{\phi_{31}^2(1-\phi_{21}^2)+\phi_{32}^2(1-\phi_{22}^2)+\phi_{33}^2(1-\phi_{23}^2)}
 \end{bmatrix}
 \begin{bmatrix}
 \frac{2n\beta_o}{\pi^2(2i-1)^2} & \frac{4}{\pi(2i-1)} & \frac{8}{n\beta_o} \\
 \frac{2n\beta_o}{\pi^2(2i-1)^2} & \frac{4}{\pi(2i-1)} & \frac{8}{n\beta_o} \\
 \frac{2n\beta_o}{\pi^2(2i-1)^2} & \frac{4}{\pi(2i-1)} & \frac{8}{n\beta_o}
 \end{bmatrix}$$

(5-16)

In this case one may determine the maximum responses, as a function of $[\phi]$, to be

$$\left[\begin{array}{l}
 x_i |_{\max} \quad \dot{x}_i |_{\max} \quad \left[\ddot{x}_i + \frac{4\ddot{z}_x \sin \left[\frac{(2i-1)\pi z}{2\ell} \right]}{\pi(2i-1)} \right]_{\max} \\
 \bar{r}\theta_i |_{\max} \quad \dot{\bar{r}}\theta_i |_{\max} \quad \ddot{\bar{r}}\theta_i |_{\max} \\
 y_i |_{\max} \quad \dot{y}_i |_{\max} \quad \left[\ddot{y}_i + \frac{4\ddot{z}_y \sin \left[\frac{(2i-1)\pi z}{2\ell} \right]}{\pi(2i-1)} \right]_{\max}
 \end{array} \right] \leq S_v \sin \left[\frac{(2i-1)\pi z}{2\ell} \right]$$

$$\left[\begin{array}{l}
 \frac{2\sqrt{2} \quad n\beta_o}{\pi^2 (2i-1)^2} \quad \frac{4 \sqrt{2}}{\pi(2i-1)} \quad \frac{8\sqrt{2}}{n\beta_o} \\
 \frac{4 \sqrt{3} \quad n\beta_o}{3\pi^2 (2i-1)^2} \quad \frac{8 \sqrt{3}}{3\pi(2i-1)} \quad \frac{16\sqrt{3}}{3n\beta_o} \\
 \frac{2\sqrt{2} \quad n\beta_o}{\pi^2 (2i-1)^2} \quad \frac{4 \sqrt{2}}{\pi(2i-1)} \quad \frac{8\sqrt{2}}{n\beta_o}
 \end{array} \right] \quad (5-17)$$

If the mode shapes are uncoupled, the absolute sum and root mean square combinations in the principle directions would each have only one component, and hence would be identical; thus as mentioned above the scale factor of $\sqrt{2}$ in equation (5-16) would be dropped and that equation would reduce to

$$\begin{bmatrix}
 x_{iu}|_{\max} & \dot{x}_{iu}|_{\max} & \left[\ddot{x}_{iu} + \frac{4\ddot{z}_x \sin\left[\frac{(2i-1)\pi z}{2\ell}\right]}{\pi(2i-1)} \right]_{\max} \\
 \bar{r}_{i\theta}|_{\max} & \dot{\bar{r}}_{i\theta}|_{\max} & \ddot{\bar{r}}_{i\theta}|_{\max} \\
 y_{iu}|_{\max} & \dot{y}_{iu}|_{\max} & \left[\ddot{y}_{iu} + \frac{4\ddot{z}_y \sin\left[\frac{(2i-1)\pi z}{2\ell}\right]}{\pi(2i-1)} \right]_{\max}
 \end{bmatrix}$$

$$= S_v \sin\left[\frac{(2i-1)\pi z}{2\ell}\right]
 \begin{bmatrix}
 \frac{2n\beta_o}{\pi^2(2i-1)^2} & \frac{4}{\pi(2i-1)} & \frac{8}{n\beta_o} \\
 0 & 0 & 0 \\
 \frac{2n\beta_o}{\pi^2(2i-1)^2} & \frac{4}{\pi(2i-1)} & \frac{8}{n\beta_o}
 \end{bmatrix} \quad (5-18)$$

The maximum relative displacements, relative velocities and absolute accelerations due to the three th_i modes are given by equation (5-17) for coupled modes and by equation (5-18) in the case for which the mode shapes are uncoupled. Most previous research is confined to the case of uncoupled modes, and results such as given by equation (5-17) are not exposed. It is of interest to note that if coupled rotational and translational modes occur, a comparison of equations (5-17) and (5-18) indicates that translational motions may be increased by a factor of $\sqrt{2}$ over that expected from uncoupled modes, and furthermore significant rotational motions may result which are not encountered if only translational modes are studied.

From equations (5-17) and (5-18) it is possible to determine the maximum relative displacements and absolute accelerations at the center of mass of the building, as well as the maximum rotations and rotational accelerations. Two other response values of interest are the average base shear and the overturning moment. By defining V_{xi} , V_{yi} , M_{xi} and M_{yi} to be the contributions of the i^{th} mode to the maximum average base shear and overturning moment in the x and y directions respectively, one may write

$$V_{xi} = \int_0^{\ell} m \left[\ddot{x}_i + \frac{4\ddot{z}_x \sin\left[\frac{(2i-1)\pi z}{2\ell}\right]}{\pi(2i-1)} \right]_{\max} dz, \quad V_{yi} = \int_0^{\ell} m \left[\ddot{y}_i + \frac{4\ddot{z}_y \sin\left[\frac{(2i-1)\pi z}{2\ell}\right]}{\pi(2i-1)} \right]_{\max} dz,$$

$$M_{xi} = \int_0^{\ell} mz \left[\ddot{x}_i + \frac{4\ddot{z}_x \sin\left[\frac{(2i-1)\pi z}{2\ell}\right]}{\pi(2i-1)} \right]_{\max} dz, \quad M_{yi} = \int_0^{\ell} mz \left[\ddot{y}_i + \frac{4\ddot{z}_y \sin\left[\frac{(2i-1)\pi z}{2\ell}\right]}{\pi(2i-1)} \right]_{\max} dz.$$

(5-19)

Furthermore, the average weight of one floor and its tributary mass in an n-story building is

$$W_o = \frac{mg\ell}{n}, \quad (5-20)$$

convenient moments which characterize the structural geometry in the x and y directions are M_{Rx} and M_{Ry} , respectively, where

$$M_{Rx} = mg\ell w_x \quad \text{and} \quad M_{Ry} = mg\ell w_y \quad (5-21)$$

in which w_x and w_y , as shown typically in figure 16, are the appropriate dimensions in the x and y directions. For a rectangular, nominally symmetric, building w_x and w_y may be taken as one-half the overall plan dimensions of the structure.

Equations (5-16) through (5-21) are combined to give equations for the base shears and overturning moments in both the strongly coupled and uncoupled cases.

$$V_{xi} = \frac{16\sqrt{2} W_o S_v}{\beta_o g \pi (2i-1)} \sqrt{\phi_{11}^2 (1-\phi_{21}^2) + \phi_{12}^2 (1-\phi_{22}^2) + \phi_{13}^2 (1-\phi_{23}^2)} \leq \frac{16\sqrt{2} W_o S_v}{\beta_o g \pi (2i-1)},$$

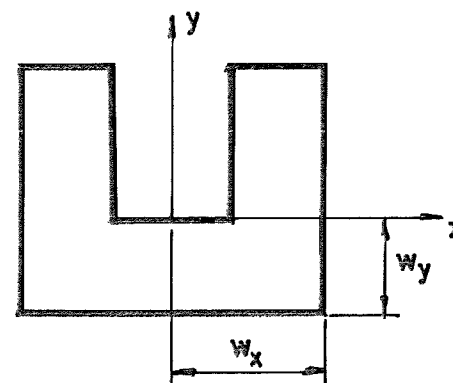
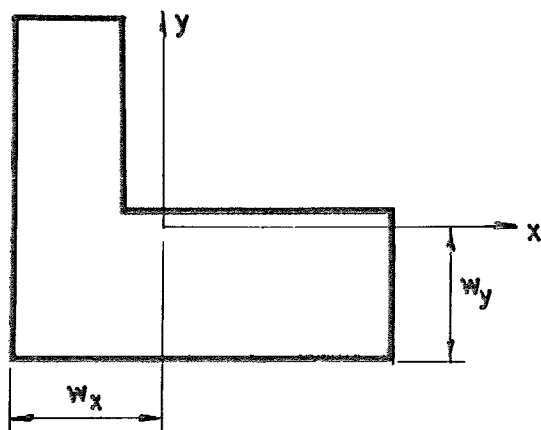
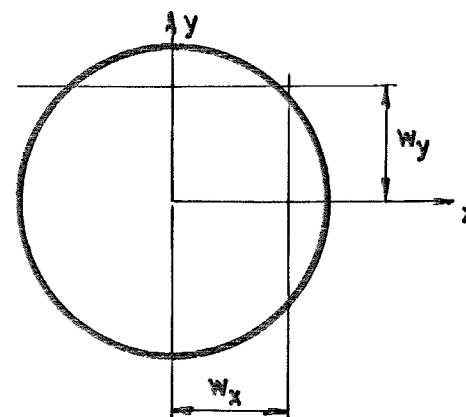
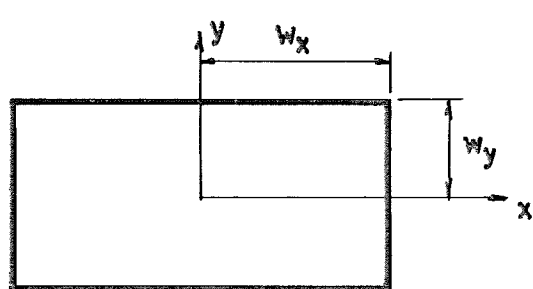
$$V_{yi} = \frac{16\sqrt{2} W_o S_v}{\beta_o g \pi (2i-1)} \sqrt{\phi_{31}^2 (1-\phi_{21}^2) + \phi_{32}^2 (1-\phi_{22}^2) + \phi_{33}^2 (1-\phi_{23}^2)} \leq \frac{16\sqrt{2} W_o S_v}{\beta_o g \pi (2i-1)},$$

$$V_{xiu} = \frac{16 W_o S_v}{\beta_o g \pi (2i-1)} \quad \text{and} \quad V_{yiu} = \frac{16 W_o S_v}{\beta_o g \pi (2i-1)}. \quad (5-22)$$

$$\frac{M_{xi}}{M_{Rx}} = \frac{32\sqrt{2} h S_v}{\beta_o g w_x \pi^2 (2i-1)^2} \sqrt{\phi_{11}^2 (1-\phi_{21}^2) + \phi_{12}^2 (1-\phi_{22}^2) + \phi_{13}^2 (1-\phi_{23}^2)} \leq \frac{32\sqrt{2} h S_v}{\beta_o g w_x \pi^2 (2i-1)^2}$$

$$\frac{M_{yi}}{M_{Ry}} = \frac{32\sqrt{2} h S_v}{\beta_o g w_y \pi^2 (2i-1)^2} \sqrt{\phi_{31}^2 (1-\phi_{21}^2) + \phi_{32}^2 (1-\phi_{22}^2) + \phi_{33}^2 (1-\phi_{23}^2)} \leq \frac{32\sqrt{2} h S_v}{\beta_o g w_y \pi^2 (2i-1)^2}$$

$$\frac{M_{xiu}}{M_{Rx}} = \frac{32 h S_v}{\beta_o g w_x \pi^2 (2i-1)^2} \quad \text{and} \quad \frac{M_{yiu}}{M_{Ry}} = \frac{32 h S_v}{\beta_o g w_y \pi^2 (2i-1)^2}. \quad (5-23)$$



Moment arms for some floor plans

CHARACTERISTIC MOMENT ARMS FOR OVERTURNING

Figure 16

Total Response

The above response contributions for the n modes can be summed now over i to estimate the total responses of the building. The natural frequencies are arranged in a harmonic pattern as given by equation (5-10) and it is assumed that beating of different ith frequencies is not a significant factor. Therefore, r.m.s. combinations of the modal contributions are satisfactory estimates of the maxima of total responses.

The maximum relative displacement and absolute acceleration responses occur at the top of the structure where z equals ℓ, and, using a r.m.s. combination for an infinite number of modal contributions the maximum relative displacements are first estimated.

$$\begin{aligned}
 x \Big|_{\max} &\approx \frac{\sqrt{3} n \beta_o S_v}{6} \sqrt{\phi_{11}^2 (1-\phi_{21}^2) + \phi_{12}^2 (1-\phi_{22}^2) + \phi_{13}^2 (1-\phi_{23}^2)} \leq \frac{\sqrt{3} n \beta_o S_v}{6} , \\
 \bar{r}\theta \Big|_{\max} &\approx \frac{\sqrt{3} n \beta_o S_v}{6} \sqrt{\phi_{21}^2 (1-\phi_{21}^2) + \phi_{22}^2 (1-\phi_{22}^2) + \phi_{23}^2 (1-\phi_{23}^2)} \leq \frac{\sqrt{2} n \beta_o S_v}{6} , \text{ and} \\
 y \Big|_{\max} &\approx \frac{\sqrt{3} n \beta_o S_v}{6} \sqrt{\phi_{31}^2 (1-\phi_{21}^2) + \phi_{32}^2 (1-\phi_{22}^2) + \phi_{33}^2 (1-\phi_{23}^2)} \leq \frac{\sqrt{3} n \beta_o S_v}{6} .
 \end{aligned}$$

(5-24)

The maximum absolute accelerations are estimated by an r.m.s. combination of n modal contributors, as would be appropriate for a finite model of an n-story building.

$$[\ddot{x} + \ddot{z}_x]_{\max} \approx \frac{8\sqrt{2} S_v}{\sqrt{n} \beta_o} \sqrt{\phi_{11}^2 (1 - \phi_{21}^2) + \phi_{12}^2 (1 - \phi_{22}^2) + \phi_{13}^2 (1 - \phi_{23}^2)} \leq \frac{8\sqrt{2} S_v}{\sqrt{n} \beta_o}$$

$$\bar{r}\ddot{\theta} \Big|_{\max} \approx \frac{8\sqrt{2} S_v}{\sqrt{n} \beta_o} \sqrt{\phi_{21}^2 (1 - \phi_{21}^2) + \phi_{22}^2 (1 - \phi_{22}^2) + \phi_{23}^2 (1 - \phi_{23}^2)} \leq \frac{16\sqrt{3} S_v}{3\sqrt{n} \beta_o} \quad \text{and}$$

$$[\ddot{y} + \ddot{z}_y]_{\max} \approx \frac{8\sqrt{2} S_v}{\sqrt{n} \beta_o} \sqrt{\phi_{31}^2 (1 - \phi_{21}^2) + \phi_{32}^2 (1 - \phi_{22}^2) + \phi_{33}^2 (1 - \phi_{23}^2)} \leq \frac{8\sqrt{2} S_v}{\sqrt{n} \beta_o} .$$

(5-25)

The same process may be applied to the case for which uncoupled mode shapes exist. Using the subscript u, it follows that equations (5-24) and (5-25) are replaced by

$$x_u \Big|_{\max} \approx y_u \Big|_{\max} \approx \frac{\sqrt{6} n \beta_o S_v}{12} , \quad \bar{r}\theta \Big|_{\max} \approx 0 ,$$

$$[\ddot{x}_u + \ddot{z}_x]_{\max} \approx [\ddot{y}_u + \ddot{z}_y]_{\max} \approx \frac{8S_v}{\sqrt{n} \beta_o} \quad \text{and} \quad \bar{r}\ddot{\theta} \Big|_{\max} \approx 0. \quad (5-26)$$

The modal contributions to the maximum average base shears and overturning moments in the two translational directions are now summed using r.m.s. combinations (with $n \rightarrow \infty$) into total average base shears and total overturning moment ratios. Using equation (5-22) the total base shears are estimated.

$$\begin{aligned}
 v_x &\approx \frac{8W_o S_v}{\beta_o g} \sqrt{\phi_{11}^2 (1-\phi_{21}^2) + \phi_{12}^2 (1-\phi_{22}^2) + \phi_{13}^2 (1-\phi_{23}^2)} \leq \frac{8W_o S_v}{\beta_o g} , \\
 v_y &\approx \frac{8W_o S_v}{\beta_o g} \sqrt{\phi_{31}^2 (1-\phi_{21}^2) + \phi_{32}^2 (1-\phi_{22}^2) + \phi_{33}^2 (1-\phi_{23}^2)} \leq \frac{8W_o S_v}{\beta_o g} \\
 v_{xu} &\approx \frac{4\sqrt{2} W_o S_v}{\beta_o g} \quad \text{and} \quad v_{yu} \approx \frac{4\sqrt{2} W_o S_v}{\beta_o g} . \tag{5-27}
 \end{aligned}$$

The total overturning moment ratios are similarly estimated.

$$\begin{aligned}
 \frac{M_x}{M_{Rx}} &\approx \frac{8\sqrt{3} hS_v}{3\beta_o gw_x} \sqrt{\phi_{11}^2 (1-\phi_{21}^2) + \phi_{12}^2 (1-\phi_{22}^2) + \phi_{13}^2 (1-\phi_{23}^2)} \leq \frac{8\sqrt{3} hS_v}{3\beta_o gw_x} , \\
 \frac{M_y}{M_{Ry}} &\approx \frac{8\sqrt{3} hS_v}{3\beta_o gw_y} \sqrt{\phi_{31}^2 (1-\phi_{21}^2) + \phi_{32}^2 (1-\phi_{22}^2) + \phi_{33}^2 (1-\phi_{23}^2)} \leq \frac{8\sqrt{3} hS_v}{3\beta_o gw_y} , \\
 \frac{M_{xu}}{M_{Rx}} &\approx \frac{4\sqrt{6} hS_v}{3\beta_o gw_x} \quad \text{and} \quad \frac{M_{yu}}{M_{Ry}} \approx \frac{4\sqrt{6} hS_v}{3\beta_o gw_y} . \tag{5-28}
 \end{aligned}$$

Consider now responses which result from a combination of x-directed and y-directed motions, that is, relative or absolute responses in an arbitrary direction. The maxima of such responses may be maximum relative displacements, absolute accelerations or

base shearing forces. A reasonable yet conservative estimate of the maximum response considered is the square root of the sum of the squares of the maximum x and y responses, and this type of estimate is used where applicable. Let ξ be the displacement of any point of the structure in any horizontal direction.

If the matrix $[\phi]$ is equal to the identity matrix, then the motion at every point at every level of the structure is the same as the center of mass motion at that level, for no rotation is present. Therefore, the maximum translational displacements and accelerations occur at every point of the top of the structure, including the centroid, and the maximum shearing stress at the base times the floor area is equal to the average of the maximum base shear. Then from equation (5-26) it follows that the maximum relative displacement for uncoupled modes is given by

$$\xi_u \Big|_{\max} = \frac{\sqrt{3} n \beta_o S_v}{6} \quad (5-29)$$

while the maximum absolute acceleration is given by

$$[\ddot{\xi}_u + \ddot{z}]_{\max} = \frac{8\sqrt{2} S_v}{\sqrt{n} \beta_o} \quad (5-30)$$

where \ddot{z} is the ground acceleration in the ξ direction.

Let the total shearing force in an arbitrary direction be V . Then from equation (5-27) the maximum base shear is given by

$$v_u \Big|_{\max} = \frac{8W_o S v}{\beta_o g} \quad (5-31)$$

and the average stress v_u is

$$v_u \Big|_{\max} = \frac{8W_o S v}{\beta_o g A} \quad (5-32)$$

If there is strong modal coupling, for example, then rotation will cause the responses to depend upon their location in plan. The maximum relative displacements of a point at x_s and y_s relative to the centroidal axis are given by $[x - y_s \theta]_{\max}$ and $[y + x_s \theta]_{\max}$ respectively, and the same formulation applies to absolute accelerations and base shearing stresses. The maximum relative displacement is estimated by

$$\xi \Big|_{\max} = \sqrt{[x - y_s \theta]_{\max}^2 + [y + x_s \theta]_{\max}^2} \quad (5-33)$$

At any particular time the x , y and θ motions are completely specified. Therefore, if the building is of rectilinear form in plan, the maximum of ξ , which occurs when both $[x - y_s \theta]^2$ and $[y + x_s \theta]^2$ are at their respective independent maxima, occurs at an exterior corner. For simplicity consider rectangular buildings, then $\xi \Big|_{\max}$ occurs at one of the four corners for which

$$x_s^2 + y_s^2 = 3r^2 \quad (5-34)$$

Use of an r.m.s. modal combination results in the equation

$$\xi \Big|_{\max} \approx \frac{\sqrt{6} n \beta_o S_v}{6}$$

$$\sqrt{2 - \left[\frac{-y_s}{\bar{r}} (\phi_{21}^3 \phi_{11} + \phi_{22}^3 \phi_{12} + \phi_{23}^3 \phi_{13}) + (\phi_{21}^4 + \phi_{22}^4 + \phi_{23}^4) + \frac{x_s}{\bar{r}} (\phi_{21}^3 \phi_{31} + \phi_{22}^3 \phi_{32} + \phi_{23}^3 \phi_{33}) \right]} \quad (5-35)$$

which for a rectangular building is subject to equation (5-34). The radical on the right hand side of equation (5-35), as a function of the orthogonal matrix $[\phi]$, is maximized by 1.38 for any rectangular building and hence one may write

$$\xi \Big|_{\max} \leq 1.38 \left(\frac{\sqrt{6} n \beta_o S_v}{6} \right) . \quad (5-36)$$

The same approach may be applied to find the maximum absolute acceleration, $\ddot{\xi} + \ddot{z}$, for a nominally symmetric rectangular building, and it follows that

$$[\ddot{\xi} + \ddot{z}]_{\max} \approx \frac{16S_v}{\beta_o \sqrt{n}}$$

$$\sqrt{2 - \left[\frac{-y_s}{\bar{r}} (\phi_{21}^3 \phi_{11} + \phi_{22}^3 \phi_{12} + \phi_{23}^3 \phi_{13}) + (\phi_{21}^4 + \phi_{22}^4 + \phi_{23}^4) + \frac{x_s}{\bar{r}} (\phi_{21}^3 \phi_{31} + \phi_{22}^3 \phi_{32} + \phi_{23}^3 \phi_{33}) \right]} \quad (5-37)$$

where equation (5-34) is satisfied. Consequently the equation

$$[\ddot{\xi} + \ddot{z}]_{\max} \leq 1.38 \left(\frac{16S_v}{\beta_o \sqrt{n}} \right) , \quad (5-38)$$

which is applicable to a uniform rectangular building of arbitrary relative dimensions, results.

Again the same approach may be applied to determine that the maximum base shear and base shearing stress are given by the equations

$$v|_{\max} = \frac{8W_o S_v}{\beta_o g} \sqrt{(1-\phi_{21}^2)^2 + (1-\phi_{22}^2)^2 + (1-\phi_{23}^2)^2} \leq \frac{8\sqrt{2} W_o S_v}{\beta_o g} \quad \text{and} \quad (5-39)$$

$$v|_{\max} = \frac{8\sqrt{2} W_o S_v}{\beta_o g A}$$

$$\sqrt{2 - \left[\frac{-y_s}{r} (\phi_{21}^3 \phi_{11} + \phi_{22}^3 \phi_{12} + \phi_{23}^3 \phi_{13}) + (\phi_{21}^4 + \phi_{22}^4 + \phi_{23}^4) + \frac{x_s}{r} (\phi_{21}^3 \phi_{31} + \phi_{22}^3 \phi_{32} + \phi_{23}^3 \phi_{33}) \right]} \quad (5-40)$$

As a consequence of equation (5-40) the base shearing stress for a nominally symmetric rectangular building satisfies the equation

$$v|_{\max} \leq 1.38 \left(\frac{8\sqrt{2} W_o S_v}{\beta_o g A} \right) \quad (5-41)$$

for which equality is a distinct possibility.

In this section it is seen that the maximum relative displacements and absolute accelerations of the center of mass, as well as average or total base shears and overturning moments may be $\sqrt{2}$ or about 40% larger than would be expected if the mode shapes are assumed uncoupled, and that significant rotational motions, not present if

the modes are uncoupled may exist. Furthermore, the combination of translational and rotational motions may account for a local relative displacement, absolute acceleration or base shearing stresses which are $1.38 \sqrt{2}$ or about 1.95 times larger than would be expected if the modes are assumed uncoupled.

These observations of the response of a simplified structure suggest that the calculations of earthquake response, based upon the assumption that the modes are uncoupled, may significantly underestimate the true response, particularly near the perimeter of the structure. Therefore, in designing tall buildings to resist earthquakes, it is recommended that either specific provisions, which guarantee that the modes are essentially uncoupled, be designed into the structure or that the determination of earthquake response include the possibility of strong modal coupling.

VI. APPLICATION TO THE SAN DIEGO GAS AND ELECTRIC BUILDING

Introduction

In the interest of developing a practical understanding for the work presented in the foregoing chapters, the San Diego Gas and Electric Company building is presented as an example of a tall building which possesses many of the major characteristics described earlier. It was noted in Chapter Three that a rectangular building with small eccentricities and a smooth, uniform dispersion of columns could have nearly equal fundamental periods in the three directions of motion, and hence strong modal coupling. The example chosen appears to fit these conditions and should have strong modal coupling in the vibration tests.⁽²⁾ It is seen as expected that the results of Chapter Three, being too restrictive, do not apply directly to the example and the perturbation method developed in Chapter Four is used instead. With the aid of an approximate, constant matrix of modal components determined from perturbation theory, the building response is examined to determine representative values for the eccentricities. Finally the results of Chapter Five are applied to extract the estimated earthquake response of the structure and to compare this response with that expected if the mode shapes were uncoupled.

The notation is the same as in previous chapters, and new symbols introduced in this chapter are given below.

<u>Symbol</u>	<u>Explanation or definition</u>
$\bar{F}(z)$	force defined by equation (6-6)
f_1, f_2, f_3	fundamental frequencies indexed in order of increasing frequency
$[\hat{\phi}]$	matrix of mode shapes as determined from 20th floor motions only
$[\phi]_{AN}$	$[\phi]_A$ with normalized vectors
$[\phi]_{AN_2}$	an approximation to $[\phi]_{AN}$

A Description of the Building

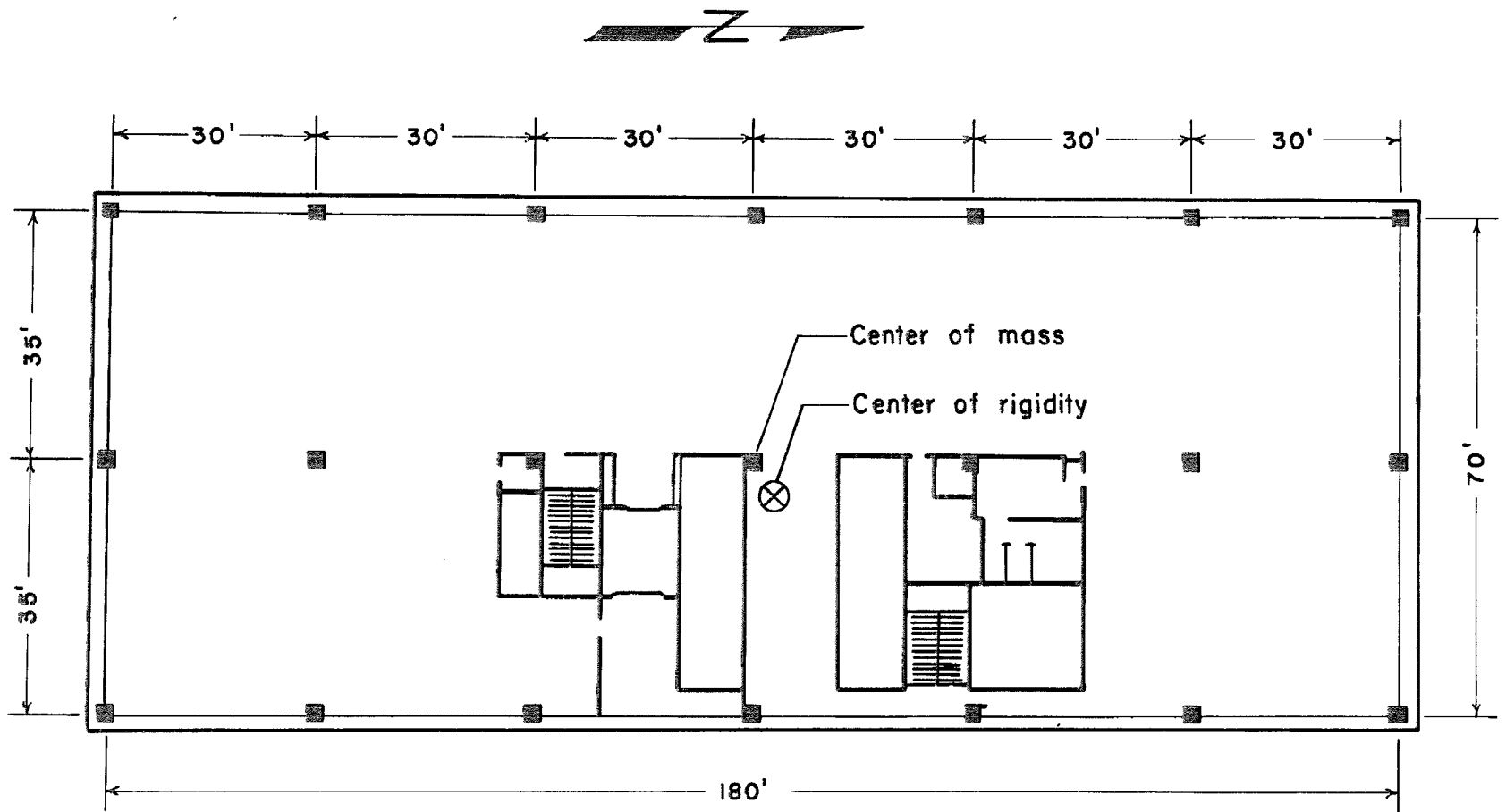
The San Diego Gas and Electric Building, located in downtown San Diego, consists of two buildings, a 22-story tower and a two-story U-shaped building separated from the tower by 3 inch seismic joints. The 291 foot tower portion is a moment resistant, ductile steel frame with the framing and mass distributed in nearly two-fold plan symmetry. A photograph of the building is shown in figure 17 while figure 18 displays a typical floor plan of the building.

Forced vibration tests using vibration generators located on the twentieth floor have recently been conducted.⁽⁴⁶⁾ From these tests it was possible to determine an approximate matrix of modal components for the three fundamental modes based exclusively on motions at the twentieth floor. The resulting matrix defined by $[\hat{\phi}]$ is not orthogonal but its vectors are normalized in a Euclidean sense.



SAN DIEGO GAS AND ELECTRIC BUILDING

Figure 17



-125-

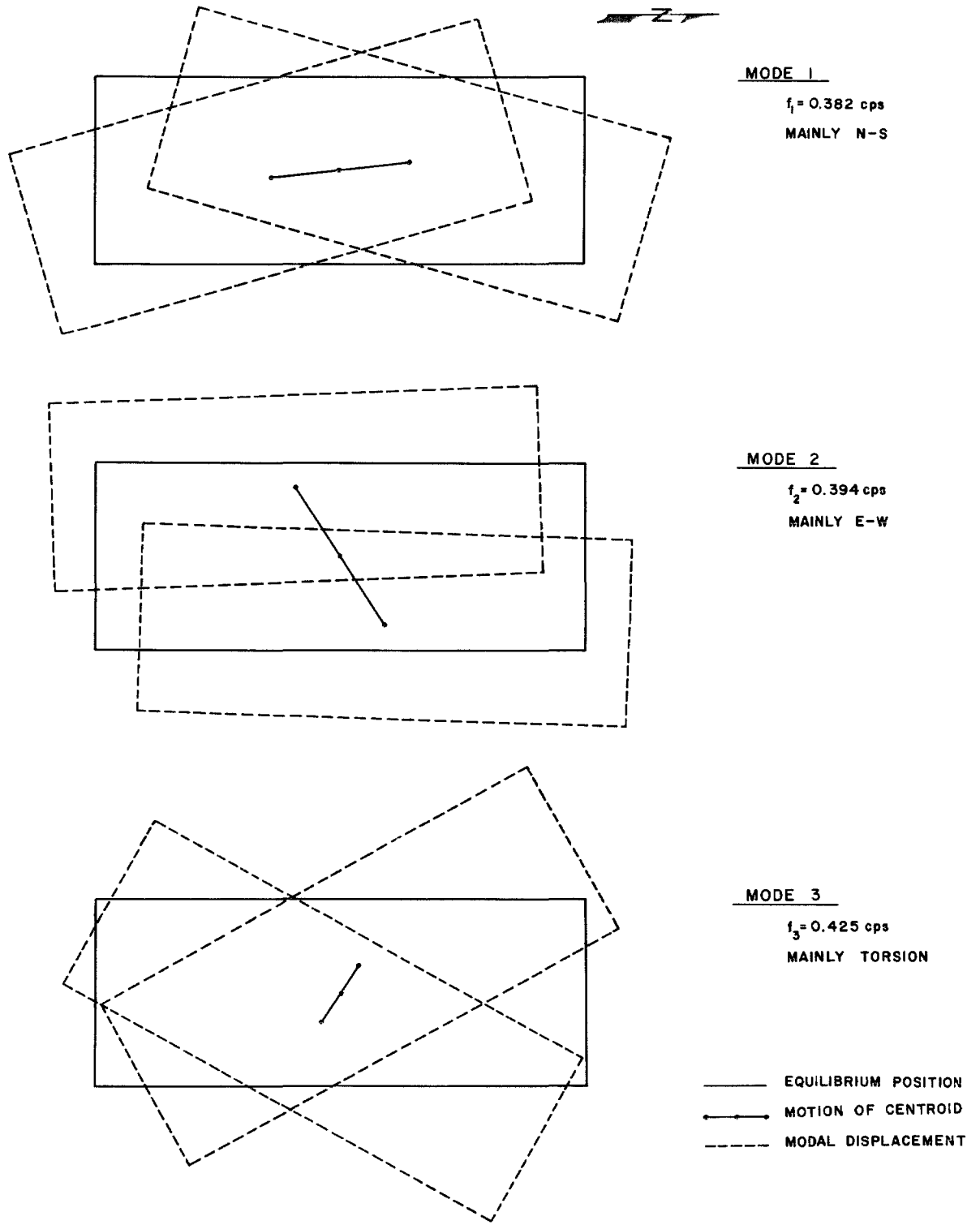
TYPICAL PLAN, 4th - 17th FLOORS
 SAN DIEGO GAS & ELECTRIC BUILDING

Figure 18

$$[\hat{\phi}] = \begin{bmatrix} 0.85 & -0.54 & -0.21 \\ 0.52 & -0.07 & 0.92 \\ 0.09 & 0.84 & -0.33 \end{bmatrix} \quad (6-1)$$

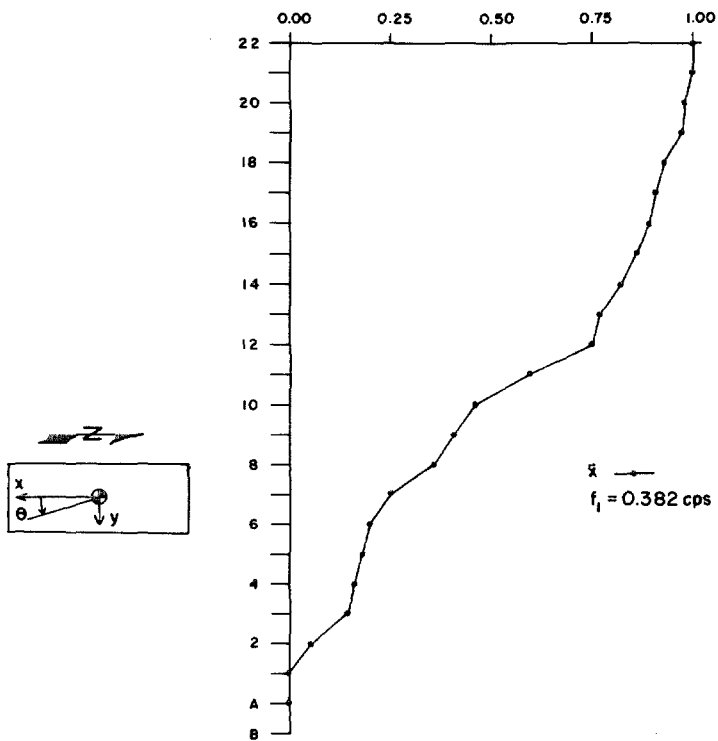
where the first, second and third columns of $[\hat{\phi}]$ represent the approximate mode shapes associated with the frequencies $f_1 = 0.382$ cps, $f_2 = 0.394$ cps, and $f_3 = 0.425$ cps, respectively. The mode shapes so determined may be displayed as shown in figure 19 which indicates the motion of the twentieth floor vibrating in each of the fundamental mode shapes. The motion, which is necessarily exaggerated for display purposes, proceeds from one dashed outline to the other through the solid outline which represents the equilibrium position of the floor. The motion of the center of mass is also indicated in figure 19.

If the matrix of modal components is constant with height, it is also orthogonal. (Appendix I). Plots of the three components of the fundamental mode shapes shown in figures 20 and 21 indicate that the \ddot{x} , $\ddot{\bar{\theta}}$ and \ddot{y} motions are in a nearly constant ratio for the full height of the building.⁽²⁾ This indicates that the associated eigenvectors in the matrix of modal components, as determined at any level, are nearly the same and hence there is a constant orthogonal matrix of modal components, $[\phi]$, representative of the whole structure. Because of insufficient data it was not possible to determine a matrix of modal components for every level, and so $[\phi]$ was not determined as an average of such matrices. Instead $[\phi]$ was determined by finding

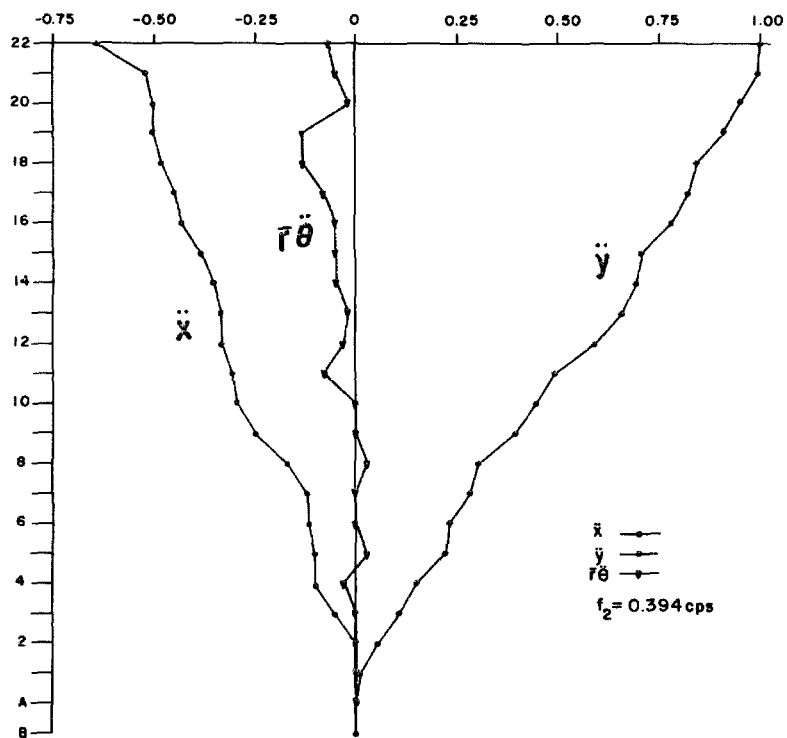


FUNDAMENTAL MODES AT THE 20th FLOOR

Figure 19



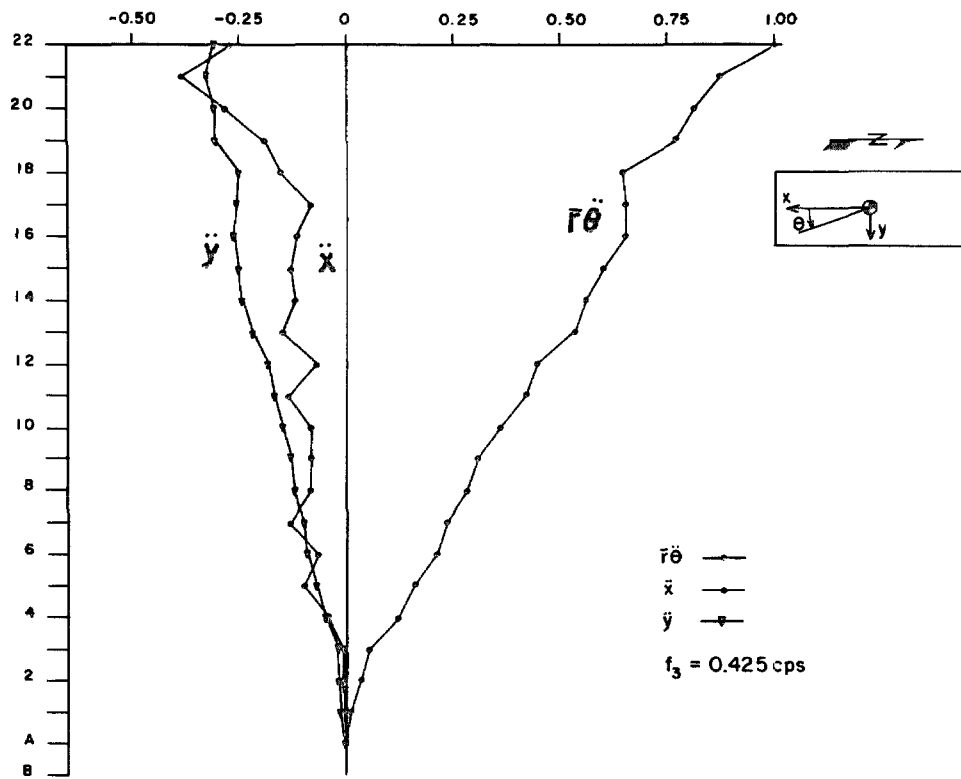
FIRST MODE SHAPE
(N-S MOTION ONLY)



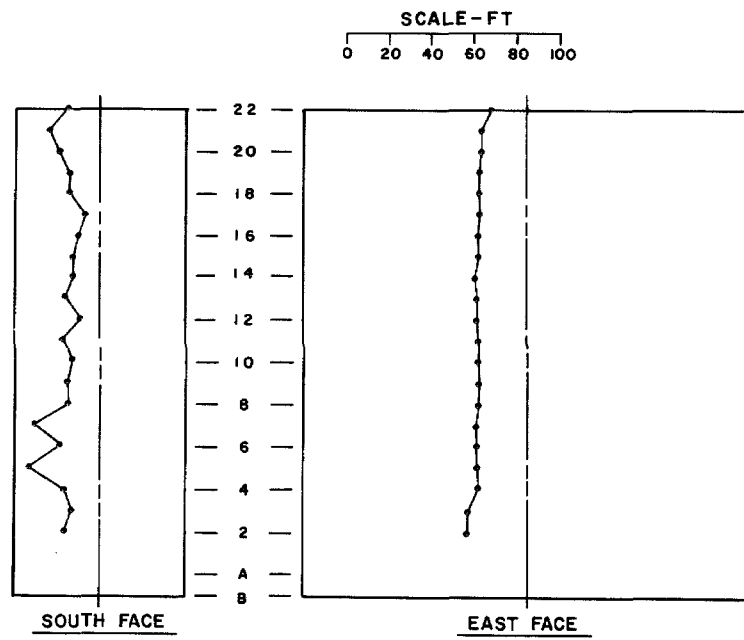
SECOND MODE SHAPE

FIRST AND SECOND FUNDAMENTAL MODES

Figure 20



MODE SHAPE



CENTER OF ROTATION

THIRD FUNDAMENTAL MODE

Figure 21

a best orthogonal fit to $[\hat{\phi}]$, the twentieth floor estimate of the matrix of modal components, which was taken to be representative choice for $[\phi]$. The orthogonal matrix so determined is given by

$$[\phi] = \begin{bmatrix} 0.82 & -0.41 & -0.43 \\ 0.49 & 0.10 & 0.87 \\ 0.30 & 0.91 & -0.28 \end{bmatrix} \quad (6-2)$$

The vectors of the matrices $[\hat{\phi}]$ and $[\phi]$ are graphed in \ddot{x} (South) \ddot{y} (East) space as shown in figure 22 to indicate the nearness of $[\phi]$ to $[\hat{\phi}]$.

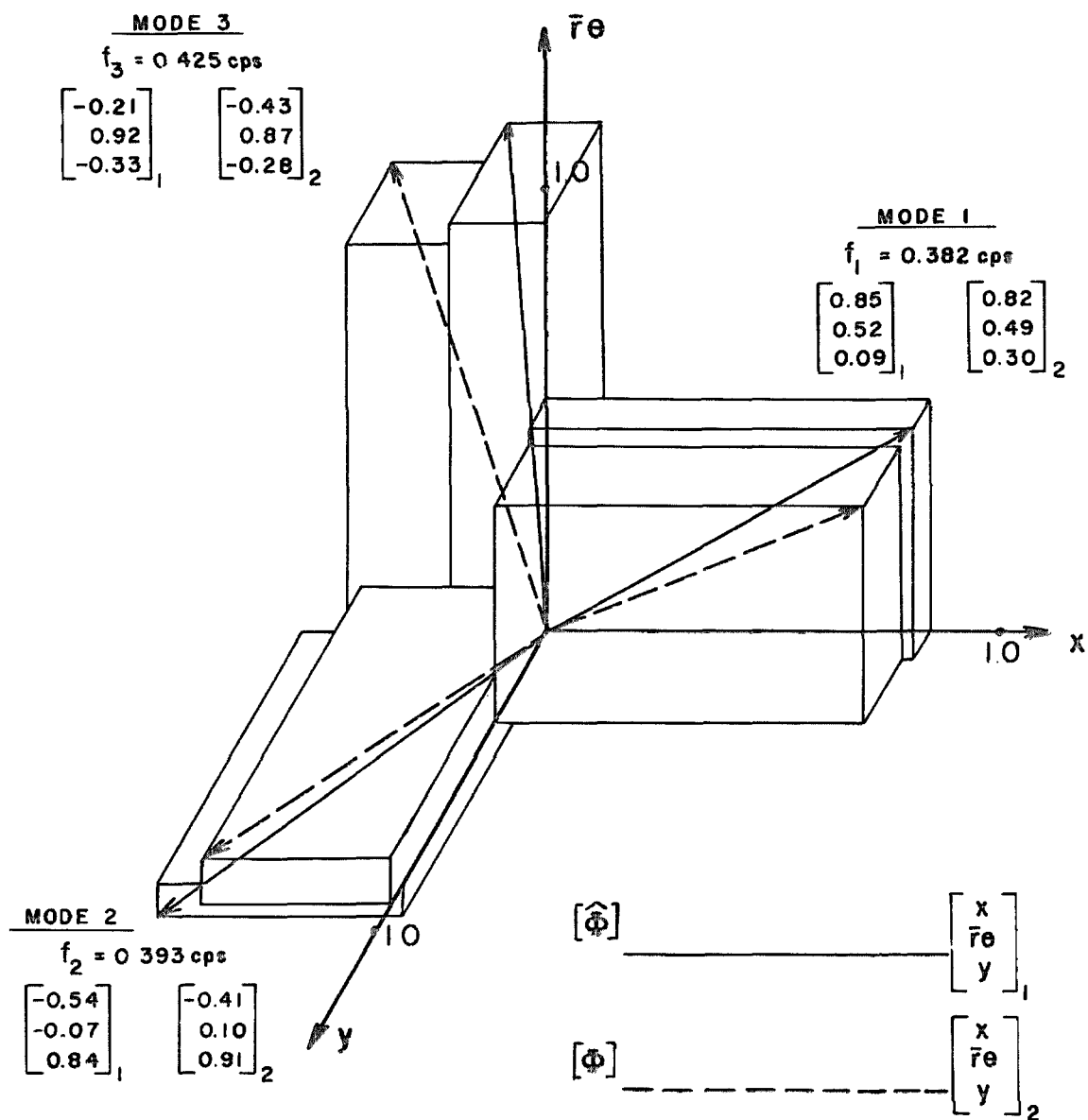
Locating the Center of Rigidity

Since the mode shapes have nearly equal relative components of motion⁽²⁾ it is assumed that equation (6-2) adequately describes the matrix $[\phi]$ for the full height of the structure. From equation (3-18) the matrix $[F(z)]$ can be deduced if $[F_\lambda(z)]$ along with $[\phi]$ is known. The plotted mode shapes for the three fundamental modes are nearly of the same shape, approximately a straight line as seen in figures 20 and 21. Using this straight line approximation equation (3-24) can be integrated to produce

$$F_k(z) = \frac{\omega_{1k}^2}{\rho_{1k}(z)} \int_z^\ell m(\bar{z}) \rho_{1k}(\bar{z}) d\bar{z} = \frac{\omega_{1k}^2}{\rho_1(z)} \int_z^\ell m(\bar{z}) \rho_1(\bar{z}) d\bar{z}$$

for $k = 1, 2, 3$ (6-3)

where $\rho_1(z)$ is the linear mode shape factor for each of the three



NORMALIZED FUNDAMENTAL MODES - 20th FLOOR

Figure 22

fundamental modes.

It is seen in equation (6-3) that the k dependence of $F_k(z)$ is assumed only by the natural frequencies ω_{1k} . Therefore equation (6-3) can be written as

$$F_k(z) = (2\pi f_k)^2 \bar{F}(z) \quad \text{for } k = 1, 2, 3 \quad (6-4)$$

where

$$2\pi f_k = \omega_{1k} \quad \text{for } k = 1, 2, 3, \quad (6-5)$$

and for simplicity

$$\bar{F}(z) = \frac{1}{\rho_1'(z)} \int_z^{\lambda} m(\bar{z}) \rho_1(\bar{z}) d\bar{z} \quad (6-6)$$

Substituting the experimentally determined values for the three fundamental frequencies f_1 , f_2 and f_3 , as listed in figure 19, into equation (6-4) produces $[F_\lambda(z)]$.

$$[F_\lambda(z)] = \bar{F}(z) \begin{bmatrix} 5.755 & 0 & 0 \\ 0 & 6.091 & 0 \\ 0 & 0 & 7.124 \end{bmatrix} \quad (6-7)$$

Equations (6-2) and (6-7) are now substituted into equation (3-18) so that $[F(z)]$ may be determined.

$$[F(z)] = \bar{F}(z) \begin{bmatrix} 6.050 & -0.518 & 0.043 \\ -0.518 & 6.791 & -0.299 \\ 0.043 & -0.299 & 6.142 \end{bmatrix} \quad (6-8)$$

A comparison of equations (3-5) and (6-8) indicates that the eccentricity ratios are given by

$$\frac{\bar{y}_f}{\bar{r}} = \frac{0.518}{6.050} = 0.0856 \quad \text{and} \quad (6-9)$$

$$\frac{\bar{x}_f}{\bar{r}} = \frac{-0.299}{6.142} = -0.0487 \quad . \quad (6-10)$$

For the San Diego Gas and Electric Building \bar{r} is approximately equal to 55.7 ft., based on a uniform mass distribution over the 70 ft. by 180 ft. floor area. Use of this value for \bar{r} in equation (6-9) and (6-10) gives

$$\bar{y}_f = 4.77 \text{ ft.}, \quad \bar{x}_f = -2.71 \text{ ft.}, \quad \text{and} \quad \sqrt{\bar{x}_f^2 + \bar{y}_f^2} = 5.49 \text{ ft.} \quad (6-11)$$

Based upon the assumption that the center of mass and the center of area are coincident, the approximate location of the center of rigidity is shown in figure 18. It is of interest to note that although the center of mass and center of rigidity for this structure are separated by only 5.49 ft., compared to overall dimensions of 70 ft., by 180 ft., strong modal coupling is present. This result is a direct consequence of the closeness of the natural frequencies.

From equation (3-5) which follows directly from the equations of motion for the continuous model it is seen that the upper right and lower left hand corner elements of $[F(z)]$ are zero. In equation (6-8) these elements are small, indicating that the matrix $[\phi]$ chosen to represent the mode shapes of the San Diego Gas and Electric Building is, in this sense at least, compatible with the observed natural frequencies.

Application of the Approximate and Perturbation Analyses

As another approach to the problem, assume that $[F(z)]$ is given by equation (6-8) and determine the natural frequencies and matrix of modal components which result. Using the perturbation theory for perturbation about $[I]$ or the equivalent approximate analysis defined in Chapter III for $[\phi]$ near $[I]$, it is possible to determine to second order the relative natural frequencies and to first order the matrix of modal components.

Because of the fact that the fundamental frequencies and hence the diagonal elements of $[F(z)]$ for the San Diego Gas and Electric Building are labeled in increasing order of magnitude, and because of the fact that F_2 is larger than F_3 as calculated from equations (3-41) and (3-42), the values of F_2 and F_3 as well as the second and third rows of $[\phi]$ as determined from the approximate analysis are interchanged. Thus from equations (3-40) through (3-42), with $[F(z)]$ from (6-8)

$$\begin{aligned}
 F_1 &= \left\{ 6.050 + \frac{(-0.518)^2}{(6.050 - 6.791)} \right\} \bar{F}(z) = 5.687 \bar{F}(z) \quad , \\
 F_2 &= \left\{ 6.142 + \frac{(-0.299)^2}{(6.142 - 6.791)} \right\} \bar{F}(z) = 6.003 \bar{F}(z) \quad \text{and} \\
 F_3 &= \left\{ 6.791 + \frac{(-0.518)^2}{(6.791 - 6.050)} + \frac{(-0.299)^2}{(6.791 - 6.142)} \right\} \bar{F}(z) = 7.293 \bar{F}(z) \quad .
 \end{aligned}$$

(6-12)

The approximate natural frequencies as determined from this equation and equation (6-4) are given by

$$f_1 = 0.380 \text{ cps.}, f_2 = 0.391 \text{ cps.}, \text{ and } f_3 = 0.430 \text{ cps.} \quad (6-13)$$

It is seen, as expected, that these values are in close agreement with the experimentally determined values for the fundamental natural frequencies as listed in figure 19.

The matrix $[\phi]_A$ given by equation (3-47), with the second and third rows interchanged is

$$[\phi]_A = \begin{bmatrix} 1 & 5.15 & -0.70 \\ 0.70 & 0.47 & 1 \\ 0.46 & 1 & -0.47 \end{bmatrix}. \quad (6-14)$$

Normalizing the eigenvectors of $[\phi]_A$ gives the matrix $[\phi]_{AN}$ where

$$[\phi]_{AN} = \begin{bmatrix} 0.77 & 0.98 & -0.54 \\ 0.54 & 0.09 & 0.77 \\ 0.35 & 0.19 & -0.36 \end{bmatrix}. \quad (6-15)$$

The first and third columns, or eigenvectors of $[\phi]_{AN}$ are in close agreement with the corresponding columns of $[\phi]$ as given by equation (6-2). However, because the approximate or perturbation theory is not applicable, the second columns disagree radically. It is seen that the largest component of the second column of $[\phi]_A$ is 5.15, while for the application of the approximate, as indicated by equations (3-40) and (3-47), or perturbation analysis, this particular element should be less than unity in absolute value. As such it can be inferred, without knowledge of the experimentally determined value for $[\phi]$ that the first and third columns of $[\phi]_A$ or $[\phi]_{AN}$ are satisfactory

approximations and the second column should be determined from the orthogonality condition with respect to the first and third columns. A further indication that such a procedure is needed is the fact that the second column of $[\phi]_{AN}$ is far from being orthogonal to the first or third columns; while the first and third columns are themselves nearly orthogonal.

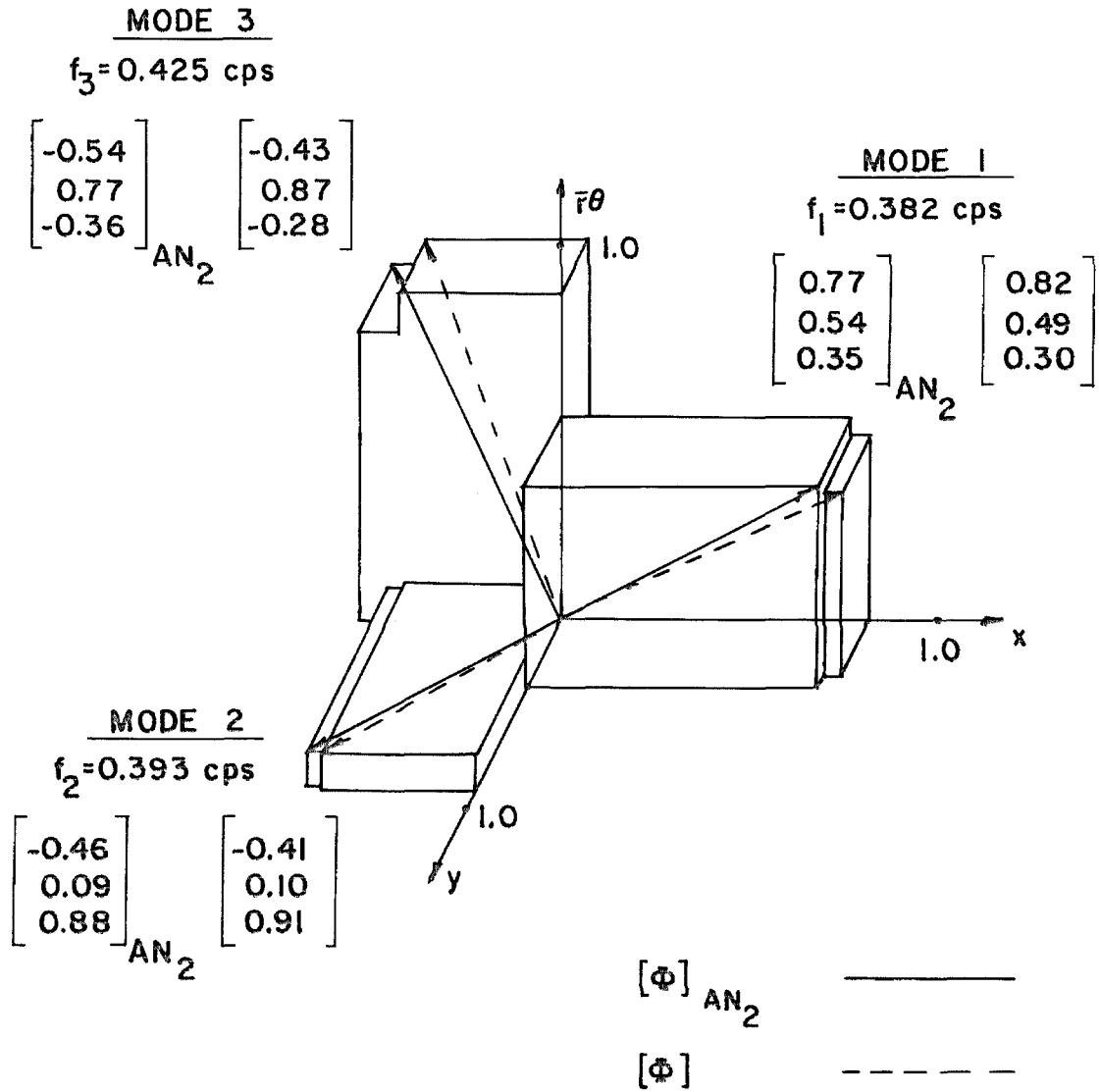
The resulting improved approximation for $[\phi]_{AN}$, denoted by $[\phi]_{AN_2}$ is given by

$$[\phi]_{AN_2} = \begin{bmatrix} 0.77 & -0.46 & -0.54 \\ 0.54 & 0.09 & 0.77 \\ 0.35 & 0.88 & -0.36 \end{bmatrix} . \quad (6-16)$$

This equation is in very close agreement with the experimentally determined matrix of modal components, equation (6-2). A comparison of the vectors of $[\phi]_{AN_2}$ and $[\phi]$ is shown in figure 23.

Earthquake Response

The estimated earthquake response of the San Diego Gas and Electric Building, in terms of relative displacements, etc., may be determined using the results of Chapter V. Based upon an average fundamental period of 2.50 seconds, the 22-story building has the constant β_0 approximately equal to 0.114. The average interfloor spacing is 13.5 feet, and the moment arms w_x and w_y , are 90 feet and 35 feet respectively. The relative displacements are expressed in feet; the absolute accelerations are expressed in ft./sec.² and the



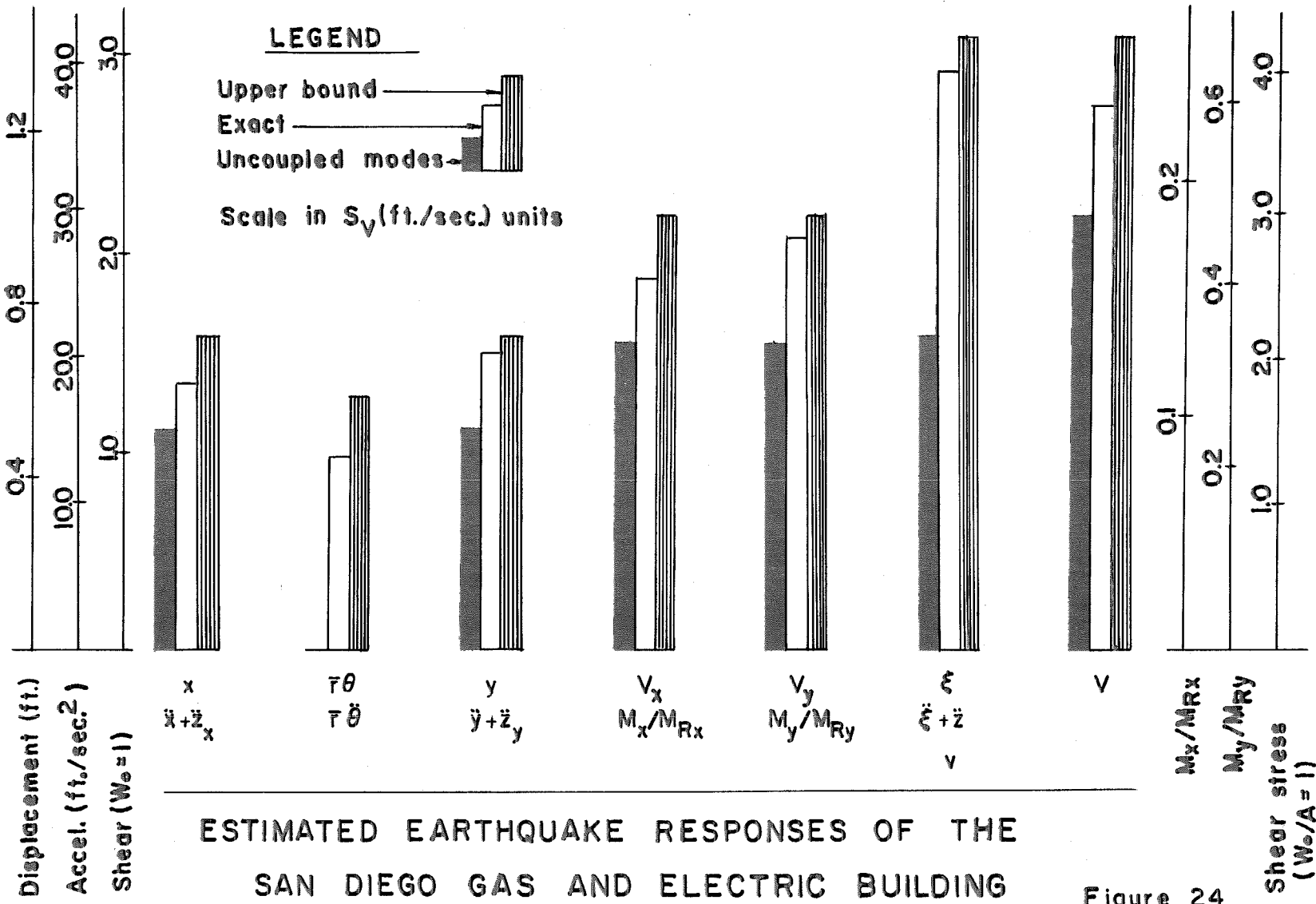
FUNDAMENTAL MODES FROM PERTURBATION THEORY

Figure 23

velocity spectrum, S_v , is given in ft./sec. The base shears are expressed in the same units as the average floor weight W_o , and the overturning moment ratios are dimensionless. The shearing stresses are expressed in the same units as the average floor weight W_o divided by the plan area A .

The responses are determined from the matrix of modal components, equation (6-2), as determined from the fundamental modes and assumed appropriate for the higher modes of the San Diego Gas and Electric Building. As an upper bound based upon the assumption that there is strong modal coupling, the maximum responses that would occur for any $[\phi]$ are calculated also. In addition, earthquake response based upon the assumption that the mode shapes are uncoupled (an assumption which from the symmetry appears attractive) are presented for comparison. The three schemes for determining the responses, of which only the first depends on the exact fundamental modal coupling in the building, may then be compared. The appropriate maxima of the earthquake response parameters for the San Diego Gas and Electric Building, as calculated using these three schemes, are illustrated in figure 24.

From figure 24 it is seen that the estimated earthquake response of the San Diego Gas and Electric Building is much greater than would be expected if the mode shapes are assumed to be uncoupled. In fact, if the resistance is uniformly distributed over the floor area, as is the case for this building, the 5% accidental eccentricity prescribed by the Uniform Building Code⁽²⁴⁾ for a static design accounts



ESTIMATED EARTHQUAKE RESPONSES OF THE
SAN DIEGO GAS AND ELECTRIC BUILDING

Figure 24

for only a 30% increase in ξ , $\ddot{\xi} + \ddot{z}$ and v . This 30% increase should be compared with 85% for a dynamic analysis of the San Diego Gas and Electric Building and with 95% for the upper bound on strong modal coupling. Furthermore, the accidental eccentricity in a code design does not imply an increase in any of the other response parameters considered, with the exception of rotation.

These approximate findings suggest that either the building code design requirements which account for rotational motions of buildings during an earthquake should be made more stringent, or a more realistic dynamic study should be made so that a more rational design using the matrix of modal components can follow. Because strong modal coupling can increase the earthquake response so drastically, it is felt that designs for which the modes are relatively uncoupled should be sought. Based upon this thesis, a rectangular building would either be designed with a central core or with peripheral shear walls, but not with a smooth distribution of columns over the floor area, for which translational and rotational frequencies could be nearly equal.

VII. SUMMARY AND CONCLUSIONS

Experience has shown that the major features of dynamic response of many tall buildings are capable of description by a shear beam model. For this reason the equations of motion for shear beams, both discrete and continuous, are examined in Chapter II, with attention confined to linear response for simplicity. Motivated by vibration tests of buildings which exhibit coupled modes, the shear beam models considered are three-dimensional, rather than the much simpler and more common one-dimensional models. After showing the equivalence of discrete and continuous formulation of the model, the continuous model is used for convenience.

In Chapter III the dynamic properties of the continuous, three-dimensional model, particularly modal coupling, are investigated. It is found that there is a class of models representative of many tall buildings for which there exists a constant orthogonal matrix of modal components, i.e., for which the components x , $\bar{r}\theta$ and y in each mode are in one of three constant, orthogonal ratios. A particularly simple subclass of this class is one with uncoupled modes, for which the matrix of modal components $[\phi]$ is given by $[I]$. The class with a constant matrix of modal components includes buildings with two-fold plan symmetry as well as buildings with eccentricity and stiffness ratios invariant with height. Nominally symmetric rectangular buildings in this class with corresponding translational and torsional frequencies, well-separated, such as buildings with

either central cores or peripheral shear walls as primary resistive elements, tend to have relatively uncoupled modes. However buildings with nearly equal translational and torsional frequencies, as expected with an even distribution of columns over the floor area, can have strong modal coupling. Exact and approximate schemes for determining $[\phi]$ are presented in Chapter III, the latter being applicable when $[\phi]$ is near $[I]$.

In Chapter IV a perturbation scheme is developed to widen the scope of the analysis because it is thought that many buildings would be nearly members of this class, although not members in an exact sense. Based upon the assumptions that the lines of mass and rigidity centers are nearly vertical as well as the assumption that the three i^{th} modes are of nearly the same shape, a constant first order matrix of modal components is found. The natural frequencies are similarly estimated to second order. A first order perturbation about $[\phi]$ equals $[I]$ is shown to be equivalent to the approximate solution for $[\phi]$ near $[I]$ developed in Chapter III.

In Chapter V the earthquake response as a function of modal coupling is investigated using as an example a simple structure with constant properties. Taking the ground acceleration as translational without rotational components, rotation in the structure is manifested only through modal coupling. The rotational motions arising from coupled translational and rotational modes are shown to result in larger responses than would be expected from uncoupled modes.

A further increase in response results from a beating type effect particularly for nominally symmetric structures with strong modal coupling, for which translational and torsional frequencies are nearly equal. Usually the maximum of combined earthquake responses, with any dominant frequency components well-separated, may be taken as the r.m.s. of the respective response maxima. However, when beating is present, this r.m.s. combination should be replaced by an absolute sum of the modal responses considered.

For the simplified structure considered in Chapter V the combination of rotational and beating effects can result in significantly increased response, by as much as 95%, on the perimeter of a rectangular building relative to that expected for uncoupled modes. In Chapter VI this is compared with an 85% increase in perimeter response expected for the San Diego Gas and Electric Company building based upon the assumption that the fundamental modal coupling, as determined from vibration tests,⁽²⁾ applies to the higher modes as well. As a further comparison, the 5% accidental eccentricity prescribed by the Uniform Building Code for symmetric buildings results in a 30% stress increase on the perimeter.⁽²⁴⁾ The beating effect alone, which is not considered in the Uniform Building Code, can increase the responses which do not depend on rotation, such as base shear or overturning moment, by as much as 40%.

From this thesis it is seen that strong modal coupling, which might include both rotational and beating effects, can result

in significant increases in response unaccounted for in the usual present-day design practices. Therefore it is recommended that 1) current statically based code design requirements regarding rotational components of earthquake response be made more stringent or 2) a more rational dynamic analysis which includes modal coupling as a possibility be incorporated in design.

REFERENCES

1. Los Angeles Annual Builders Guide, Vol. III, Inter-State Educational Association, Los Angeles, California, (1926), p. 83.
2. Jennings, P.C., Matthiesen, R.B. and Hoerner, J.B., "Forced Vibration of a 22-Story Steel Frame Building," Earthquake Engineering Research Laboratory, California Institute of Technology and Earthquake Engineering and Structures Laboratory, University of California at Los Angeles, (February, 1971).
3. Ayre, R.S., "Interconnection of Translational and Torsional Vibrations in Buildings," Bulletin of the Seismological Society of America, (April, 1938). pp. 89-130.
4. Ayre, R.S., "Experimental Response of an Asymmetric, One-Story Building Model to an Idealized Transient Ground Motion," Bulletin of the Seismological Society of America, (April, 1943) pp. 91-119.
5. Ayre, R.S., "Methods for Calculating the Earthquake Response of 'Shear' Buildings," Proceedings of the World Conference on Earthquake Engineering, Berkeley, California, (June, 1956), pp.13-1 to 13-24.
6. Jacobsen, L.S. and Ayre, R.S., "Engineering Vibrations," McGraw-Hill Book Co., (1958), pp. 335-344.
7. Shiga, T., "Torsional Vibrations of Multi-Storied Buildings," Proceedings of the Third World Conference on Earthquake Engineering, Vol. 2, Auckland and Wellington, New Zealand, (1965), pp. 569-584.

8. Shepherd, R. and Donald R.A.H., "Seismic Response of Torsionally Unbalanced Buildings," Journal of Sound and Vibration, Vol. 6 No. 1, (1967) pp. 20-37.
9. Skinner, R.I., Skilton, D.W.C., and Laws, D.A., "Unbalanced Buildings and Buildings with Light Towers Under Earthquake Forces," Proceedings of the Third World Conference on Earthquake Engineering, Vol. 2, Auckland and Wellington, New Zealand, (1965), pp. 586-602.
10. Penzien, J., "Earthquake Response of Irregularly Shaped Buildings," Proceeding of the Fourth World Conference on Earthquake Engineering, Vol. 2, Santiago, Chile, (1969), pp. A3-75 to A3-89.
11. Hart, G.C., "Three Dimensional Dynamic Analysis of Two Colombian High Rise Buildings," Bulletin of the Seismological Society of America, (August, 1969), pp. 1495-1515.
12. Shepherd, R., "Predictions of the Response of a Torsionally Unbalanced High Rise Building to Earthquake Loading," First Australian Conference on Mechanics of Structures and Materials, Sydney, Australia, (1967).
13. Irwin, A.W. and Heidebrecht, A.C., "Dynamic Response of Coupled Shear Wall Buildings," ASCE National Structural Engineering Meeting, Baltimore, Maryland, (April, 1971).
14. Medearis, K., "Coupled Bending and Torsional Oscillations of a Modern Skyscraper," Bulletin of the Seismological Society of America, (August, 1966), pp. 937-946.
15. Bouwkamp, J.G. and Blohm, J.K., "Dynamic Response of a Two-Story Steel Frame Structure," Bulletin of the Seismological Society of

- America, (December, 1966), pp. 1289-1303.
16. Penzien, J. and Chopra, A.K., "Earthquake Response of an Appendage on a Multi-Story Building," Proceedings of the Third World Conference on Earthquake Engineering, Vol. 2, Auckland and Wellington, New Zealand, (1965), pp. 476-490.
 17. Berg, G.V., "Earthquake Stresses in Tall Buildings with Setbacks," Second Symposium on Earthquake Engineering, Section IV, Roorkee, India, (1962), pp. 267-284.
 18. Loyar, E.A., "Torsion in Plan of Buildings," Chilean Conference on Seismology and Earthquake Engineering, (July, 1963), pp. B3.1-1 to B3.1-13.
 19. Shibata, H., Sato, H. and Shigeta, T., "Aseismic Design of Machine Structure," Proceedings of the Third World Conference on Earthquake Engineering, Vol. 2, Auckland and Wellington, New Zealand, (1965), pp. 552-568.
 20. Shiga, T., Shibata, A., Onose, J., "Torsional Response of Buildings to Strong Motion Earthquakes," Proceedings of Japan Earthquake Engineering Symposium, Tokyo, Japan, (1966), pp. 209-214.
 21. Newmark, N.M., "Torsion in Symmetrical Buildings," Proceedings of the Fourth World Conference on Earthquake Engineering, Vol. 2, Santiago, Chile, (1969), pp. A3-19 to A3-32.
 22. Englekirk, R.E., and Matthiesen, R.B., "Forced Vibration of an Eight-Story Reinforced Concrete Building," Department of Engineering, University of California at Los Angeles, (January, 1966).

23. Hoerner, J.B. and Jennings, P.C., "Modal Interference in Vibration Tests," Journal of the Engineering Mechanics Division, ASCE, (August, 1969), pp. 827-839.
24. "Uniform Building Code," 1970 Edition, Vol. 1, International Conference of Building Officials, Pasadena, California, (1970), p. 121.
25. Housner, G.W., and Outinen, H., "The Effect of Torsional Oscillations on Earthquake Stresses," Bulletin of the Seismological Society of America, (July, 1958), pp. 221-229.
26. Bustamante, J.I. and Rosenbluth, E., "Building Code Provisions on Torsional Oscillations," Proceedings of the Second World Conference on Earthquake Engineering, Vol. 2, Tokyo, Japan, (1960), pp. 879-894.
27. Rosenbluth, E., "The Earthquake of 28 July 1957 in Mexico City," Proceedings of the Second World Conference on Earthquake Engineering, Vol. 1, Tokyo, Japan, (1960), pp. 359-369.
28. Trifunac, M.D., "Wind and Microtremor Induced Vibrations of a Twenty-two Story Steel Frame Building," Earthquake Engineering Research Laboratory, California Institute of Technology, Pasadena, California, (1970).
29. Blandford, R.R., McLamore, V.R. and Aunon J., "Structural Analysis of Millikan Library from Ambient Vibrations," Earth Sciences, (February, 1968).
30. Crawford, R. and Ward, H.S., "Determination of the Natural Periods of Buildings," Bulletin of the Seismological Society of America, (December, 1964), pp. 1743-1756.

31. Ward, H.S. and Crawford, R., "Wind Induced Vibrations and Building Modes," Bulletin of the Seismological Society of America, (August, 1966), pp. 793-813.
32. Trifunac, M.D., "Ambient Vibration Test of a Thirty-Nine Story Steel Frame Building," Earthquake Engineering Research Laboratory, California Institute of Technology, Pasadena, California, (July, 1970).
33. Kuroiwa, J.H., "Vibration Test of a Multistory Building," Earthquake Engineering Research Laboratory, California Institute of Technology, Pasadena, California, (June, 1967).
34. Nielsen, N.N., "Dynamic Response of Multistory Buildings," Ph.D. thesis, California Institute of Technology, Pasadena, California, (June, 1964).
35. Blume, J.A., "Period Determinations and Other Earthquake Studies of a Fifteen-Story Building," Proceedings of the World Conference on Earthquake Engineering, Berkeley, California, (June, 1956), pp. 11-1 to 11-27.
36. Alford, J.L. and Housner, G.W., "A Dynamic Test of a Four-Story Reinforced Concrete Building," Bulletin of the Seismological Society of America, (January, 1953), pp. 7-16.
37. Weinberger, H.F., "A First Course in Partial Differential Equations," Blaisdell Publishing Company, Waltham, Massachusetts, (1965).
38. Courant, R. and Hilbert, D., "Methods of Mathematical Physics," Interscience Publishers Inc., Vol. I, New York, (1953).

39. Giberson, M.F., "The Response of Nonlinear Multi-Story Structures Subjected to Earthquake Excitation," Ph.D. thesis, California Institute of Technology, Pasadena, California, (1967).
40. Cole, J.D., "Perturbation Methods in Applied Mathematics," Blaisdell Publishing Company, Waltham, Massachusetts, (1968).
41. Jennings, P.C., "Spectrum Techniques for Tall Buildings," Proceedings of the Fourth World Conference on Earthquake Engineering, Vol. 2, Santiago, Chile, (1969), pp. A3-61 to A3-74.
42. Housner, G.W. and Jennings, P.C., "Generation of Artificial Earthquakes," Journal of the Engineering Mechanics Division, ASCE, (February 1964), pp. 113-150.
43. Housner, G.W., "Behavior of Structures during Earthquakes," Journal of the Engineering Mechanics Division, ASCE, (October, 1959), pp. 109-129.
44. Alford, J.L., Housner, G.W. and Martel, R.R., "Spectrum Analyses of Strong-Motion Earthquakes," A Report on Research Conducted under Contract with the Office of Naval Research, California Institute of Technology, Pasadena, California, (August, 1951, revised August 1964).
45. Merchant, H.C., "Mode Superposition Methods Applied to Linear Mechanical Systems under Earthquake Type Excitation," Ph.D. Thesis, California Institute of Technology, Pasadena, California, (1961).

46. Hudson, D.E., "Synchronized Vibration Generators for Dynamic Tests on Full-Scale Structures," Earthquake Engineering Research Laboratory, California Institute of Technology, Pasadena, California (November, 1962).
47. Caughey, T.K. and O'Kelly, M.E.J., "General Theory of Vibration of Damped Linear Dynamic Systems," Dynamics Laboratory, California Institute of Technology, Pasadena, California, (June, 1963).

APPENDIX I

A CONSTANT MATRIX OF MODAL COMPONENTS DIAGONALIZES $[F(z)]$

If a constant orthogonal matrix diagonalizes $[F(z)]$, it follows directly that $[\phi]$ is a matrix of modal components as defined by equation (3-19). Here it is assumed that $[\phi]$ is a constant non-singular matrix of modal components and that the mode shapes satisfy the self-adjoint differential equation, (3-11), with $[F(z)]$ continuous. It is here shown that $[\phi]$ is an orthogonal matrix which diagonalizes $[F(z)]$. Substitute equation (3-19) into the first of equation (3-11).

$$\{[F(z)]\rho'_{ik}(z)[\phi]\{\tilde{e}_k\}\}' + m(z)\omega_{ik}^2\rho_{ik}(z)[\phi]\{\tilde{e}_k\} = \{\tilde{0}\} \quad \text{for } k = 1, 2, 3. \quad (\text{I-1})$$

This equation may be premultiplied by $[\phi]^{-1}$ and rewritten as

$$[[\phi]^{-1}[F(z)][\phi]\rho'_{ik}(z)]' + m(z)\omega_{ik}^2\rho_{ik}(z)[I]\{\tilde{e}_k\} = \{\tilde{0}\} \quad \text{for } k = 1, 2, 3 \quad (\text{I-2})$$

The matrix $[F^*(z)]$, with components $F^*_{pk}(z)$, is defined by

$$[F^*(z)] = [\phi]^{-1}[F(z)][\phi] \quad . \quad (\text{I-3})$$

This equation is substituted into equation (I-2) and the p^{th} row is

$$[F^*_{pk}(z)\rho'_{ik}(z)]' + \delta_{pk}m(z)\omega_{ik}^2\rho_{ik}(z) = 0 \quad (\text{I-4})$$

which can be integrated, subject to the boundary conditions.

$$F_{pk}^*(z) = \frac{\delta_{pk} \omega_{1k}^2}{\rho_{1k}'(z)} \int_z^{\ell} m(\xi) \rho_{1k}(\xi) d\xi . \quad (I-5)$$

The slope of fundamental mode shape, $\rho_{1k}'(z)$, vanishes only at $z = \ell$, and since $[F(z)]$ is continuous, $[F^*(z)]$ is also continuous. Therefore, the off-diagonal elements of $[F^*(z)]$ vanish, and $[F^*(z)]$ is diagonal. Since $[F(z)]$ is symmetric, it is diagonalized only by an orthogonal matrix, and hence $[\phi]$ is a constant orthogonal matrix which diagonalizes $[F(z)]$ as indicated by equation (3-18).

APPENDIX II

NECESSARY AND SUFFICIENT CONDITIONS FOR A CONSTANT $[\phi]$.

If $[\phi]$ is constant, $[\phi]$ diagonalizes both $[F(\bar{z})]$ and $[F(z)]$ for any constant \bar{z} and variable z in the closed interval $[0, \ell]$. It follows from matrix algebra that the symmetric matrices, $[F(\bar{z})]$ and $[F(z)]$, are diagonalized by the same orthogonal matrix if and only if $[F(\bar{z})]$ and $[F(z)]$ commute.⁽⁴⁷⁾ Furthermore,

$$[[F(\bar{z})][F(z)]]^T = [F(z)]^T[F(\bar{z})]^T = [F(z)][F(\bar{z})], \quad (\text{II-1})$$

and hence $[F(\bar{z})]$ and $[F(z)]$ commute if and only if $[F(\bar{z})][F(z)]$ is symmetric. Assuming the product

$$\begin{bmatrix} F_x(\bar{z}) & \frac{-\bar{y}_f(\bar{z})}{\bar{r}}F_x(\bar{z}) & 0 \\ \frac{-\bar{y}_f(\bar{z})}{\bar{r}}F_x(\bar{z}) & F_\theta(\bar{z}) & \frac{\bar{x}_f(\bar{z})}{\bar{r}}F_y(\bar{z}) \\ 0 & \frac{\bar{x}_f(\bar{z})}{\bar{r}}F_y(\bar{z}) & F_y(\bar{z}) \end{bmatrix}$$

$$\begin{bmatrix} F_x(z) & \frac{-\bar{y}_f(z)}{\bar{r}}F_x(z) & 0 \\ \frac{-\bar{y}_f(z)}{\bar{r}}F_x(z) & F_\theta(z) & \frac{\bar{x}_f(z)}{\bar{r}}F_y(z) \\ 0 & \frac{\bar{x}_f(z)}{\bar{r}}F_y(z) & F_y(z) \end{bmatrix}$$

is symmetric, it follows that

$$F_x(\bar{z})\bar{y}_f(z)F_x(z) + \bar{y}_f(\bar{z})F_x(\bar{z})F_\theta(z) = \bar{y}_f(\bar{z})F_x(\bar{z})F_x(z) + F_\theta(\bar{z})\bar{y}_f(z)F_x(z), \quad (\text{II-2})$$

$$\bar{y}_f(\bar{z})F_x(\bar{z})\bar{x}_f(z)F_y(z) = \bar{x}_f(\bar{z})F_y(\bar{z})\bar{y}_f(z)F_x(z) \quad \text{and} \quad (\text{II-3})$$

$$F_\theta(\bar{z})\bar{x}_f(z)F_y(z) + \bar{x}_f(\bar{z})F_y(\bar{z})F_y(z) = \bar{x}_f(\bar{z})F_y(\bar{z})F_\theta(z) + F_y(\bar{z})\bar{x}_f(z)F_y(z). \quad (\text{II-4})$$

If division by zero does not occur, equations (II-2) through (II-4) may be rewritten as

$$\frac{\bar{y}_f(z)F_x(z)}{F_x(z) - F_\theta(z)} = \frac{\bar{y}_f(\bar{z})F_x(\bar{z})}{F_x(\bar{z}) - F_\theta(\bar{z})}, \quad (\text{II-5})$$

$$\frac{\bar{x}_f(z)F_y(z)}{\bar{y}_f(z)F_x(z)} = \frac{\bar{x}_f(\bar{z})F_y(\bar{z})}{\bar{y}_f(\bar{z})F_x(\bar{z})} \quad \text{and} \quad (\text{II-6})$$

$$\frac{\bar{x}_f(z)F_y(z)}{F_\theta(z) - F_y(z)} = \frac{\bar{x}_f(\bar{z})F_y(\bar{z})}{F_\theta(\bar{z}) - F_y(\bar{z})}. \quad (\text{II-7})$$

Therefore the matrix of modal components, $[\phi]$, is constant if and only if the terms

$$1) \frac{\bar{y}_f(z)F_x(z)}{F_x(z) - F_\theta(z)}, \quad 2) \frac{\bar{x}_f(z)F_y(z)}{\bar{y}_f(z)F_x(z)} \quad \text{and} \quad 3) \frac{\bar{x}_f(z)F_y(z)}{F_\theta(z) - F_y(z)}$$

when defined are constant.

If any of the equations (II-5) through (II-7) include a division by zero for all z and \bar{z} , the corresponding equation in (II-2) through (II-4) is satisfied identically and the constraint on $[F(z)]$ which results is no longer of consequence. For example, if $\bar{y}_f(z)$ vanishes for all z and the matrix of modal components is constant, the second constraint is eliminated and it is only necessary for the third constraint given by

$$\frac{\bar{x}_f(z)F_y(z)}{F_\theta(z) - F_y(z)}$$

to be constant. The first constraint also vanishes in this case because it is satisfied identically.

APPENDIX III

THE FORM OF $[F(z)]$ AND $[F_\lambda(z)]$ IF $[\phi]$ AND THE
ECCENTRICITY RATIOS ARE CONSTANT

If the eccentricity ratios $\bar{x}_f(z)/\bar{r}$ and $\bar{y}_f(z)/\bar{r}$ are constant, and there is a constant matrix of modal components, it follows from Appendix II that

$$1) \frac{F_x(z)}{F_x(z) - F_\theta(z)}, \quad 2) \frac{F_y(z)}{F_x(z)} \quad \text{and} \quad \frac{F_y(z)}{F_\theta(z) - F_y(z)}$$

are constant. The first constraint can be written as

$$\frac{F_x(z)}{F_x(z) - F_\theta(z)} = \frac{1}{c} \quad (\text{III-1})$$

from which it follows that

$$F_x(z)(1-c) = F_\theta(z) \quad (\text{III-2})$$

This equation, the second constraint above and the form of $[F(z)]$ imply that $[F(z)]$ is a scalar multiple of a constant matrix. From equation (3-18) it follows that $[F_\lambda(z)]$ is also a scalar multiple of a constant matrix.